2010

Cell-Taught Gene Therapy for the Preservation and Regeneration of Cardiac Tissue Following Chronic Heart Failure

Srividya Sundararaman
Cleveland State University

CELL-TAUGHT GENE THERAPY FOR THE PRESERVATION AND REGENERATION OF CARDIAC TISSUE FOLLOWING CHRONIC HEART FAILURE

SRIVIDYA SUNDARARAMAN

Bachelor of Technology (B.Tech)

Chemical Engineering

Madras University, Chennai

May 2003

Masters of Science (S.M)

Molecular Engineering of Biological and Chemical Systems

Singapore-MIT-Alliance, Singapore

July 2004

Submitted in partial fulfillment of requirements for the degree of

DOCTOR OF ENGINEERING IN APPLIED BIOMEDICAL ENGINEERING

at the

CLEVELAND STATE UNIVERSITY

December, 2010

This dissertation has been approved
for the Department of Chemical and Biomedical Engineering
and the College of Graduate Studies by

_____

Dissertation Committee Chairperson, **Marc S. Penn, M.D., Ph.D.**
Department of Chemical and Biomedical Engineering

_____
Date

_____

Joanne Belovich, Ph.D
Department of Chemical and Biomedical Engineering

_____
Date

_____

Crystal Weyman, Ph.D
Department of Graduate Studies

_____
Date

_____

Paul Fox, Ph.D
Department of Biological Geological and Environmental Sciences

_____
Date

_____

Kai Wang, M.D., Ph.D.
Department of Chemical and Biomedical Engineering

_____
Date

_____

John Barnard, Ph.D.
Department of Chemical and Biomedical Engineering

_____
Date

DEDICATION

I dedicate this work to

My parents, Mr. G. Sundararaman and Mrs. Geetha Sundararaman

for letting me follow my dreams and for believing that I could achieve them

ACKNOWLEDGMENTS

I would like to thank my advisor, Dr Marc Penn, whose vision and guidance during these past five years have helped get this substantial piece of work done as smoothly as possible, for providing me with the right opportunities, and always encouraging me to do the best I can. I would also like to thank him for giving me the opportunity to work with Juventas, Inc. as that helped shape the initial aspects of this thesis. In that regard, I would like to thank Drs. Rahul Aras, Joe Pastore and Tim Miller for their guidance, support and for introducing me to the world of taking lab results to the clinical arena. I would like to thank my committee members Drs. Joanne Belovich, Crystal Weyman, Paul Fox, Kai Wang and John Barnard for their critical evaluation and suggestions that helped shape and fortify this thesis. I would also like to thank Dr Vinod Labhasetwar for generously allowing me to use his facilities and for guiding me with the nanoparticle work.

I would like to thank everyone (past and present) in the Penn lab. Matt, for knowing every protocol and teaching them to me and for keeping the lab from burning down. Amanda, Udit and Nik for being in my boat as fellow graduate students, for encouraging me and never giving up. Mary, Jing, Kristal, Feng, Yanming, Xiorong, Nil, and Mazen for their kind and generous support and time. Farhad, for introducing me to the world of rodents, from surgeries to post op care. Zoran, Kathy and Jeannie for training me in echocardiography. Ranjan for his help with the microarray analysis. Radhika and Shiva for their patience with me while I learnt the formulation and testing of nanoparticles.

I would like to express my gratitude to Becky Laird and Darlene Montgomery at the ABE department in CSU. Their help in organizational and administrative aspects of my doctoral journey were instrumental in my timely completion of this arduous task.

However, none of this would have been possible without the support and encouragement from my friends and family.

Pulak, Chaitu, Vivek, Mitya, Anil, Gati, Uma, and Sushma for setting an example, for enjoying this journey and being optimistic when I was not.

My parents, for their constant support, unwavering faith and undying patience. Priya, Karthick, Athimber, and Vidhya for their support and love. Shruti and Smriti for being full of life and reminding me of how much I am loved. And Guru, for supporting me through the most difficult times and encouraging me to never give up.

Thank you, for this is your achievement as much as mine.

CELL-TAUGHT GENE THERAPY FOR THE PRESERVATION AND REGENERATION OF CARDIAC TISSUE FOLLOWING CHRONIC HEART FAILURE

SRIVIDYA SUNDARARAMAN

ABSTRACT

Heart failure is the primary cause of mortality and morbidity in the Western world. Although cell therapy has demonstrated improvement in cardiac function, these benefits are being attributed to the activation of paracrine factors, rather than the differentiation and integration of the transplanted cells into the host tissue. Based on this knowledge the focus of this thesis work was to deliver paracrine factors, and evaluate its effect on cardiac function.

Gene therapy has evolved as a promising option to deliver pro-angiogenic proteins to infarct zones, thus providing cardiac benefit. This study has identified a gene design without the use of viral vectors, to deliver transient, yet therapeutic levels of an angiogenic chemokine, Stromal-Derived-Cell-Factor-1 (SDF-1) in rodents with chronic heart failure, and has reported significant improvement in cardiac function. The use of Kozak sequences and translational enhancers helped boost gene expressions which could be accurately measured using bio-fluorescence imaging techniques. This improvement in

gene expression was directly proportional to the improvement in cardiac function in rodents with chronic heart failure.

However effective plasmid delivery, via the systemic route, requires the encapsulation and targeting of the plasmid to infarct zones. An infarct-specific peptide was identified with the help of phage panning techniques and nanoparticles, formulated with poly lactide-co-glycolide (PLGA), were employed to encapsulate a fluorescent dye, 6-Coumarin (6C). Targeted and efficient delivery was achieved by tagging the surface of the nanoparticles with the targeting peptide. Another aspect of this study was to identify novel paracrine factors responsible for reverse ventricular remodeling, following the treatment of chronic heart failure with mesenchymal stem cell (MSC) therapy, using microarray analysis.

Overall, this study has identified the design and delivery technique for a therapeutic, cardiac-benefitting gene to the infarct zone, in rodents with heart failure. These results can be translated to a clinical setting, providing relief to patients with chronic heart failure. This study has also paved the way for future research in developing novel cardiac drugs, by identifying cardiac specific genes, responsible for reverse ventricular remodeling.

TABLE OF CONTENTS

Page

LIST OF TABLES

LIST OF FIGURES

CHAPTER I

INTRODUCTION

1.1 Research Interest in Heart Failure

Heart failure is a major cause of morbidity and mortality in the modern world. The conventional therapies involve a replacement of the tissue, either by designing total artificial hearts made with the use of biocompatible metals, or using a xenogenic transplant. However, the number of patients who die every year, or who are at risk has increased dramatically, leading researchers to focus on preventing the occurrence of an acute myocardial infarction, or to repair the tissue and thus provide relief to the chronic conditions associated with it and improving the quality of life.

Ischemic heart disease, caused by reduced blood supply in the heart and thus the damage associated with it, is a leading cause for heart failure. Current therapies involve preventive measures in order to stop cardiac myocyte loss in an acute stage, or to

optimize the reversal of ventricular remodeling in a chronic condition. The heart is a highly aerobic organ requiring a constant supply of oxygen in order to continue its function. The cells of the heart, specially the muscle cells or myocytes, are terminally differentiated and thus do not repair themselves following damage. A reduction in oxygen, due to reduced blood supply, can lead to the death of the cells in that tissue, almost immediately.

This damage elicits an inflammatory process where the dead muscle cells are replaced by a scar region, which is not an ideal replacement to the loss in function. This action, then leads to a cascade of lower cardiac output and the compensation mechanisms caused henceforth. The combination of ventricular fibrosis, muscle cell hypertrophy, dilation of the ventricle, thickening of the ventricular wall, and thinning of the scar tissue is termed ventricular remodeling. These pathological conditions are symptomatic of a more progressive condition known as chronic heart failure.

Current research is now focused on reversing this ventricular remodeling, by inducing angiogenesis in the infarct region, thus providing oxygen to injured myocardium in the infarct border zones, or in triggering a cascade of pathways that can provide the right signals to regenerate the myocardium either with the concomitant use of stem cells or without.

1.2 Chemokine Mediated Repair

Cell therapy has evolved as a promising option for cardiac repair for more than a decade. Pre-clinical and clinical studies have demonstrated the potential of skeletal myoblasts, multiple autologous or syngeneic stem cell populations, including Hematopoietic (HSC), Mesenchymal (MSC) Stem Cells, and Multipotent Adult Progenitor Cells (MAPC) to improve cardiac function when delivered in the peri-infarct period in animal models as well as human trials. For cell therapy to provide substantial clinical impact, the cells transplanted should be able to survive in a hypoxic environment and must protect themselves from being degraded by the host's immune system. The other option for successful cell therapy is to use multipotent stem cells, capable of differentiating to the cells of the cardiac lineage and then engrafting into the host tissue to replace the damaged or dying cells.

Although cell therapy has shown to provide cardiac functional benefit by improving the cardiac output, there is limited evidence that point to the improvement as arising from the differentiation of these cells to cardiac myocytes. This has led to the belief that the improvement in cardiac function is not due to regeneration of the myocardium but rather due to the paracrine effects which then help improve angiogenesis, matrix remodeling, cell signaling to help stem cells from the bone marrow to home to the ischemic myocardium, and cell survival to name a few.

Consistent with this hypothesis are recent studies by us and others, demonstrating that the benefit of stem cell therapy is increased by the over-expression of specific factors, namely Stromal Derived Cell factor -1 (SDF-1), Monocyte Chemoattractant Protein-3 (MCP-3), and others. The over-expression of SDF-1, in ischemic tissue, leads to increased stem cell homing, neovascularization, and preservation of cardiac myocytes due to the binding of SDF-1 to its receptor CXCR4, which is present on the cell surface of hematopoietic cell populations. Although SDF-1 is shown to be elevated in injured tissue; the naturally occurring transient increase of this chemokine, is not sufficient to provide a significant improvement in cardiac function.

Other studies in our laboratory have demonstrated that MSC home to myocardial tissue in response to MCP-3 when transfected a month after inducing myocardial infarction in rodents, and that re-establishment of MCP-3 weeks after AMI re-establishes MSC homing to the heart leading to ventricular remodeling and improved function. However the pathways that mediate the benefits associated with cardiac remodeling are poorly defined. Similar results are obtained from varied stem cell sources with limited evidence that these different cell types actually differentiate into cardiac myocytes. The conclusion that the majority of the improvement observed is not due to the regeneration of cardiac myocytes, but rather due to the paracrine factors released by the engrafted stem cells, has led to growing number of research in identifying these paracrine factors.

Sophisticated software is currently available to analyze and identify the changes in gene expression following cell therapy. The use of whole genome analysis is made

possible with the help of Affymetrix's and Ilumina's software systems, that can identify changes in gene behavior, whether it is differential or not. Other software, such as DAVID and Ingenuity Pathway Analysis, provide effective techniques in order to decipher the information present in the large datasets.

Gene therapy has provided an efficient method of expressing these chemokines *in vivo* and assessing their effects in animal models. In cardiac applications, this method has evolved as a potential target for encoding angiogenic proteins which lead to repair of the myocardium, following a promotion of blood vessel growth in the injured area, which helps revive the hibernating myocardium. Although, this is a promising field and the expectation is that it can provide functional benefit, there are no clinically approved gene therapy treatment options available today. One reason is that most gene therapy trials use viral techniques, which pose a serious threat to the life of the patient due to immunological reactions, and tumor developing potentials.

The alternative method is to use naked plasmid or DNA which then has a drawback of having low transcription efficiencies, and the potential to degrade in the host environment. In order to bridge this gap between low transcription and immunological reactions, it is necessary to understand mechanisms which will provide a platform for high transcriptions and not pose a risk towards pathological damage. Another concern to be addressed with gene therapy is to avoid the degradation of these genes in the host tissue when delivered systemically. The use of polymeric devices has gained popularity

in order to optimize the delivery of plasmids to specific organs with the focus being on safety and efficacy.

1.3 Research Focus

Our overall goal with this thesis is to determine a gene therapy based approach to provide benefit to myocardium with chronic heart failure, stemming from ischemic injury. We would like to develop and optimize a gene drug, which effectively translates to a cardiac benefiting protein and can provide significant improvements in cardiac function. Towards this main goal of designing and delivering a cardiac benefiting gene drug, we would like to optimize the delivery of this drug by understanding the principles required to systemically deliver this to the injured cardiac tissue. Having done that, we would have developed a drug, capable to providing cardiac relief that can be delivered systemically to patients, thus minimizing the trauma associated with multiple surgeries.

However, the need for more efficient drugs to support the prevention and regeneration of cardiac tissue, and reverse the remodeling caused by ischemic injury, leads us to focus on other cardiac pathways, responsible for this remodeling, following treatment with mesenchymal stem cells. This will provide us with leads to follow, in future, for other candidates that may be able to provide a better benefit to the myocardium and improve quality of life in patients.

1.4 Specific Aims

Hypothesis 1

Adult stem cell therapy for preventing and treating cardiac dysfunction is due to paracrine factors; therefore, the results of cell therapy can be achieved by gene transfer. To effectively design a gene it is necessary to manipulate the gene expression *in vivo*. A bioluminescent reporter can be used as a method to determine real time information on gene expression for plasmid profiling. This reporter will utilize optical imaging in order to determine changes in expression of a plasmid with the reporter gene and other enhancer elements.

Specific Aim 1

The goal of this study was to determine if re-establishing myocardial plasmid SDF-1 expression without the concomitant delivery of cells would provide a significant benefit in cardiac function by increasing myocardial vascular density in an ischemic cardiomyopathy condition. This study aimed to design and monitor the expression of the naked plasmid for effective gene therapy capable of expressing and sustaining expression in rodent hearts. We also wanted to evaluate if optical imaging could provide detailed information about changes in gene expression, with modifications to the plasmid design.

Therefore, the primary focus of this study was to investigate the role of naked SDF-1 gene when delivered in chronic ischemic hearts *in vivo*. Transient expressions of the naked SDF-1 plasmids were monitored for corresponding functional responses mediated in rodent ischemic hearts. To manipulate gene expressions, our secondary focus was to identify a gene design for efficient delivery of the SDF-1 gene into the ischemic myocardium. We investigated the role of transcription enhancers, Kozak sequences, and cardiac specific promoters for this purpose.

Hypothesis 2

A safe, effective and targeted delivery of naked plasmid to the heart, without having to reopen the chest, is important for targeted, systemic delivery of drugs to the myocardium. Infusion of phage display libraries within M13 bacteriophage may be useful in identifying specific targeting ligands in the infarct region of the heart.

Poly lactide co glycolide (PLGA) derived polymeric devices may be able to encapsulate drugs and deliver them safely to tissues via the systemic circulation. The targeting peptide when tagged to the polymeric complex, may be viable and in its active form, and will be able to direct the polymeric complex to the injured myocardium. The PLGA polymer will then be able to release the encapsulated material into the area of injury.

Specific Aim 2

The main focus with this aim was to engineer a targeted delivery carrier for gene drugs into the ischemic myocardium. The delivery of genes involves two complicated aspects: the targeting of the gene into the region of interest, and carriers for the maintenance and delivery of the gene *in vivo* without degrading it. Our primary focus was divided into two secondary focuses, a) To identify a peptide sequence, via phage panning to target the genes to the ischemic myocardium when injected intra-venously, b) to utilize nanoparticles for the encapsulation of the naked genes to prevent degradation of the DNA and tagging targeting peptides to the surface of these devices to mediate effective delivery of the DNA.

We wanted to identify one or a few ligands that have a high affinity for infarct tissue and are specific to the heart. This can then be used to tag polymeric devices to infuse therapeutic genes to the ischemic myocardium. Our goal then, was to design a nanoparticlulate carrier capable of encapsulating a fluorescent dye, and delivering it to the myocardium, with the help of a tagging peptide. The uptake and *in vivo* trafficking will be monitored to determine the dose, time, and other aspects associated with this delivery system.

Hypothesis 3

Recruitment of stem cells mediated improvement, in ventricular function is due to reverse ventricular remodeling. In previous studies, we have shown that Monocyte Chemoattractant Protein -3 (MCP-3) based recruitment of mesenchymal stem cell therapy leads to the expression of paracrine factors capable of improved ventricular function without the differentiation of cardiac myocytes, or blood vessel growth in the microenvironment. This reverse ventricular remodeling is attributed to paracrine factors secreted in the microenvironment.

Whole genome analysis provides sophisticated, yet specific information on all genes in the genome that are affected as a result of the application of therapy. Therefore whole genome analysis would be a viable option to identify pathways associated in the changes that lead to functional improvement thereby leading us to paracrine factors associated with this improvement.

Specific Aim 3

The primary focus of this aim is to identify cardiac pathways associated with reversing ventricular remodeling, following therapy with mesenchymal stem cells and then identifying proteins associated with ischemic disease and repair.

The goal is to identify candidate proteins responsible for the improvement in cardiac function when mesenchymal stem cells are recruited to the injured heart tissue due to MCP-3 over-expression. To understand and identify these proteins and pathways we shall employ whole genome analysis and back that with pathway analysis studies. Important aspects of genome wide experiments will be the large number of genes assessed and the high sensitivity of this approach.

CHAPTER II

BACKGROUND

2.1 Cardiovascular Disease

Cardiovascular disease ranks among the leading causes of morbidity and mortality in the world today with more than 80 million people who suffer from one or more forms of it, just in the United States. Cardiovascular disease is a pathological condition affecting the normal functioning of the heart due to an injured or overworked heart muscle, or an electrical imbalance determining the rhythm. These fall under a general umbrella of four types; dilated cardiomyopathy, restrictive cardiomyopathy, hypertrophic cardiomyopathy and arrhythmogenic cardiomyopathy. The causes for any of these forms can be due to bacterial or viral infections, genetic mutations and predispositions, the growth and build up of fatty components in the arteries and heart walls, abuse of cardio toxic substances, like caffeine and alcohol, or a secondary symptom of other chronic conditions, such as

hypertension and diabetes. Any or all of these forms have the potential to develop into a more progressive heart failure. While each of these conditions can cause a clinically significant cardiomyopathy, the focus of this work is primarily on ischemic cardiomyopathy.

2.1.1 Myocardial Infarction:

One of the more common types of cardiovascular diseases is Myocardial Infarction (or Acute Heart Attack) which occurs when there is a lack of blood supply to the heart. This condition affects more than 8 million people in the United States with 1.1 more being added each year.[1] The most common cause is due to a coronary artery disease (CAD); when a plaque ruptures and causes intra coronary thrombosis and disrupt blood flow, distal to thrombosis. The extent of damage to the heart depends on the duration of ischemia, and can lead to permanent damage if not treated immediately.

The cells of the heart tissue are terminally differentiated and thus do not repair themselves following damage. Following lack of blood supply, the myocytes, endothelial cells, nerves and fibroblasts die by a process called necrosis. This is then followed by an influx of inflammatory components, including macrophages, neutrophils and granulocytes that replace the viable muscle with a dead scar region, which is not an ideal replacement to the loss in function. The ventricular wall with a scar tissue lining which is unable to contract during the pumping action of the heart is not able to provide the same cardiac output as a healthy, viable wall. To compensate for this loss in output the

ventricle enlarges by either hypertrophy of the cardiac cells or by increase in ventricular volume, corresponding to thinning of the scar tissue. These conditions lead to a progressive heart failure condition.[2, 3]

Damaged heart, incapable of pumping the right amount of blood, can also lead to a life threatening condition, cardiac arrhythmia. Cardiac arrhythmias are conditions when the heart is unable to synchronize its pumping action thus causing abnormal beats or rhythms. Often times this leads to insufficient supply of blood pumped from the heart and may lead to cardiac arrest.[4]

2.1.2 Heart Failure

The combination of ventricular fibrosis, muscle cell hypertrophy, dilation of the ventricle, thickening of the ventricular wall, and thinning of the scar tissue is termed ventricular remodeling. These pathological conditions are symptomatic of a more progressive condition known as chronic heart failure.[3, 5]

Heart failure is among the leading causes of morbidity in the Western world, with a prevalence of 5.4 million Americans and an incidence of 690,000 cases being added each year. Coronary Artery Disease leading to Acute MI is the most common cause for heart failure. Other causes may be due to some or various forms of cardiomyopathy, attributed by genetic dispositions, personal lifestyles, cardio toxic abuse, pregnancy, radiation, and other chronic conditions such as diabetes, hypertension etc.

As heart failure is a progressive condition, the diseased state is classified into various classes based on the quality of life, class 1 for patients who are least affected physically by the condition and class 4 for those who are severely limited in their day to day activity and class 2 and 3 in between these two. Pathologically, the disease is classified based on the condition of the heart muscle, Stage 1 is a classification for patients at risk for heart disease, due to lifestyle choices, or secondary conditions but with no cardiac tissue compromise. Stage 4 is assigned to patients with structural heart disease and previous symptoms of heart failure.[3, 6]

The same pathways that are triggered as a response to acute cardiac injury, when sustained for longer periods of time, lead to a progression of events causing chronic heart failure. Some of these are mediators present in the circulatory system, such as angiotensin II,[7, 8] which is released as a result of low cardiac output can lead to increase in cardiac hypertrophy, others such as norepinephrine, cause cardiotoxicity and arrhythmias,[9] and TNF-α which decrease contractility.[10] A family of peptides, also used as a diagnostic tool, is β-natriuretic peptides that are released as a response to increased ventricular pressure, can cause vasodilation.[11] These cytokines released in response to myocardial injury, can worsen cardiac and endothelial dysfunction with the progression to heart failure.

2.2 Current Treatment Options for Heart Failure

Heart failure is not an isolated event that can be controlled or reversed after its occurrence. The current treatment options involve alleviating the symptoms associated with it and preventing a worsening of the condition. There are currently no available options to entirely cure a person of this condition. For patients without any structural damage or physical limitations, the simplest solution is to prevent the occurrence for one. This involves a few drugs that can help prevent the damages caused by secondary components. However, these are not sufficient for patients dealing with advanced stages of heart failure thus a number of other treatment options have been developed in the last few decades that support the heart from assistance to total replacement.

2.2.1 Cardiac Devices

Implantable cardiac defibrillators (ICDs) are devices that are connected to the heart tissues via electrodes. When the leads detect an abnormality in the beating action, e.g. tachycardia or fibrillation, they send a signal to the pulse generator, stored in the upper chest under the skin, which then sends a pulse or a shock to the heart thus setting the rhythm back for the pumping to continue. Cardiac Resynchronization is a technique by which electrical leads are placed on the atria and ventricles and these are then connected to a small battery operated device placed under the skin. The device sends electrical pulses routinely to the atria and ventricles which then contract in tandem. Such a procedure allows for effective ventricle ejection, reduction in ventricular size, and

improvement in cardiac function. A Left Ventricular Assist Device (LVAD) or a Total Artificial Heart (TAH) is used in patients with hearts that have completely lost the capability to function. Revascularization of the ventricle is a viable option when the left ventricle may be capable of functioning again. The myocardium may either be ischemic, infracted, stunned, or hibernating. Ischemic myocardium is one where the supply of blood to it, has been disrupted. The flow of blood back to it will repair the damage done relatively quickly. Stunned myocardium is one, where there is muscular dysfunction due to prolonged ischemia.[12] Revascularization will benefit the patient over a period of time. Hibernating myocardium is one where revascularization may or may not respond to revascularization, although revascularization coupled with other forms of functional assistance may provide benefit. Infarcted tissue is one where scar tissue has progressed with the lack of myocytes in the region. Revascularization may not provide any benefit in such situations.[3, 12]

2.2.2 Cell Therapy for Heart Failure

Cell Therapy has evolved as a promising mechanism for cardiac repair for more than a decade. The potential of several different populations of cells, including fetal cardiomyocytes, skeletal myoblasts, bone marrow derived progenitor cells, and embryonic stem cells has been studied in animal models and clinical populations in an attempt to repair the damage in ischemic cardiac tissue.[13-15] Ideally, the right type of cell should be able to survive in a hypoxic environment, with reduced angiogenesis, and

should be able to interact with the host cardiac tissue and integrate with it in order to facilitate contraction of the tissue, synchronous with existing heartbeats.

The first studies used fetal cardiomyocytes, which retain the potential to grow as they possess the required growth factors and signals necessary to do so. Leor et al studied the ability of human and rat fetal cardiomyocytes to engraft in ischemic rat myocardium following coronary ligation.[16] These cells engrafted and survived for up to 2 months post transplantation. Similar results were observed with cells encapsulated within bioengineered grafts with improved vasculogenesis in the graft tissue and improved LV function.[17,18] The improvement in LV function is due to improved morphological engraftment, coupled with the improvement of electrical conduction and rhythmic contractions of the ventricle.[19,20] Fetal cardiomyocytes have been shown to couple and integrate with host cardiomyocytes through gap junction proteins, such as N cadherins and connexin-43.[19]

Although fetal cardiomyocytes successfully engrafted with the host tissue, a scar region differentiated the newly formed myocardium and the host myocardium. Similar results with xenogenic neonatal and fetal cardiomyocytes have showed significant engraftment to host tissue and improvement in cardiac function in larger animals.[13] In spite of increasing evidence, proving successful transplantation of fetal cardiomyocytes, the use of these cells in treating patients leads to ethical concerns. The use of xenogenic cells is accompanied by immunological concerns and its clinical significance has not been tested.[21]

Skeletal myoblasts are rapidly mobilized following injury and have the potential to proliferate in ischemic conditions. Also, they are not stem cells therefore can retain their lineage, thus reduce the risk for uncontrolled proliferation into various cell types and are autologous, thus eliminating the need for xenogenic transplantation. The first studies were performed in rabbits with cryoinjured myocardiums.[22,23] Transplantation of autologous skeletal myoblasts, have since shown a trend towards engraftment to host tissue and improved cardiac function capable of being taken to larger animals and towards a clinical perspective.[24-26] This engraftment is not coupled to the host tissue via the gap junction proteins, nor does it trans-differentiate to cardiac cells, but occupies the scar zone as multinucleated striated cells and improvement in function is only detectable in these pockets of striated myotubes directly proportional to the number of cells injected.[22, 27] This has led researchers to believe that the cardiotropic benefit attained by skeletal myoblast transplantation is due to paracrine factors released by these cells and the cardiac tissue, but these factors have been ill defined.[28, 29] Also, the engraftment is independent of the host cardiac cells and thus may lead to ventricular arrhythmias.

Bone marrow derived cells include whole bone marrow preparations,[30,31] hematopoietic bone marrow stem cells (HSC),[32, 33] mesenchymal stem cells (MSC),[34, 35] multipotent adult progenitor cells (MAPC),[36] and endogenous cardiac stem cells populations,[37] all of which have been shown to improve cardiac function in animal models and clinical perspectives. These cells can be modified to change their phenotype in vitro in order to differentiate into cells of the cardiac lineage before they are transplanted into the ischemic myocardium, or are transplanted into the myocardium and

are transdifferentiated *in vivo* or elicit paracrine factors that assist in the improvement in cardiac function due to the activation of other survival and angiogenic pathways. Embryonic stem cells and induced pluripotent stem cells have recently become more attractive options due to their totipotency, thus the ability to differentiate into cardiomyocytes.[14, 38, 39]

However, from a clinical perspective, there a many challenges involved, apart from the regulatory and ethical concerns. Embryonic stem cells are limited in the purification of specific lineages, concerns regarding the formation of teratomas, in vitro differentiation and in vivo engraftment into host tissues. Induced pluripotent stem cells can overcome the graft rejection and ethical concerns but the risk of teratoma formation still exists.

2.2.3 Cell Taught Gene Therapy

While there is clearly emerging evidence that future cell based therapies will ultimately yield clinical benefit, it is also becoming clear that, in the absence of embryonic or induced pluripotent stem cells, the benefits achieved may be in the absence of myocardial regeneration. Rather, the benefits of adult stem cell based therapies appear to be due to paracrine effects delivered following cellular homing and engraftment in the injured myocardium. If paracrine effects dominate the benefits of adult cell based therapies, then one could postulate that adult stem cell based therapies will evolve into a new wave of gene therapies.[40] This new wave of gene therapy will not be based on gene

product that we believe the normal myocardium should have; but rather will be based on gene targets that cell therapy would have taught us that benefit the myocardium in an injured state.

The primary genes of interest were the vascular endothelial growth factor (VEGF) gene family, as well as fibroblasts growth factor (FGF). These gene products were demonstrated in studies in vitro to induce endothelial and smooth muscle cell proliferation. In preclinical studies, in the absence of atherosclerosis, the administration of VEGF or FGF protein or gene transfer led to significant capillary and arteriolar blood vessel growth.[37,41, 42] While no clinical product has evolved from these studies to date, significant advances in know-how and knowledge in the field of myocardial gene therapy were achieved by providing a better understanding of vectors, doses, and backbones that help design it.

2.3 Stem Cell Therapy for Cardiac Failure

Using cell therapy as means for providing cardiac benefit was developed because having a viable tissue was better than a collagenous scar tissue in the myocardium. Initial studies were performed with skeletal myoblasts and when that led to engraftment led arrhythmias, researchers moved to more versatile forms of bone marrow derived pluripotent cells.[43] Stem cell therapy began with the hope of differentiating these cells, either *in vivo* or *in vitro* to replace the lost or damaged cardiac cells.

Early studies with hematopoietic cells showed great improvements in cardiac benefit by myogenesis following transplantation of ckit+ cells.[44] This study further led to clinical trials, but the earlier studies representing myocardial differentiation of hematopoietic cells have not been corroborated by subsequent studies.[15] Instead the improvement in function was attributed to increase in angiogenesis and arteriogenesis.[45,46] Moreover, unknown parameters such as timing of delivery, methods of purification and storage of a single cell population, selection of patient population and techniques for cell delivery have limited the clinical trials giving rise to heterogeneity within the trials themselves.[47]

Other cell populations, including mesenchymal stem cells, and multipotent adult progenitor cell, have been shown to improve cardiac function in animal models but most theories regarding the differentiation of these cells to cardiomyocytes have been limited and not unanimous. In fact, MSCs have been exploited as the more attractive option for cell delivery as they can be easily proliferated in vitro, they secrete a variety of growth hormones, such as IGF, HGF, VEGF etc,[48-50] elicit paracrine factors, *in vivo*, such as sfrp2, SDF-1, MCP-3 etc,[51-54] and thereby are able to provide repair in more than one aspect of tissue damage. Currently, the focus of research has shifted from myogenic differentiation to peripheral parameters that improve the environment around the infarct zone to provide for cardiac benefit.

2.3.1 Homing Factors

The first few steps required for efficient cardiac tissue repair with stem cell therapy is the need for targeting the cells to the area of injury and to engraft it there. Traditionally, homing occurs as a stress response, when certain factors are released by cells, following injury, as a signal to recruit either stem cells from the bone marrow and inflammatory cells in order to begin the repair process.

One such chemokine is SDF-1 which is shown to be elevated in an injured myocardium and recruits stem cells to the area providing cardiac benefit.[55] We, in our lab have also shown that MSCs infused intravenously home to the heart one day post MI but not when infused 14 days after MI. This is attributed to the fact that SDF-1 peaks one day post MI and drops by 7 days. Moreover, plasma elevation of SDF-1 induces hematopoietic stem cell and platelet migration to the area of injury.[56] Apart from adult tissue, stem cell homing has been shown to be critical in mice fetuses, where the elimination of either the homing factor (SDF-1) or its receptor, CXCR4, is fatal for development due to the lack of homing of the essential cells to the interstitial space to form blood vessels.[57, 58]

The homing of mesenchymal stem cells is a slightly more complicated process, as the molecular mechanisms that define these are not completely understood. Mesenchymal Stem Cells possess the CXCR4 receptors on its surface and therefore migrate towards the SDF-1 chemotactic gradient. However, the amount of CXCR4 receptors are limited and

this limits the amount of MSC migration leading to limited tissue benefit. Endothelial progenitor cells, precursors to blood vessels, respond to IL-8, released in injured tissues, and prevent apoptosis.[59,60] However, these cells are not capable of angiogenesis, probably due to reduced function in a hypoxic environment. In our lab, we have demonstrated the homing of MSCs as a response to Monocyte Chemoattractant Protein -3 (MCP-3).[52] LAD ligated rodents were infused with MSCs and Cardiac Fibroblasts to show that only MSCs migrated to the myocardium and cardiac fibroblasts did not. Using a DNA assay, monocyte chemoattractant protein was identified to be a myocardial homing factor for stem cells.

Transplanting cardiac fibroblasts over expressing MCP-3 in the myocardium we have been able to show an elevation in MSC homing to the heart immediately after MI, and late after MI. Reestablishing the homing factors can lead to reestablishing homing of stem cells. We also observed that the over expression of SDF-1 immediately after AMI, leads to the recruitment of cardiac stem cell like cells to the area of injury. Interestingly, although these cells are positive for cardiac myosin, they are not differentiated cardiac myocytes. These cells also possess CXCR4 on their cell surfaces thus determining their lineage to be cardiac stem cells. Also, optical mapping studies demonstrated that these cells are capable of de-polarizing in vivo, therefore may possess the ability to contract. The recruitment of cardiac stem cell like population into the infarct zone can alter electrical activity and may have a significant impact on the electrical functions of the myocardium.[61]

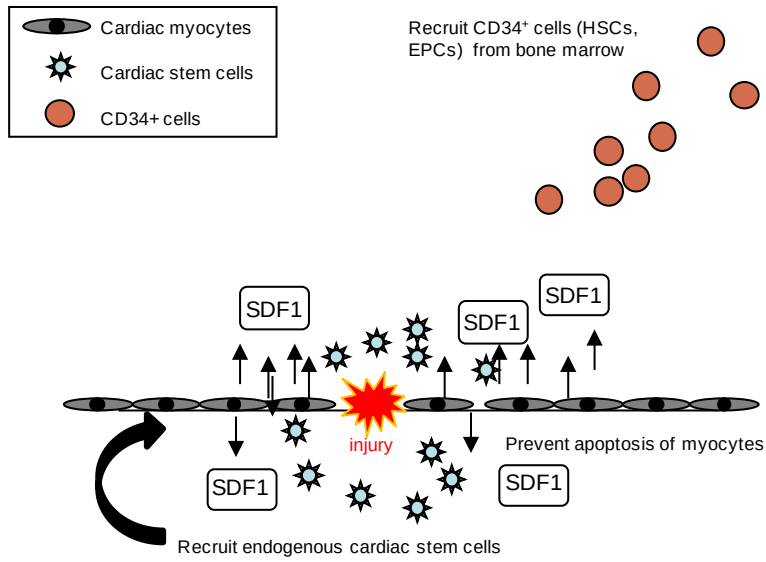

Figure 2-1: Role of SDF-1 in AMI as a homing factor for stem cells

2.3.2 Role of SDF-1 in Acute Myocardial Infarction

It has been established that $CD34^+$ cells home to the infarct zone, following Acute Myocardial Infarction (AMI). To understand the triggers signaling the targeting of these cells from the bone marrow to the heart, initial studies were performed to determine the levels of mobilizing cytokines in the serum plasma. The increase in the amount of CD34+ cells correlated to the increase in levels of G-CSF (Granulocyte colony stimulating factor) and an increase in SDF-1 (Stromal derived cell factor-1).[62]

To understand the role of G-CSF and SDF-1 in promoting homing in AMI, rodents were injected with G-CSF in the presence and absence of cells over expressing SDF-1, transplanted in the cardiac tissue. G-CSF was not sufficient to mobilize the bone marrow derived cells, establishing the role of SDF-1 as the homing agent.[55] Further studies

identifying the role of SDF-1 in mobilization of CD34+ cells was demonstrated with emphasis on the SDF-1 CXCR4 axis playing a pivotal role, in the homing of stem cells.[63] Stem cells, positive for the CD34 marker, in the bone marrow possess the receptor CXCR4. An increase in SDF-1, a ligand for CXCR4, in the plasma leads to the targeting of the CD34+ cells.

This homing is prevalent in the first 12 hours following injury and then drops significantly over a week. Furthermore, the levels of the stress cytokines are proportional to this homing effect, where levels of VEGF and SDF-1 increase following AMI after the first day, and continue to increase for 3 days following injury.[64] The levels then start dropping to normal levels by the end of a 7 day follow up.[55] The initial theory regarding the trans-differentiation of these early cardiac marker cells, following the homing to ischemic tissue was refuted in a study from our lab, to identify trophic factors to be the cause of the repair mechanism. Rodents with AMI were treated with infusions of mesenchymal stem cells over expressing SDF-1, and showed great improvements in cardiac function. This improvement was attributed to a decrease in apoptotic nuclei, a decrease in scar tissue formation and a significant improvement in vessel density in the infarct zone.[35]

Subsequent studies have followed regarding the use of SDF-1 without the concomitant use of cells, to over-express SDF-1 in infarcted regions to understand the improvement in cardiac functions thereafter. SDF-1 protein injections was the most straightforward of these and injecting SDF-1 directly into the center of an infarct

demonstrated improved cardiac benefit by increased neovascularization in infarct zones and reduction in scar sizes, but the effect was short lived and failed to provide clinically relevant results.[33, 65, 66] To prolong the effect of SDF-1, controlled release of the protein was then studied. SDF-1 protein encapsulated within nanofibers, when injected immediately after coronary ligation, has shown to provide improvement in cardiac function coupled with increase in vascular density.[67] A controlled release of SDF-1 provided by a PEGylated fibrin patch when placed in situ after coronary ligation in mice, showed a marked improvement in cardiac function following recruitment of CD34+ cells. The improvement was more prominent after 2 weeks and was sustained at 4 weeks.[68] SDF-1 promotes cell survival immediately after MI and also helps reverse ventricular remodeling and prevents heart failure.

2.3.3 Role of SDF-1 in CHF

As established earlier, our lab has also shown that MSCs infused intravenously home to the heart one day post MI but not when infused 14 days after MI.[69] This is attributed to the fact that SDF-1 peaks one day post MI and drops by 7 days. To determine if the homing reaction produced by SDF-1 could elicit a meaningful response late after injury, rodents were infarcted via LAD ligation, and were allowed to develop a chronic heart failure model for 2 months. In this time, the ventricular cavity had dilated, the scar tissue had developed and viable myocardium in the ischemic region had died due to apoptosis. 8 weeks after ligation, control fibroblasts, or those over-expressing SDF-1 were transplanted into the ischemic myocardium. Animals that received the SDF-1 expressing

cardiac fibroblasts, had a greater number of proliferating cells, including, CD117+ (hematopoietic stem cells), CD45+ (leukocytes), CD34+ (hematopoietic stem cells, endothelial progenitor cells) and vWF + (endothelial cells) cells in their heart tissues. Apart from acting as a homing factor for these cells, the presence of the angioblasts and paracrine factors released by the recruited cells, led to a significant improvement in cardiac function, as determined by their fractional shortening.[69]

2.3.4 Molecular Mechanisms Involved in SDF-1 CXCR4 axis

CXCR4 is present in CD34+ cells, such as hematopoietic stem cells, endothelial progenitor cells, and cardiac stem cells.[64,70-72] Following myocardial infarction, the mRNA expressions of SDF-1 has been shown to be elevated in the left ventricular anterior and posterior walls in animal studies.[55, 69] Cells with the CXCR4 receptor, stem cells, now migrate towards a SDF-1 chemotactic gradient and thus home towards the ischemic myocardium. SDF-1 present in systemic circulation is sufficient to mediate this recruitment.[61,70] When SDF-1 binds to its receptor CXCR4 it leads to the activation of other paracrine factors such as P selectin ligand, E selectin ligand,[73] Very late antigen VLA4, VLA5 etc, on the surface of hematopoietic stem cells.[74] These ligands bind to the receptors P selectin, E selectin, Intracellular Adhesion Molecule (ICAM) on endothelial cells and allow them to roll over the endothelial cell layer allowing for transmigration along the cell layer thus recruiting cells to the area of injury.[74-76]

The interaction of SDF-1 ligand with the G-protein coupled receptor, CXCR4 triggers intracellular pathways involving Akt phosphorylation, Ca2+ influx, mitogen-activated protein kinases (MAPKs) phosphorylation, activation of PI3 Kinases, and JAK STAT pathway activation.[77] Following SDF-1 up regulation in the infarct zone, phosphorylation of Akt and up regulation of VEGF are observed which leads to cell preservation.[53, 78] Cell survival can also be attributed to downstream signaling of Akt involving BAD, NF-kB, and NO from e NOS.[79] Also, SDF1 CXCR4 coupling activate both PI-PLC and PI3K, which activates PKC.[80] PKC activation induces Pyk2 and ERK activation, leading to adhesion and chemotaxis as well as gene transcription via MAPK activation. MAPKs are a family of protein kinases that consist of ERKs, p38, MAPK and JNK which mediate apoptosis. PKC also mediates the activation of NF-kB which in turn mediates MMP-9 production allowing for matrix remodeling and reducing the scar tissue which in turn allows for reverse ventricular remodeling.[81, 82]

2.4 Overview on Gene Therapy

Gene therapy involves the manipulation of nucleotide sequences involving the recognition, selection and integration of the desired genes in a chromosome. Since early 1990's up to now, more than 900 clinical trials involving gene therapy in various disease conditions, such as cancer, monogeneic diseases, vascular diseases, immunogenic diseases, etc have been carried out.[83, 84] The most evident application of gene therapy is to replace a defective/abnormal gene by its normal counterpart in order to benefit the organism, by supporting normal functioning. This replacement is preferred to be a stable,

safe and permanent one, in order to constitutively provide normalcy in the organ. Another application of gene therapy involves suppressing an unwanted reaction by the organ, such as in cancerous tissue, in order to prevent the growth of tumors. Genes can also be used as a drug or a prodrug, which encodes for an enzyme or a protein that can act as a cytotoxic drug to eliminate the tumor and its environment. This application of genes as prodrugs can also be used to promote the growth of certain growth factors or enzymes that may help provide relief to repair injured tissues or organs.

2.4.1 Gene Therapy in Heart Failure

Significant pioneering work was done in the 1990's in the field of cardiovascular gene therapy. Gene therapy was involved not only in therapeutic purposes, but played a significant role in diagnosis of key participants in the heart failure process. Multiple studies regarding the apoptosis of cardiac myocytes following ischemia have been reported, and the role of TNF-α in cardiac dilation, procaspase-8 in dilated cardiomyopathy, and gp180 molecules in cardiac apoptosis following pressure overload have been elucidated.[10, 85, 86]

As therapeutic options in cardiac applications, gene therapy studies are responsible for preventing apoptosis and promoting survival signaling. The members of the PI-3 kinase pathway also include Akt phosphorylation that leads to survival and growth of myocytes, as seen in the prenatal heart.[87, 88] Insulin Like Growth Factor-1 is another pro

survival protein that prevents naturally occurring apoptosis.[89] SDF-1 has been shown to prevent apoptosis, and induce the growth of vessels in ischemic zones. [66]

However, in a heart failure condition the focus is on inducing angiogenesis in an attempt to treat "no option" patients who are presented with diffuse coronary artery disease and chronic ischemia. The genes of interest could be characterized as those that investigators believed would benefit the myocardium, not necessarily those that were inherently needed by the heart. These genes would provide peripheral support to the ischemic tissue, by enriching the environment thus promoting cardiac benefit. The primary genes of interest are those of the vascular endothelial growth factor (VEGF) gene family, as well as fibroblasts growth factor (FGF).[90, 91] In a protein form, these factors were not sufficient to elicit any clinically meaningful results.[92,93] Growth factors have short half lives, and thus it was hypothesized that a gene therapy approach would allow for prolonged sustenance and effect. These gene products were demonstrated in studies in vitro to induce endothelial and smooth muscle cell proliferation.[94-96] In preclinical studies, in the absence of atherosclerosis, the administration of VEGF or FGF gene transfer led to significant capillary and arteriolar blood vessel growth.[97, 98] However, none of these gene therapy products have been approved for clinical use in cardiovascular patients yet.

2.4.2 Advantages and Disadvantages of Gene Therapy

Initial studies regarding transplantation of skeletal myoblasts in ischemic regions in the heart have not been able to provide enough functional benefit in the heart. Moreover,

this effect was lost in a 4 month follow up.[27] More concerning, is the fact that this cell-therapy treatment may lead ventricular arrhythmias.[25] Gene therapy is a more straight forward approach where the ultimate goal is either to over-express a gene such as to achieve therapeutic levels of cardioprotective protein, or the knocking-down of genes that may lead to cardiotoxicity. However, the first clinical study with gene therapy led to the death of a patient, due to immune toxicity. Gene therapy has to battle a few factors that lead to its inefficacy in clinical trials.[84, 99]

Transient Expression: It is undesirable to let genes integrate into the host genome such as to provide this constitutive effect for future generations. However, it is necessary to have a transient supply of the therapeutic DNA for a clinically relevant period of time. The cells that inherit the DNA must also be able to proliferate, survive and stably express this DNA for the same period of time. This will prevent the need for patients to undergo multiple rounds of the therapy in order to sustain the therapeutic level of benefit. Furthermore, the level of proteins translated directly relate to the amount of DNA injected into the patient. However, the corollary may also pose a risk, where unregulated gene expression leading to unchecked protein levels may have detrimental effects.

Immunotoxicity*:* For an effective, stable DNA expression, these plasmids are packaged into viral vectors and then introduced into the patient. The main advantage of viral vectors is that it yields very high transfection efficiencies. However, viral vectors pose numerous safety and efficacy issues, ranging from toxicity and immune and inflammatory responses, to gene control and targeting issues. The presence of such

foreign bodies can lead to an enhanced immune reaction by the body, hoping to destroy this foreign object, thus reducing the effectiveness of the enhanced gene. This can further lead to the immune system attacking healthy tissues and can pose a high risk to the organ. Furthermore, the immune system's enhanced response to invaders it has encountered before makes it difficult for gene therapy to be repeated in patients.

Cardiovascular Applications: Unlike single gene mutation disorders, where the defective gene can be replaced by the normal gene sequence, cardiovascular diseases come with multiple symptoms, from loss of contractility, loss of blood vessels, loss of growth factors, increased inflammatory reactions, deposition of collagenous scar etc. Treating such conditions with gene therapy will only be possible with treating it early and before the tissues are beyond repair. In chronic heart failure, although there may be methods of providing cardiac benefit and an improved life style for the patient, it is difficult to bring the heart back to a normal healthy tissue.

2.4.3 Non Viral verses Viral Constructs

Delivering the genetic material into a host cell involves the use of vectors, which could either be viral or non viral. Direct injection of naked DNA is widely employed in gene transfer studies as it is relatively safe, is cost effective and can be produced in large quantities in bacteria and can also be manipulated by standard recombinant techniques.[100] Moreover, it possesses low immunological toxicity, is water soluble and heat stable. In earlier cardiovascular diseases, this method was widely used for the same reasons. On the

other hand, naked DNA has low transfection efficiencies, can be degraded rapidly and generally needs targeting or condensing agents to penetrate the cell wall. [101]

It has been seen in the past that transfection decreases with increase in animal size.[102] Expression levels are slightly lower in rats than mice and significantly decrease with rabbits and pigs which make it unsuitable for large animal studies.[102,103] Greater expression of the gene can be achieved by complexing the DNA with compounds such as cationic polymers,[104] lipopolymers,[105] PEI,[106] and liposomes.[107] Such compounds not only protect the DNA from degradation but also condense them into smaller sizes so that it can mediate uptake by the cell. Despite alternative approaches, non viral delivery methods yield transient and non site specific expressions, which make it non feasible for conditions that require long lasting expressions such as cardiomyopathies.

The major advantage of viral vectors is that its yields very high transfection efficiencies. The difference between viral transduction efficiencies and non viral ones are due to the difference in uptake mechanisms between the two. In contrast to non viral vectors, which may get degraded in the presence of lysosomes, viral vectors are readily bound to cell surface receptors, which prevent native degradation of the virus.[108]

	Advantages	Disadvantages
Naked plasmid	Safe Cost effective Bulk processing available Low toxicity Water soluble Heat stable	Low transfection efficiency Transient expression
Adenovirus	High transfection efficiency Can be taken up by all cell types Easy to produce Tropism for multiple cell types	Adverse immunological responses Transient expression patterns High toxicity
Adeno associated virus	Non pathogenic vectors Long term expression patterns High transduction efficiency Can be taken up by all cell types Low immune responses	Limited transgene capacities Difficult to produce in large quantities
Lentivirus	Long term expression patterns Can integrate into all cell types Can be driven by various promoters	Safety issues Difficult to produce in large quantities Low transduction efficiency

Table 2-1: Comparison between viral and plasmid vectors for gene delivery

2.4.4 Naked Plasmids

Most commonly, non viral delivery techniques involve the use of naked plasmid alone, or naked DNA either encapsulated within polymeric delivery systems or liposomes in order to protect DNA from degradation and to allow for a consistent expression over time.[109, 110] The use of non viral vectors can circumvent most issues associated with viral vectors, mainly safety associated with immunotoxicity. On the other hand, unencapsulated DNA can be modified, with the help of transcriptional and translational

enhancers, in order to achieve similar benefits. Other aspects that affect the transfections involved with naked plasmid delivery are based on technical details such as the number of injections, the time of delivery, the amount of DNA used, site of injection and so forth as described in the table below.[96, 102, 107]

Dose	Needle	Area	Number of injections	Time of injection	Treatment
20 μg / 100 μl of saline	Curved 30 gauge	Infarct border zone	4 to 5	1 week after infarct	Naked with bFGF and PGDF
15 μg / 200 μl of sucrose	30 gauge	Infarcted area	1	2 weeks after infarct	HVJ liposome method
500 μg / 150 μl of saline	24 gauge	Left anterior border zone	1	24-50 days after infarct	phVEGF
60 μg / 100 μl of saline	30 gauge	border zone	1	1 week after infarct	phVEGF and adVEGF
50 μg / 100 μl of saline	30 gauge	Left anterior free wall	1	At the time of infarct	HIF1 and VP16; phVEGF

Table 2-2: Various parameters involved in gene delivery

2.4.5 Translational Enhancers

Enhancers are a short sequence of nucleotides either present upstream or downstream to the transcription activator site, or the start codon and can boost the transcription or translation of the RNA to protein. A Kozak sequence is a short sequence present upstream of the transcription activation site and generally contains the full consensus

sequence, GCC GCC A/T CC ATG G, three bases before the start codon. The Kozak sequence slows the rate of ribosomal scanning and thereby improves the chance of translation by ensuring that the start codon is recognized.[111] Similarly, the 5' untranslated region (UTR) can affect the translation of mRNA, by either inhibiting or enhancing translation. If the untranslated region has more number of AU rich regions and is poorly structured, it allows for easy ribosomal scanning and thus helps the ribosomes to recognize the translation initiation codon.[112] The UTR of the human t cell leukemia virus (HTLV) conforms to this poor structure and thus enhances translation when present upstream to the activation site.[113]

2.4.6 Transfection Agents

Transfection agents prevent the degradation of naked plasmid by encapsulating them and then releasing them into the cell. These encapsulating agents can either be polymeric or liposomes. These are either made of polymers, proteins or lipids and coat the DNA such that they allow for timed release and also protect the DNA from being damaged. Moreover, they condense the DNA to smaller sizes to mediate better uptake by the cell.

2.5 Encapsulation and Systemic Gene Delivery

2.5.1 Poly Lactide co Glycolide nanoparticles

Research involving the delivery of DNA or plasmids as therapeutic agents has grown rapidly. The need to safely and efficiently deliver these genes to the tissue of interest has resulted in a rapid growth of research in the use of polymeric nanoparticles as delivery vehicles for these transiently expressing, easily degradable therapeutic agents. Although, recent advances have led to almost 100 clinical trials with nanoparticles as carriers for drugs, there is no drug loaded within nanoparticles which has been approved for human use yet. This is partly due to the fact that the targeting of nanoparticles to cells has been a challenge.[114]

DNA plasmids have a polynucleotide structure and thus are negatively charged which poses a challenge for traversing the tissue layers, and they are easily degraded in the system. In order to overcome this, genes need to be properly condensed to a size that can be taken up by cells. Once they are taken up by cells, the plasmid may be lost due to endosomal sequestration of the nanoparticle, loss of nanoparticle by exocytosis, or lysosomal degradation of the nanoparticle in the cytoplasm. Therefore, an efficient delivery of plasmid DNA to the cell nucleus requires the condensation of the plasmid to allow encapsulation within the nanoparticle, stability during formulation and *in vivo*, ability to target the tissue or cells of choice by either a surface ligand or by possessing a specific promoter element in the plasmid, or both, capability of release from the

nanoparticle following endocytosis into the cell, and ability to be taken up by the nucleus in its active form.

Polymeric nanoparticles are being widely used as delivery agents for plasmids because of their stability,[115] ability to bind targeting ligands to the surface,[116] regulated control over the release kinetics of the encapsulated plasmid in the cytoplasm, ability to be degraded *in vivo*,[117-119] following the release of the plasmid, and are approved for use in human trials by the FDA.[120]

Generally, nanoparticles encapsulating plasmids are formulated using a variety of techniques such as; double emulsion solvent evaporation technique,[121] salting out,[122] nano precipitation,[123] cross flow filtration,[124] or emulsion diffusion technique.[125] The most common of these techniques is the double emulsion method where the hydrophilic plasmid is dissolved in an aqueous solution with sucrose or albumin as stabilizing agents and the polymer is dissolved in an organic phase. A primary, water in oil, emulsion is formulated between the aqueous phase and the organic solvent. This is then added drop wise to another aqueous phase with a polymeric surface activator, poly vinyl alcohol (PVA), to formulate a secondary, oil in water, emulsion.[126] This is then allowed to evaporate slowly to remove all the organic solvents, and form hydrophobic nanoparticles encapsulating the hydrophilic plasmid, with surface activators that alter the hydrophobicity of this complex.[127]

The surface activation is a key step in this process, since the surface comes in contact with cell membranes, and thus is the determining factor for the internalization of the nanoparticle in the cell. PLGA nanoparticles enter into the cell by endocytosis partially by pinocytosis and partially by receptor mediated endocytosis and this process is concentration and time dependent.[127] Other factors, such as size of the nanoparticle, affect cell internalization, with smaller size of the nanoparticle facilitating easier uptake than larger ones.[119] Nanoparticles escape the endo lysosomes and enter into the cytoplasm immediately after, within the first 10 minutes. However, some studies have demonstrated that a significant amount of these nanoparticles escape the cells via exocytosis and only about 15% of the nanoparticles remain in the cytoplasm.[127]

Some factors that affect the release of nanoparticles in the cytoplasm are dependent on the surface characteristics, such as the zeta potential, hydrophilicity and surface charge, all governed by the surface activator, poly vinyl alcohol (PVA). An excess of PVA on the surface, if not removed completely during formulation alters a process called surface charge reversal. In an acidic lysosome, the nanoparticles change their surface charge from anionic to cationic, destabilize the vesicle membrane, and get released from them into the cytoplasm. An excess PVA prevents this occurrence and the nanoparticles do not release from the lysosomes and exit the cells via exocytosis.[120]

This portion of released nanoparticles degrades slowly and releases the encapsulated plasmid over a controlled period of time. The release of plasmid in the cytoplasm can be altered by varying formulation parameters, such as polymer to plasmid ratio or molecular

weight and composition of the polymer used. Higher molecular weight polymers allow for more plasmid loading within the nanoparticles and thus release more plasmid per nanoparticle, facilitating greater gene transfections. Other factors, such as higher viscosity, better emulsifying properties also allow for greater loading and smaller nanoparticle sizes, thus greater uptake and release of more DNA into the cells. The hydrophobicity of polymers affects loading and release, with less hydrophobic particles providing better release. Surface activators also help in altering the hydrophobicity.[121, 128]

Formulations of the polymer complex with the plasmid, involving the type of polymer, the method of formulation, surface activators, size of the resulting nanoparticles and zeta potentials (surface charge of the particles) all have an effect on encapsulation and delivery of the plasmid and can be modulated to provide the required results.

2.5.2 Targeting Factors

Targeting ligands aid nanocarriers to effectively direct them to a specific cell or tissue type to maximize efficacy of the encapsulated plasmid or drug in the specific tissue.[129] Initial targeting studies were used for tumors, in order to prevent angiogenesis, and thus prevent the growth of tumor cells, but leave the healthy tissue around it intact.[130] These ligands exclusively bind to specific receptors on the cell surface with high affinity. Some of the common ligands that have been studied are peptides, antibodies, sugars, vitamins and certain chemical compounds. Once these ligands bind to the cell surface, the

uptake occurs by a receptor mediated endocytosis, via clathrin dependent or independent pathway.[127, 131]

To formulate a ligand tethered polymer/DNA complex, the ligand molecule is either linked directly or via a linker polymer to covalently bind to the surface of the polymer complex.

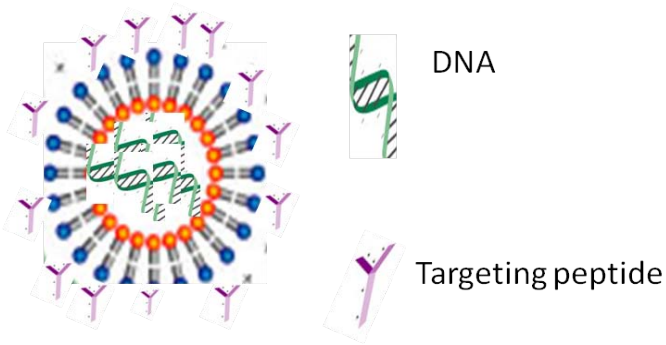

Figure 2-2 : Schematic of the encapsulation of DNA within PLGA nanoparticles

There is a lot of research involving the receptors on cell surface that target these homing ligands. A great body of research is dedicated to looking at integrin based members of cell adhesion receptors. Proteins of the extra cellular matrix such as fibronectin bind to a three amino acid sequence peptide commonly known as RGD, for Arg-Gly-Asp[132,133] on specific integrins over expressed in angiogenic endothelial cells of tumor tissues.[134,135] This led researchers to tap this targeting moiety to deliver siRNAs and other inhibitor drugs to these tissues to hamper its growth and block blood flow to this region, resulting in targeted tumor tissue damage.[136]

Other peptide sequences such as the Luteinizing Hormone - Releasing Hormone (LHRH) is also a tumor targeting ligand as its receptor is commonly found in various tumor (breast, ovarian) tissues.[137] Certain iron binding ligands, such as transferrin and lactoferrin, are common receptor binding proteins specially used for lung targeting and traversing the blood brain barrier in the brain,[138,139] although in gene transfections studies, lactoferrin mediated delivery demonstrated a greater transfections efficiency as compared to transferrin mediated delivery.[140] A similar ligand protein is epidermal growth factor (EGF) that binds to the EGF receptor (EGF-R).[141,142] Another similar ligand protein is the Receptor associated protein (RAP) that binds to low density lipopolysaccharides (LDL) on the cell surface.[143] Several sugars, such as galactose, mannose, and folates bind to specific moieties on the cell surfaces such as asialoglycoprotein receptors on hepatocytes,[144] mannose receptors on macrophages, and dendritic cells,[145] and folate receptors on tumor cells.[146]

Other technologies involve combinatorial libraries, such as RNA display, yeast display or bacterial display to identify certain small peptide molecules that target specific cell types.[147] A novel yet powerful strategy that is being used nowadays is called *in vivo* phage panning using a phage display library.[148] Phages are screened by allowing them to bind to specific cell receptors in the tissue of interest. After several rounds of screening followed by purification and amplification of the primary candidates, a robust and highly specific ligand-receptor binding target is identified.

2.6 Phage Panning

Bacteriophages or phages are viruses to bacteria that can replicate their DNA in a bacterial cell. Generally phages have a single stranded DNA in them, and can infect E coli. A phage clone has a foreign gene introduced into a phagemid vector, such that it possesses the phage and a replication plasmid to enhance transformations. A phage display library has multiple copies of various clones, with sequences for a number of known and unknown peptides attached to the fusion coat protein plasmid in the M13 genome of phagemid vectors.[149] The peptides are comprised of 7 amino acids, formed from all possible permutations from the genome sequence of the organism. When these phage particles enter into a bacterial cell, the genome is now released from inside the phage vector and is displayed on the surface, while the coat protein remains attached to the phage vector. On identifying a receptor to these peptides, the ligand binds to the receptor tagging the phage with it. Phage panning studies with specific epitopes (receptor) or the tissue with the epitope employs this specificity to identify the phage that binds to it, which is then isolated, amplified, and sequenced to reveal the peptide sequence that binds to the epitope of interest.

The principle behind phage panning is to identify the clone that binds to an epitope with the affinity and selectivity that other clones do not bind to or do so with poor affinity. To achieve this, multiple rounds (or pans) of binding the phage to the epitope, identifying the bound phage, eluting the unbound phage, amplifying it and sequencing the bound phage are carried out. For *in vivo* identification of ligands specific to receptors, animals

are infused with multiple copies of phages expressing a library. This is allowed to circulate for 2 hours, to ascertain the removal of unbound phage from the tissues (organs and tumors). Residual phages still bound to the target organs are harvested. This residual phage is purified, amplified and infused into the animal for a second round. After multiple rounds, it will now be possible that very few phages express specificity to the tissue.[150]

Several studies with this principle has led to specific ligands for traversing the intestinal mucosa and targeting the goblet cells,[151] traversing layers of the skin to deliver drugs intradermally,[152] targeting pancreatic cells,[153] tumor cells,[154] lymph channels,[155] and vascular endothelium.[156]

In vitro affinity binding to identify targets for these antigens have been tapped for tumor targeting ligand selections. Certain antigens, specific for tumor cells such as urokinase plasminogen activator (uPA), epidermal growth factor receptor (EGF-R), Thomsen Friedenreich tumor associated antigen etc, are plated on a dish and phages are allowed to bind to them. Unbound phage is eluted and the bound phage is amplified and sequenced, after multiple rounds, to identify targets to these receptors.[157]

Although phage display seems to be able to provide crucial information regarding targeting ligands which can then be synthesized chemically, and tagged with photo or radio labels to help imaging, or be tagged to liposomes and polymeric gene carriers to deliver encapsulated drugs to organs, it has some serious drawbacks. First of all, in vivo

screening can be done only in animal models which limit translating this information to humans, if the targets that bind these 7-mers are not identified. In such scenarios, it may or may not be useful to use these ligands to target or image tissues in humans. This extrapolation might also lead to secondary organ damage.[158] In recent times, human panning for identifying targeting ligands are being performed but this is limited in the number of subjects that can be used for this study, as organs need to be excised following phage injections.[159] However *ex vivo* screenings on intact organs can be used to determine targeting peptides in human organs.[160]

Other smaller drawbacks are based on the size of the phage particles, thus the vascular space and mostly the endothelial layer are targeted for receptors. Secondly, the affinity to certain receptors may be due to the large copies of libraries infused into the organ rather than a specific affinity of the peptide in itself, which is revealed by low affinities seen with mono copies. Thus there is a great deal of work to be done in optimizing this system towards ideal screening platforms.[161]

2.7 Gene Profiles in Tissue Regeneration

Following the human genome project, that has identified the sequences to all genes in the human body, researchers began to study how these genes affect each other. Gene expression profiling is a tool used to study the expression of multiple, or in some cases, all genes at the same time. Following treatment, a gene expression profile would help understand how all genes respond to the therapy.[162,163] The ones that are closely

associated with the damaged organ, will have significant changes in expression as a response to therapy, and genes that are not affected will have no change in expression as a response to the therapy. Monitoring the changes in gene expression for multiple genes at one time will provide a comprehensive knowledge of many genes that may be associated with the disease state. During the early part of this century, following the human genome project, studying the effect of all the genes in response to therapy would require hours of labor but today, the same study, identifying the same data can be done in a few hours due to advances in chip technology and fluorescence detection. Several studies have identified novel pathways and peptides associated with cardiac tissue damage using genome wide studies. The role of chronic Akt mediated hypertrophy and heart failure was established.[164] Novel paracrine factors associated with tissue repair, following Akt- modified stem cell transplantation has been attributed to a secreted frizzled related protein 2 (sfrp 2) that mediates myocardial survival and tissue repair.[54]

2.7.1 Whole Genome Analysis

A gene chip is a matrix of sequence specific oligonucleotides, arranged in a specific order, and bound to a solid surface (quartz) at the bottom. This system is known as a microarray chip. One company that has revolutionized the microarray chip with providing comprehensive data and easy experimentation is Affymetrix.[165] The affymetrix chip has about 16 to 20 probe pairs for each gene. Each probe pair consists of a perfect match to the gene of interest, and a mismatch to the same gene. The difference in

intensity between this perfect match and mismatch is what will be provided at the end of the analysis.

The degree of discrimination, R, which determines the ratio of the difference between the perfect and mismatch to the sum of the two will be calculated. R= PM-MM /PM+MM. An increase in gene expression would be determined by an R value of 1 or close to 1.

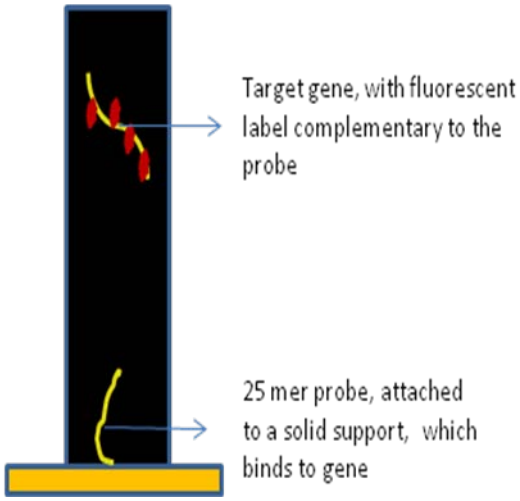

Figure 2-3 : Schematic of a microarray chip

According to the Wilcoxon signed rank test, two parameters are analyzed a) change in gene expression (up or down regulation) and b) the p value. If the p value is greater than 0.05, the gene will be excluded from the list. The fold changes between the control and sample genes will be measured and based on these results, a new set of genes, with highest fold changes, will be identified. The chip is normalized using the Robust Multi Averaging (RMA) software.[166,167] This software allows users to normalize the

background and also negate misidentified mismatch data and also determine fold changes between the original gene and the up regulated or down regulated gene.

2.7.2 Pathway Studies

Pathway analysis tools help in searching and exploring the relationships between genes that are associated in any given pathological condition. The relationships then help researchers understand the functionality associated with these genes. These tools are structured in order to define the location of these genes in the cellular compartments. Moreover they define the interactions between genes to endogenous chemicals, drug targets and other genes within their network. This then provides a mechanistic understanding of all genes and their targets, thus illustrating the pathways that are involved in the given process. These networks and pathways are mostly pre defined and provide comprehensive information to the researcher. The Ingenuity Pathway Analysis software is a tool to understand the various pathways involved in the genes that have changed after the treatment process.[163] It can provide information on the signaling pathway involved in the whole process. Other software, such as Spotfire, helps cluster the genes and thus form groups which helps in gene profiling.

CHAPTER III

GENERAL METHODS

3.1 Cell Culture

3.1.1 Harvesting Rat Mesenchymal Stem Cells

Rat bone marrow was isolated by flushing rat femurs and tibias with 0.6 ml DMEM repeatedly until all of it is extracted. Clumps of bone marrow were gently minced using a 20 gauge needle and a 10 ml syringe. Cells were then be removed by Percoll density gradient. This bone marrow was then washed with PBS three times to remove all debris and then plated in a dish with MSC media, comprising 10% FBS and 1% antibiotic in low glucose DMEM, and incubated at 37ºC for three days.

The mesenchymal stem cells adhere to the plate leaving the endothelial cells in suspension. The floating endothelial cells were removed and the media was changed in order to obtain a pure population of MSC cells. After four passages, this culture was then sorted negatively for CD45 and CD34, by magnetic cell sorting to remove endothelial cell types and in order to obtain a double purified population of MSCs.

3.1.2 Isolation of Cardiac Fibroblasts

The left ventricles of 3 to 5 rats were pooled together, minced and placed in 100 U/ml of collagenase XI and trypsin at 37 ºC for 10 minutes in a shaking incubator. The cell suspension was filtered out using gauze filtration and minced tissue was collected. The cell suspension was centrifuged at 2000 rpm for 10 minutes to sediment the cells. The cells were seeded in Ham's modified DME medium supplemented with 10 % FBS and 1% antibiotic containing Penicillin and Streptomycin. Non adherent cells were removed after 2 hours of incubation and the adherent cells were washed twice with phosphate buffered solution (PBS). The resulting adherent fibroblasts were cultured in Ham's modified DMEM medium supplemented with 10% FBS and 1% antibiotic containing Penicillin and Streptomycin on T75 flasks and incubated in 37ºC and 5% CO2.

3.1.3 Stem Cell (Mesenchymal Stem Cell) culture

Harvested mesenchymal stem cells were cultured on tissue culture plates. Cells were added to media comprising Dulbecco's minimum essential medium supplemented with

10% fetal bovine serum and 1% antibiotic of penicillin and streptomycin. Cells were allowed to adhere to the bottom of the plate and proliferate in a 5% CO_2 and 37° C. Media was changed every 2 days. When the plate was confluent, cells were detached from the bottom of the plate by washing twice with Phosphate buffered solution, and then incubated for 5' at 37°C with trypsin EDTA. Cells were pipetted to break down clumps mechanically and then re-plated at a concentration of 1 million cells per plate in the specific medium.

3.1.4 Cardiac Fibroblasts culture

Cardiac fibroblasts were cultured on tissue culture plates in a similar fashion as described for mesenchymal stem cells but with a specific cardiac fibroblasts media comprising equal parts of Dulbecco's minimum essential medium and F12 medium supplemented with 10% fetal bovine serum, 1% antibiotic solution with penicillin and streptomycin, and 1% L-glutamine.

3.1.5 Cell Freezing

Cells were detached from the tissue culture plate using Trypsin-EDTA. A pellet of 1 million cells was collected by centrifuging the cell solution (Cells in Trypsin) at 2000 rpm for 5 minutes. Each cell pellet was dissolved in 1 ml of DMSO (dimethyl sulfoxide) and Fetal Bovine Serum at a ratio of 6:4 (600 µl of DMSO and 400µl of FBS). These

were then transferred to a Nunc cryovial and slowly frozen at -80°C for 1 week and then in liquid nitrogen for long term storage.

3.2 Plasmid Constructions

3.2.1 pCMV

The pCMV Luc plasmid was generated by digesting the Luciferase gene from a pGL3 vector (Promega), using the following primers: Forward: 5'- GAATTCGTCG ACTATGGAAGACGCCAAAAACATAAAGAAAGGC-3'; Reverse: 5'-TCTAGAAAG CTTTTACACGGCGATCTTTCCGCCCT TC-3', and subsequently ligating it onto a pcDNA3.1 vector (Invitrogen, Carlsbad, CA). The Forward Primer has the restriction enzymes EcoRI & SalI; the Reverse Primer has HinDIII and XbaI. The resulting PCR product was digested with EcoRI and XbaI, gel-purified and ligated into an EcoRI-XbaI digested pcDNA3.1+ (Invitrogen) backbone.

3.2.2 pCMVe

The pCMVe Luc vector was a kind gift from Copernicus. This plasmid was generated by ligating a Luc gene onto a pcDNA3.1 vector with a Kozak sequence and an RU5 sequence at the 5' end of the plasmid, followed by a polyA tail.

3.2.3 pMHC

The luciferase gene from pCMV vector was digested and ligated into a pBSK.αMHC vector (a kind gift from Jeffery Robbins Lab at the University of Cincinnati Medical Center, Children's Hospital Medical Center) to generate the pMHC Luc vector. The MHC promoter is a mouse alpha myosin heavy chain promoter in pBluescript SK (+) vector (Stratagene, Agilent Technologies, La Jolla, CA) with a 23bp linker region and a Human Growth Hormone Poly A tail (hGH).

3.2.4 pMHCe

This plasmid was generated by ligating a Luc gene onto an αMHC vector with a Kozak sequence and an RU5 sequence at the 5' end of the plasmid, followed by a polyA tail.

The Luc gene was sub cloned out of the vector and the SDF-1 cDNA was inserted to generate the pCMV SDF-1, pCMVe SDF-1 and the pMHC SDF-1 vectors respectively. For the SDF-1 plasmids, the hSDF-1 gene was cloned from the mRNA of human foreskin fibroblasts using the primers, Forward: 5'- GCTAGCGTCGACATGAACGC CAAGGTCGTGGTCGTGCTGGTC-3'; Reverse: 5'-AAGCTTTTACTTGTTTAAGGC TTTCTCCAGGTAC TCCTGAAT-3'.

3.2.5 Plasmid Amplification and Validation

The DNA was amplified using 250mL of LB Broth (Ampicillin) resistance and 50uL of the frozen bacteria plasmid stock. It was cultured overnight in a shaking incubator at 37^{o}C at 225rpm. The DNA was isolated from the bacterial prep using the PureLink HiPure Plasmid Filter Maxiprep Kit (Invitrogen, Carlsbad, CA) as per the manufacturer's instructions. The DNA was then measured at 260/280nm for concentration using a Nanodrop 3000 fluorospectrometer (Thermo Fischer Scientific, Waltham, MA).

The CMV driven Luc plasmids, pCMV-Luc and pCMVe Luc were transfected onto 293FT cells and the αMHC driven Luc plasmids, pMHC Luc were transfected onto H9C2 cardiomyoblasts at 50% confluence at 300,000 cells per well in a 6 well plate using the FUGENE Transfection kit (Roche Basel, Switzerland) as per the manufacturer's instructions. The cells were exposed to luciferin at 10µg per ml of PBS per well and the chemiluminescence emitted was quantified using a cooled couple device camera from the Xenogen Imaging Systems.

3.3 Animal Handling

All animals were maintained in the AAALAC approved rodent facility of the Cleveland Clinic Foundation that is staffed by a full time veterinarian and trained technicians. The Animal Research Committee of the Cleveland Clinic Foundation reviews and approves all protocols. All animals were maintained under sodium

pentobarbital anesthesia by i.p. injection during the surgical procedures. Once surgery is complete, bupivacaine (0.5%), a local anesthetic was injected along the sternal wound which provided analgesia for ~18 hours. The animals were treated with Buprenorphine after the procedure at a concentration of 0.3 mg/kg up to 3 days after surgery. For euthanizations, the animals were treated with an overdose of sodium pentobarbital at the time of sacrifice. This mode of euthanasia is consistent with the recommendations of the Panel on Euthanasia of the AVMA. We routinely use Buprenorphine as an analgesic in our protocols.

All animal experiments were approved by the Institutional Animal Care and Use Committee and we followed the guidelines provided by them. All animals were 8 week old, weighing 200-225 grams, Lewis rats (Jackson Laboratories Bar Harbor, ME) for the chronic heart failure study.

3.3.1 LAD Ligations

Briefly, LAD ligation was performed in rats anesthetized with sodium pentobarbital, 50 mg/kg. Animals were intubated and ventilated with room air at 100 breaths per minute using a rodent ventilator (Harvard Apparatus Holliston MA). The chest was sterilized with ethanol, and a sternotomy was performed. The left atrium was retracted and the proximal LAD was identified visually. The proximal LAD was ligated using 6-0 prolene. We were able to verify ligation of the LAD by blanching and dysfunction of the anterior wall. The sternum and then skin was closed with 4-0 prolene with interrupted

sutures. Any residual pneumothrorax was reduced using negative pressure generated by a 20G needle placed in the closed chest, attached to a 10 ml syringe. The rat was then weaned from the ventilator over the next 10-15 minutes.

3.4 Tissue Fixation and Staining

3.4.1 Harvesting Rodent Organs

At the time of necropsy, the animals were perfused with saline to remove all residual blood from their circulation and histochoice to fix the tissues immediately. The hearts were harvested and again fixed in histochoice for 7 days.

3.4.2 Paraffin Embedding

Harvested tissues were then processed by a series of dehydration steps and then washed in hot paraffin. Plastic labeled blocks were filled with hot paraffin and the tissues were embedded into them. This was allowed to cool at 4°C for a couple days.

3.4.3 Embedding in OCT for frozen sections

At the time of necropsy, animals are perfused with saline alone, and then organs are harvested. The tissues are again washed three times in ice cold PBS and then embedded in the OCT (Optimum Cutting Temperature) compound and placed on dry ice. This is a

gel at room temperature but freezes on dry ice. This snap frozen tissue, embedded in OCT is stored at -20°C for a week.

3.4.4 Masson's Trichrome Staining

Tissues embedded in paraffin blocks are cut into 5 micron slices using a microtome. These slices are then mounted on transparent slides and stained with the Masson's Trichrome dye in a series of steps involving dehydration and staining with the dye for collagen and heart muscle. Mason's trichrome is used to quantitate the collagen content. Fibrosis size or scar tissue was deduced by the percentage of area with collagen as compared to the total area.

3.4.5 Immunohistochemistry

Tissues were fixed in formalin and embedded in paraffin blocks according to established protocols. Antigen retrieval was performed using 10 mM sodium citrate buffer (pH 6.0) and heat at 95°C for 5 min. The buffer was replaced with fresh buffer and reheated for an additional 5 min, then cooled for 20 min. The slides were washed in deionized water three times for 2 min each. Specimens were then incubated with 1% normal blocking serum with goat and donkey serum in PBS for 60 min to suppress nonspecific binding of IgG. Slides were then incubated for 60 min with the primary antibody at a dilution specified by the manufacturer in blocking buffer with serum. Slides were then washed with phosphate-buffered saline (PBS) and incubated for 45 min, with

secondary antibody at a dilution specified by the manufacturer in blocking buffer with serum in a dark chamber. After washing extensively with PBS, coverslips were mounted with aqueous mounting medium. (Vectashield Mounting Medium with DAPI, H-1200; Vector Laboratories, Burlingame, CA, USA).

3.5 Isolation of total RNA

RNA from tissue samples were isolated using the Trizol reagents. Briefly, the tissues were homogenized in Trizol in dry ice and chloroform was added to this. The aqueous phase obtained was collected and mixed with isopropanol and centrifuged to collect the samples. RNAgents denaturing solution (Qiagen, Hilden, Germany) was then added to this to dissolve the pellet. Samples were again collected with isopropanol and are centrifuged. This sample was further treated with 75% ethanol and centrifuged to collect samples. The supernatant was discarded without disturbing the pellet and the pellet is dissolved in DEPC water for future use. Further clean up of the RNA was done with the use of the Qiagen kit as per the manufacturer's instructions.

3.6 Preparation of cRNA

First-strand cDNA was synthesized using Oligo dT and Superscript II RT (Invitrogen, Grand Island, NY). Alternatively, cDNA can be prepared using OVATION RNA Amplification System (NuGen Technologies, Inc., San Carlos, CA). cDNA amplification products were fragmented and chemically-labeled with biotin to generate biotinylated

cDNA targets. Each Affymetrix gene chip for rat genome was hybridized with fragmented and biotin-labeled target (2.5 μg) in 200 μl of hybridization cocktail. Target denaturation was performed at 99°C for 2 minutes, followed by hybridization for 18 hours. Arrays were washed and stained using Genechip Fluidic Station 450, and hybridization signals were amplified using antibody amplification with goat IgG (Sigma-Aldrich) and anti-streptavidin biotinylated antibody (Vector Laboratories, Burlingame, CA).

3.7 Imaging

3.7.1 Xenogen IVIS

The animals were routinely measured for luciferase expression using a cooled coupled device camera from the Xenogen Imaging Systems. The animals were anesthetized using 2% isofluorane. Luciferin was injected intra peritoneally at a concentration of 125 mg/kg of the animal. As Luciferin is light sensitive, care was taken to minimize the amount of light in the room. After 10 minutes, within which time the luciferin would have been flushed to all parts of the body, real time images were obtained to determine the luciferase expression of the gene, as expressed by a chemiluminescence emitted by the luciferase protein in the presence of luciferin.

3.7.2 Echocardiography

We performed 2D-echocardiography on rats using a 15-MHz linear array transducer interfaced with a Acuson Sequoia C256 (Siemens, Munich, Germany). The animals were sedated with ketamine, the chest was shaved, and the sedated animal maintained in a supine position. For quantification of LV dimensions and wall thickness, we digitally record 2D clips and m-mode images in a short axis view from the mid-LV just below the papillary muscles. This anatomical location was chosen to consistently obtain measurements from the same anatomical location in different mice. Measurements were made offline using ProSolv (Indianapolis, IN). Each measurement in each animal was made 6 times, from 3 randomly chosen m-mode clips out of 5.

As a measure of left ventricular functions, shortening fractions was calculated from M mode studies.

Shortening fraction: (LVEDD-LVESD)/LVEDD *100 where,

LVEDD: Left ventricular end diastolic dimension

LVESD: Left ventricular end systolic dimension

Dimensions were measured between the anterior and the posterior walls from short axis view just below the papillary muscle. Left ventricular mass was calculated by

Left Ventricular Mass = 1.05 * ((Anterior Wall Thickness+LVEDD+Posterior Wall Thickness)^3 –LVEDD^3)

3.7.3 Confocal Microscopy Analysis

Tissues were analyzed using an upright spectral laser scanning confocal microscope (Model TCS-SP; Leica Microsystems Heidelberg, Germany) equipped with blue argon (for DAPI), green argon (for Alexa Fluor 488), and red krypton (for Alexa Fluor 594) lasers. Data were collected by sequential excitation to minimize "bleed-through." Image processing, analysis, and the extent of co-localization were evaluated using the Leica Confocal software. Optical sectioning was averaged over four frames, and the image size was set at 1,024 x 1,024 pixels. No digital adjustments were made to the images.

3.8 Nanoparticle Formulation

Nanoparticles containing BSA and 6-coumarin were formulated using a double emulsion-solvent evaporation technique. An aqueous solution of BSA (60 mg/ml, 1 ml) was emulsified in a PLGA solution (180 mg in 6ml chloroform) containing 6-coumarin (100µg) using a probe sonicator (55W for 2 min) (Sonicator® XL, Misonix, NY). The water-in-oil emulsion formed was further emulsified into 50 ml of 2.5% w/v aqueous solution of PVA by sonication (55W for 5 min) to form a multiple water-in-oil-in-water emulsion. The multiple emulsion was stirred for ~18 h at room temperature followed by for 1 h in a desiccator under vacuum to remove the residual chloroform. Nanoparticles were recovered by ultracentrifugation (35,000 rpm for 20 min at 4°C, OptimaTM LE-80K, Beckman, Palo Alta, CA), washed two times with distilled water to remove PVA,

un-entrapped BSA and 6-coumarin, and then lyophilized (−80°C and <10μm mercury pressure, SentryTM, Virtis, Gardiner, NY) for 48 h to obtain a dry powder.

3.8.1 Conjugation of nanoparticles with RR peptide

Nanoparticle surface was activated by the epoxy compound, Denacol®, followed by conjugation of the activated NPs to RR-peptide in the second step. Briefly, 60 mg of NPs were sonicated in 4 mL of borate buffer (50 mM, pH 5.0) for 30 s on an ice-bath. This was followed by the addition of 40 mg of Denacol® that was also dissolved in an equal volume of buffer and the reaction was allowed to take place for 30 min at 37 °C with gentle stirring in the presence of 50 mg of zinc tetrahydrofluroborate hydrate, which acted as a catalyst. NPs were separated by ultracentrifugation at 30,000 rpm at 4 °C for 20 min followed by three washings with borate buffer to remove any unreacted Denacol®. To conjugate RR-peptide, epoxy activated NPs were resuspended in 4 mL of borate buffer and mixed with a solution containing 200 μg of RR peptide in the same buffer. The reaction was allowed to proceed at 37 °C for 2 h with constant stirring. The unreacted peptide was then removed by ultracentrifugation as discussed above; the final NP suspension was lyophilized for 48 h to obtain a dry powder.

3.8.2 High Performance Liquid Chromatography

The mobile phase used for the HPLC analysis was acetonitrile water solution at a ratio of 65:35 supplemented with 0.005M n-heptane sulfonic acid salt. The column used

was a C8 column (Waters Technologies). The mobile phase was allowed to circulate through the column and the samples were dissolved in 100% methanol. Samples were allowed to pass through the column at a rate of 0.8 ml/minute for 5 minutes. All samples were in triplicates. Standard curves were generated with increasing concentrations of 6 Coumarin extracted with methanol overnight. Excitation and emission wavelengths were at 420 and 490 nm.

3.9 Statistical Analysis

All results are expressed as mean $\pm$ s.e.m. Statistical analysis was performed using the Students t-test.

CHAPTER IV

IN VIVO BIO-FLUORESCENCE IMAGING FOR GENE EXPRESSION

4.1 Introduction

Gene therapy has evolved as a viable method to deliver therapeutic genes, such as VEGF, FGF to ischemic myocardium following myocardial infarction. However, this is limited in its approach as there are not enough bio assays that can quantify the amount or the presence of these proteins in the injured tissue. Moreover, the expression of these plasmids is mostly studied *ex vivo,* wherein the tissue is excised and the level of reporter molecules are identified via various assays, such as optical microscopy (confocal), PCR analysis, flow cytometry, microarray analysis, and others. However, this method provides information for a single time point and for temporal analysis several animals are used, with one group of animals being sacrificed for each time point. These studies also vary

between animal groups, and have discordance due to technical errors generated during intra myocardial injections. A real time *in vivo* quantification of gene expression can provide a more cost effective and more accurate data between animal groups.

Several sophisticated imaging modalities can be used to detect physiological changes, as a response to gene therapy, including magnetic resonance imaging MRI, positron emission tomography PET, single photon emission computed tomography SPECT and others.[168, 169] However these modalities are extremely complicated, are not well suited for small animals, and are highly expensive and thus non feasible for initial studies.

Bioluminescent reporters, however, can be used as a tool to determine real time information on gene expression for plasmid expression studies. Bioluminescent reporters can provide real time, *in vivo* monitoring data for gene expression by emitting chemiluminescence at particular wavelengths. In the past, such studies were only possible with transparent or translucent objects, however, recent studies using a firefly Luciferase gene has been shown to provide non invasive quantification of expression due to its bioluminescent light source internally.[170] Luciferase, derived from the firefly, is a photoprotein used in several molecular biology studies, including *in vitro* in cells studies, tumor studies, and gene expression studies.[171-173]

This study aimed to design and validate a plasmid for effective gene therapy capable of expressing and sustaining expression in rodent hearts. We wanted to evaluate if optical imaging could provide detailed information about changes in gene expression, with

modifications to the plasmid design. Therefore, we designed a plasmid that encoded for the gene, Luciferase. This protein generates bioluminescence via a reaction in the presence of a substrate luciferin and oxygen, in order to produce photons of light. Light thus produced can be imaged via a sensitive detector present in a cooled coupled camera device.

We injected plasmids encoding Luciferase into rats that had chronic heart failure. We then serially measured the light emitted from it in the presence of an i.p. injection of luciferin. This was quantified and analyzed in order to understand the gene expression profile of this plasmid. We noticed that this profile changed when the gene was enhanced with transcriptional enhancers boosting the amount of light and the duration that the light was emitted. Utilizing a cooled camera to detect bioluminescence can help understand the gene expression profile in gene therapy and eliminate the need for complicated bioassays.

Mechanism of Biofluorescence Imaging using the IVIS 100

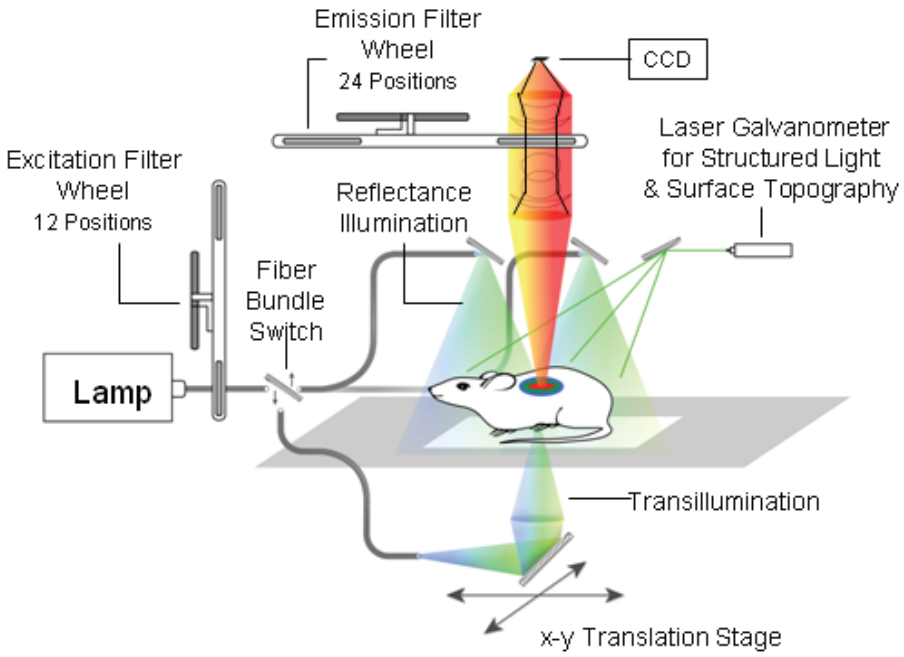

Figure 4-1 : Illustration of the mechanism involved in bioluminescent imaging.
Adapted from www.caliperls.com

When the luciferin protein interacts with oxygen it emits light but this process is extremely slow. In the presence of oxidative Luciferase, this reaction occurs almost immediately allowing this light to be quantified. The animal or cells that possess the Luciferase (Luc) gene are placed in a light tight box. An i.p. injection of luciferin is administered and this is allowed to circulate through the body. When luciferin interacts with oxygen in the presence of Luciferase, it emits chemiluminescence, which is captured by a highly sensitive charged cooled camera device. The signal here needs to be adjusted for autoluminescence and scattered luminescence.

4.2 Methods:

4.2.1 Experimental Plan

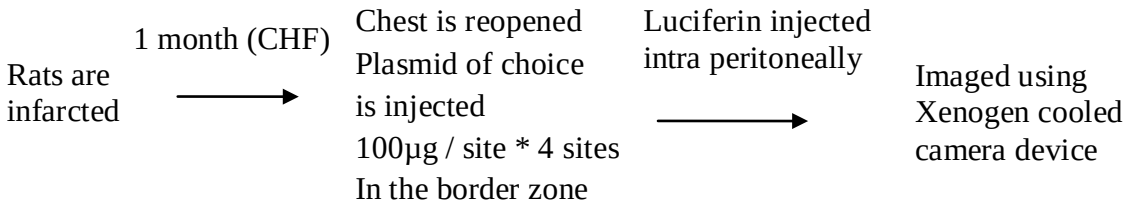

Rats were infarcted via LAD ligation and the hearts were allowed to modify to a chronic heart failure stage. 4 weeks after LAD ligation, the chests were re-opened in order to inject the plasmid into the border zone of the left ventricle. Rats were imaged using the IVIS system (Xenogen, CA) in the presence of an i.p. injection of luciferin serially till no chemiluminescent image was observed for three days in a row.

4.2.2 Optical Imaging System

All studies were performed using the IVIS 50 small animal scanner (Xenogen, Alemeda, CA) using the Luciferase filter set to match the emission characteristics of the chemiluminescence emitted from the Luciferase Luciferin reaction. Acquisitions were performed 10 minutes after an i.p. injection of luciferin to allow for maximum circulation. Illumination parameters (exposure time of 1 minute, medium lamp voltage = medium, f/stop of 2, and binning of 2) were selected for each acquisition. For in vitro studies, cell samples were placed in a black bottomed 6 well plate. Whole-body real-time scans of

anesthetized rats were acquired in prone and supine position, every day following myocardial injection of the Luciferase gene.

4.2.3 Image analysis

Images were acquired and analyzed using Living Image 2.5 software (Xenogen, Alameda, CA, SA) integrated with Igorpro (Wavemetrics, Lake Oswego, OR, USA). The digitized image intensity is expressed in arbitrary units.

For the in vitro experiments, image analysis involved the designation of regions-of interest (ROI) as the circular area of the well containing the cell concentrations to extract the average intensity (sum of the intensity of all pixels within this ROI divided by the number of pixels). For the in vivo experiments, image analysis involved the definition of the ROI in each location of enhanced fluorescence as the area having intensity larger than 50% of the peak signal intensity. This ROI was manually selected.

4.2.4 Plasmids Used

The pCMV, pCMVe and pMHC plasmids expressing the Luc gene was used for this study. Detailed descriptions of these plasmids are described above. (Chapter 3)

4.2.5 In Vitro Expression

Plasmids were transfected into HEK293A cells or H9C2 cardiomyoblasts at 50% confluence at 300,000 cells per well in a 6 well plate using the FUGENE Transfection kit (Roche Basel, Switzerland) as per the manufacturer's instructions. The cells were exposed to luciferin at 10 µg per ml of PBS per well and the chemiluminescence emitted was quantified using a cooled coupled device camera from the Xenogen Imaging Systems.

4.2.6 In Vivo Expression

8 week old male Lewis rats weighing 225-250 grams underwent LAD ligation, as previously described. 4 weeks later, the chests were re opened and the plasmid was injected, intra myocardial at 100 µg / 100 µl of plasmid in phosphate buffered solution (PBS) at 4 sites in the border zone of the infarct using a 30 gauge needle. Animals were imaged serially, one day post surgery, using the IVIS system. Five animals were used per group for each plasmid type.

4.3 Results

4.3.1 Plasmid expression in H9C2 cell lines

The inefficiency of physical delivery of non-viral plasmid DNA to cells has been well documented. One of the strategies employed to circumvent low transfection

efficiencies has been to identify vector components that yield either high levels of protein expression or enable target specific expression using tissue-specific promoters. We tested three different plasmids in the H9C2 myoblast cell line to identify a vector that would produce sufficient cardiac cell expression over approximately two weeks. Plasmids were constructed with either the ubiquitous CMV promoter or cardiac-specific αMHC promoter and the luciferase reporter gene (pCMV, pMHC and pCMVe, Figure 4-2A). We observed that CMV-driven promoters (pCMV and pCMVe) exhibited higher luciferase expression ($1.3x10^7$ arb units and $2.3x10^7$ arb units) compared to the cardiac-specific αMHC-driven plasmid (pMHC, and pMHCe at $1.1x10^6$ and $9.2x10^6$ arb units). As expected, the RU5 translational enhancer in pCMVe increased expression over pCMV and pMHC plasmids (Figure 4-2B).

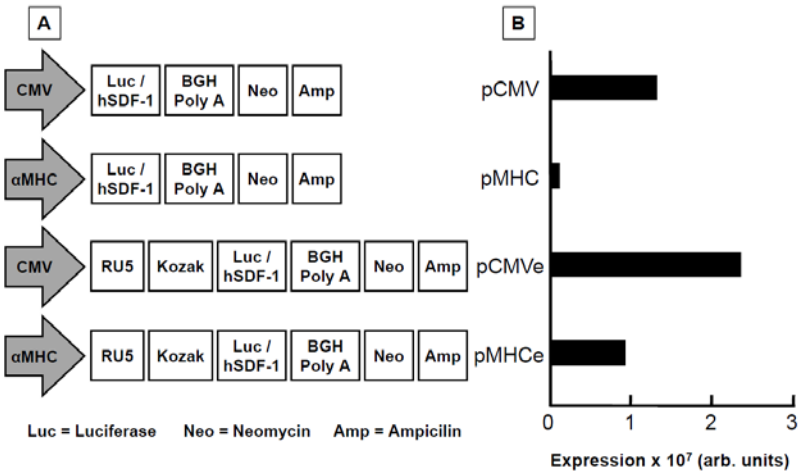

Figure 4-2: Plasmid design and *in vitro* expression profile.
A) A schematic of the gene design is shown here. The promoters, a ubiquitous CMV, or a cardiac specific αMHC present in the 5' region are used to drive the gene expression. Transcriptional enhancers, such as Kozak sequences and RU5 regions are used to boost the gene expression by multiple folds. B) The in vitro expression of luciferase activity is shown here. H9C2 cells were transfected with CMV and αMHC driven plasmids at 300,000 cells per well. Transcriptional enhancers, such as Kozak sequences and RU5 regions increase gene expression by multiple folds.

4.3.2 Evaluation of Gene Expression in rodents

We assessed *in vivo* vector expression in adult Lewis rats infarcted via a left anterior descending artery (LAD) ligation followed by direct cardiac injection with 100 µl of 1 mg/ml pCMV, pMHC or pCMVe-luc in saline into the border zone of the infarcted myocardium at the time of infarct. Control rats were injected with saline. Gene expression was quantified by measuring chemiluminescence following i.p. injection of luciferin three days after direct cardiac injection (Figure 4-3). The presence of the signal in the heart alone, rules out the possibility of the naked plasmid being flushed into the liver, or being washed away into the circulatory system

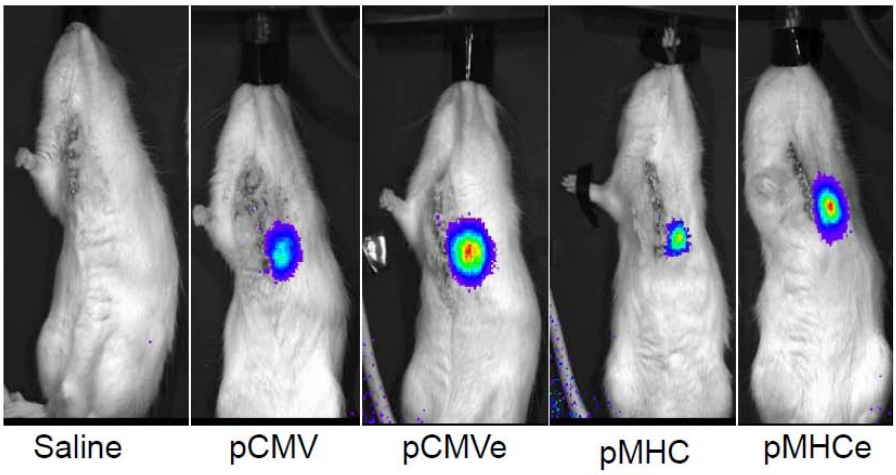

Figure 4-3 : Gene expression *in vivo* in 8 week old rodents
Animals were injected with CMV αMHC plasmids expressing the Luc gene and the images were obtained after 3 days. The luciferase gene expresses the protein which emits chemiluminescence in the presence of an i.p. injection of luciferin. This intensity is measured using a cooled coupled camera device. The greatest intensity was obtained with the gene vector with transcriptional enhancers.

4.3.3 Dose-response of cardiac gene transfer

To determine the optimal plasmid dose required for efficient myocardial transfection, we injected naked plasmid encoding luciferase (pCMV-luc) immediately after ligation of the LAD in Lewis rats at doses ranging from 0 to 500 µg in 100 µl PBS. A dose-response curve was generated for vector expression. The peak expression increased up to a dose of 100 µg and saturated at higher doses (Figure 4-4). Therefore, a dose of 100 µg was used in all subsequent experiments.

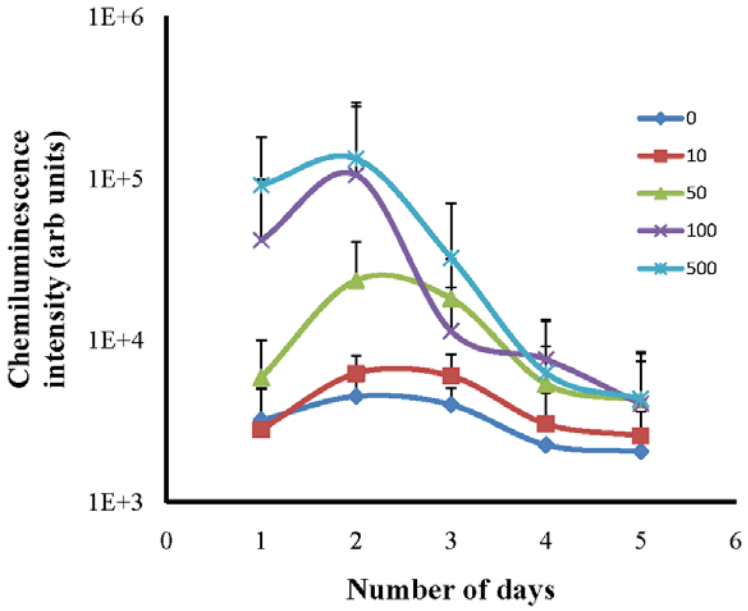

Figure 4-4 : Dose curve to determine optimal amount of plasmid *in vivo*
Infarct model of rodents were injected with CMV pcDNA3.1 Luc at varying doses of 0 µg to 500 µg in the border zone. The chemiluminescence emitted was measured every day for 5 days after the injection. The gene expression saturated at 100ug. n=3

4.3.4 Time course of vector expression in the heart

Next we determined duration of expression after cardiac gene transfer with pCMV, pCMVe and pMHC vectors. All plasmids expressed luciferase in infarcted cardiac tissue. Expression from the CMV based plasmids expressed for a short period of 5 days, whereas plasmid pMHC expressed for a longer period of 32 days. Adding elements to increase transcriptional and translational efficiency significantly affected the expression profile, with pCMVe expression lasting 15 days. Changing the promoter or adding elements to increase translational efficiency significantly affected the duration of expression (Table 4-1).

Promoter	Backbone	Model	Days of expression
αMHC	pBS	Infarcted rats	32
αMHC	pBS	Infarcted rats	40
CMV	pCDNA 3.1	Infarcted rats	5
CMV	pCDNA 3.1	Infarcted rats	16

Table 4-1 : Comparison of maximum expression time between the plasmids.
CMV and αMHC plasmids exhibited different expression profiles when injected in rodents. CMV plasmids had shorter expression time as compared to αMHC plasmids. Translational enhancers boosted expression time.

4.3.5 Comparison of peak magnitude between the different plasmids

The magnitude of luminescent intensity was determined for the three plasmids (pCMV, pCMVe and pMHC). We observed that pCMV peaked at day 3. pMHC showed maximum expression on day 7 and continued for 30 days. The αMHC promoter had a smaller magnitude of luciferase expression when compared to CMV promoters.

Compared to pCMV, the RU5 translational enhancer in the CMV plasmid (pCMVe) increased peak expression almost 10-fold. The pMHCe plasmid also improved peak magnitude as compared to pMHC plasmid to almost 10 fold. (Figure 4-5)

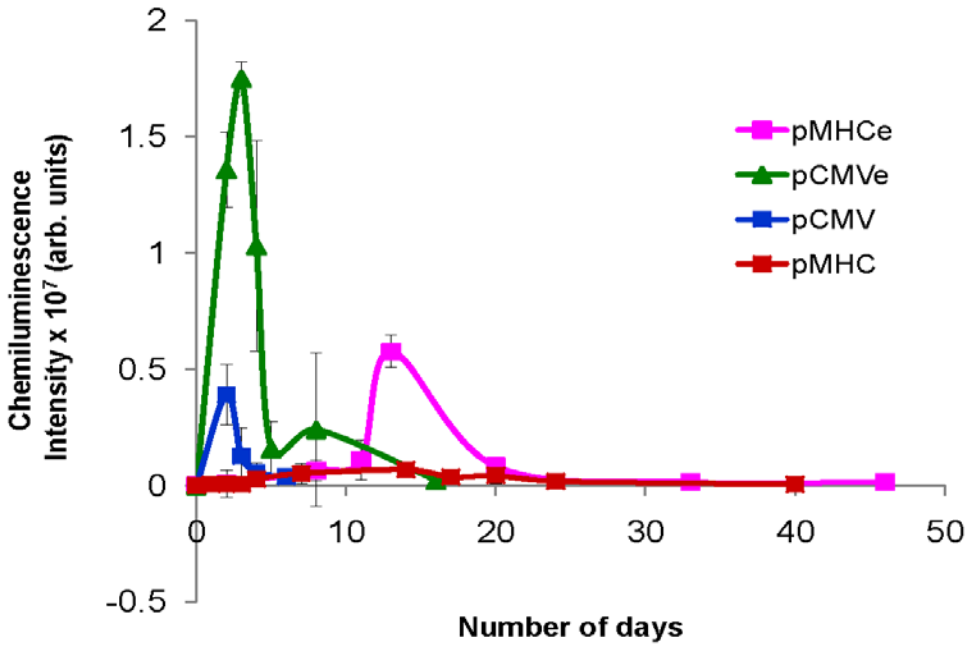

Figure 4-5 : Expression profile between various plasmid designs *in vivo*
Animals were injected with the four different plasmids and the gene expression was monitored by quantifying the chemiluminescence intensity emitted. αMHC pBS Luc had the longest expression time, 32 days, and KCPIR Luc had the maximum peak expression, $2.7x10^7$.

4.3.6 Role of promoters and backbones in plasmid design

The vectors backbones used were pcDNA 3.1, which is a standard vector used in most studies. pBS is the smallest vector and therefore provides greater uptake into the cells. pKCPIR is a modified pcDNA 3.1 backbone which has a transcriptional enhancer and an intron/exon unit inserted into the pcDNA backbone, and a modified pBS plasmid

with the enhancer elements. On comparing pCMV backbones, pMHC backbones, pCMVe backbones, and the pMHCe backbones, we observed the longest expressions were obtained by using either the pBS backbone used in the pMHC and the pMHCe plasmid. The length of plasmid expression is determined by the backbone and does not change significantly with the use of a translational enhancer element added to this. (Table 4-1).

4.3.7 Role of Transcriptional Enhancers in plasmid design

On comparing the overall magnitudes between plasmids, it can be seen that the role of transcriptional enhancers is to boost the magnitude of expression. Translational enhancers slow down ribosomal units so that the chance of the occurrence of translation is increased. Between the pCMV and pCMVe plasmids, the expression was enhanced by more than 6 fold. Similarly the use of enhancer elements in the pMHC plasmid boosted the expression by more than twice. (Figure 4-6)

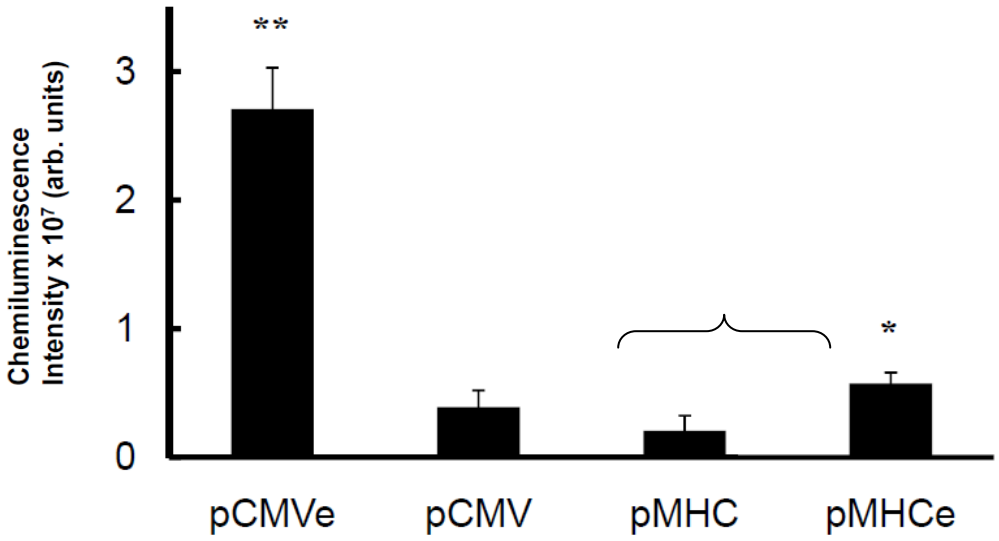

Figure 4-6 : Peak expression profile between various plasmids *in vivo*
Overall peak magnitudes describe the amount of gene expression collected over the time course of the expression period. Enhanced CMV plasmids exhibited the largest amount of expressions collected overall.

4.4 Discussion

The use of gene therapy to deliver therapeutic proteins has been utilized for providing cardiac benefit to ischemic myocardium. However, the use of viral vectors poses a threat to the host due to immunological responses and toxic concerns. The use of non viral gene therapy for the delivery of proteins is becoming an attractive option to reduce immunological responses and eliminate toxic concerns. The limitation of low transfection efficiencies, associated with non viral mediated gene transfer can be overcome with the use of translational enhancers. The need to determine the expression of a gene in vivo, without the excision of the tissue, to provide real time, accurate data has become necessary and optical imaging with the help of biofluorescence quantification

provides the tools to do so. In addition, optical imaging allows for data to be collected from the same animal over time thus reducing the number of animals required for the study, and eliminating variations between animals.[170]

To date, no study has been performed with optical imaging as a means to understand gene expressions. Our expression studies demonstrated that expression of the pCMV plasmid peaked at day 2 post gene transfer and decreased over the following two weeks. These findings are consistent with previous literature showing a peak in CMV-driven gene expression, 2 days after injection in the rat heart.[169,174] Peak expression in the presence of the RU5 element (pCMVe) was 10-fold greater than that seen in the non-enhanced CMV plasmid (pCMV).

It is noteworthy that direct injection of plasmids into the infarct border zone led to the transfection of cardiac myocytes. In our studies with plasmid delivery restricted to cardiac myocytes, using the cardiac specific αMHC promoter, there was a delay of 4 days after plasmid injection, prior to any evidence of significant expression. Furthermore, the magnitude of expression was 10-fold less than that observed with the pCMV. Although the signal was low, expression persisted for 32 days. Combining the αMHC promoter with the RU5 translational enhancer results in significant plasmid expression for up to 1 month post-injection. Replacing the biofluorescent gene to a therapeutic gene, in the same plasmids will be able to provide expression similar to the expression observed here, thus optical imaging proves to be a useful tool for gene expression profiling.

CHAPTER V

STROMAL DERIVED CELL FACTOR-1 GENE TRANSFER FOR HEART FAILURE

5.1 Introduction

We previously identified Stromal cell-Derived Factor-1 (SDF-1, a.k.a. CXCL12) as a chemokine that is transiently expressed post-tissue injury to promote stem cell homing to the myocardium.[69] SDF-1 enhances tissue repair by preventing cell death and recruiting blood borne and tissue specific stem cells to the damaged region.[69] SDF-1 is a naturally-occurring chemokine that is rapidly increased after myocardial infarction for a period of 4-5 days.[69,175] SDF-1 triggers a number of protective molecular cascades that are both anti-inflammatory[81] and anti-apoptotic to preserve cardiac tissue after injury.[176] Furthermore, SDF-1 is a strong chemoattractant of stem cells and progenitor cells that promote tissue preservation and blood vessel development. The tissue-preserving and

reparative effects of SDF-1 led us to investigate the potential role of SDF-1 in treating ischemic cardiovascular disease.

More recently, we have demonstrated that the over-expression of SDF-1 in myocardial tissue leads to recruitment of endogenous cardiac stem cells to the infarct border zone.[61] Since our original findings several groups have expanded the molecular mechanisms by which myocardial expression of SDF-1 or its receptor CXCR4 leads to preservation of cardiac myocytes and improvement in cardiac function in an acute myocardial infarction setting.[74,177] The benefit from adult stem cell therapy, for preventing and treating cardiac dysfunction, is due to paracrine factors; therefore, the results of cell therapy can be achieved by gene transfer.

We hypothesized that re-establishing stem cell homing by increasing SDF-1 expression via non-viral gene transfer into the peri-infarct tissue, late after myocardial infarction, would re-establish myocardial healing through recruitment of bone marrow derived stem cells and lead to increases in vascular density and cardiac function.[69] To date, we have re-established SDF-1 expression through a cell-based gene transfer approach using stably transfected fibroblasts,[69] mesenchymal stem cells,[35] or skeletal myoblasts transfected with an adenovirus encoding SDF-1 *ex vivo*.[66, 178] SDF-1 protein, in combination with a slow release matrix, has been shown to improve cardiac function in a model of ischemic cardiomyopathy.[179] While these data would suggest that SDF-1 alone may be sufficient to improve cardiac function, such a conclusion is premature, since matrix alone has been shown to induce ventricular remodeling.[180, 181] The goal of

this study was to determine if re-establishing myocardial SDF-1 expression without the concomitant delivery of cells is a viable strategy for increasing myocardial vascular density and cardiac function in the setting of ischemic cardiomyopathy.

In order to deliver SDF-1 to the myocardium, we injected naked plasmid DNA encoding hSDF-1 into the infarct border zone. In prior studies, this strategy has proven to be safe and non-toxic, and is not associated with the toxicities and loss of function that have been observed with adenoviral injection in the infarct border zone.[182] We characterized plasmid expression in cardiac tissue using a luciferase bioluminescence reporter system,[109] since previous non viral gene transfer studies demonstrated low transfection efficiency with this approach. We tested plasmid dose, effect of transcription enhancers, and ubiquitous versus cardiac-specific promoters to increase expression of this therapeutic gene. We identified an optimal plasmid formulation, using a biofluorescence reporter and used a similar design for this gene as well. We injected plasmid encoding SDF-1 into the heart one month after myocardial infarction. This led to a significant increase in cardiac function four weeks post-injection that could be attributed to significant increase in vessel density and a trend towards reduction in scar tissue. The degree of functional improvement correlated with the level of vector expression.

5.2 Methods:

5.2.1 Experimental Plan

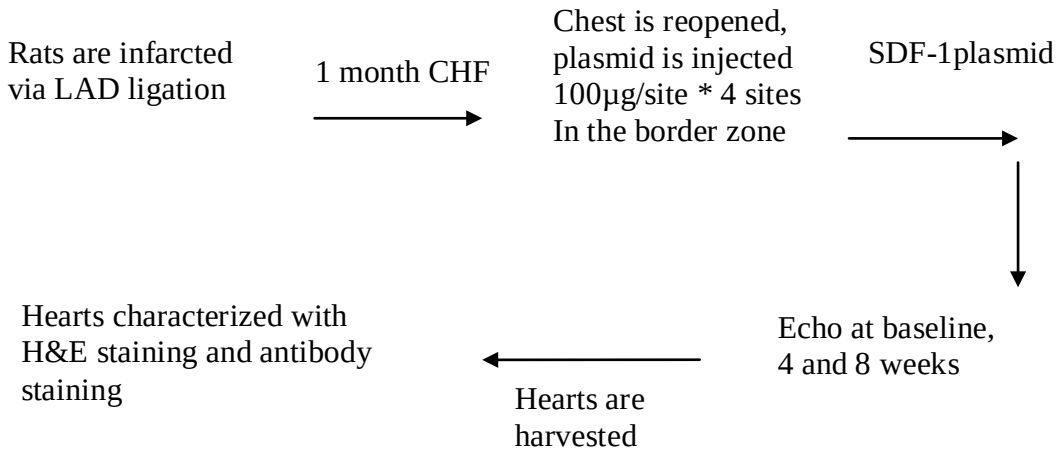

Rats were infarcted via LAD ligation, and the hearts were allowed to modify to a chronic heart failure stage. 4 weeks after LAD ligation, the chests were re-opened in order to inject the hSDF-1 plasmid into the border zone of the left ventricle dissolved in 100µg/100µl of PBS, at 4 sites spanning the infarct. Rats were imaged using the ultrasound echocardiography, before the injections, and 2 weeks, 4 weeks and 8 weeks post treatment. Hearts were then excised and characterized for vessel density, and fibrosis extent, via histochemistry studies.

5.2.2 Plasmids Used

The pCMV, pCMVe and pMHC plasmids expressing the hSDF-1 gene was used for this study. Detailed descriptions of these plasmids are described above. (Chapter 3)

5.2.3 Intramyocardial Gene Delivery

8 week old male Lewis rats weighing 225-250 grams underwent LAD ligation, as previously described. To inject the DNA, the chest was reopened four weeks post MI, applying the same procedure as above. 100 µg of DNA solution in 100 µl of saline per injection site was injected using a 30 gauge needle, for a total of 4 injection sites around the border zone. The border zone was identified by the blanched region around the LAD identified by dyskinetic motion of the anterior wall. The DNA was injected into the wall and distention of the tissue was observed when the DNA was injected. The chest was closed as mentioned above for the LAD ligation.

5.2.4 Echocardiographic Analysis

We routinely perform 2D-echocardiography on rats, pre injection, 2 weeks, 4 weeks and 8 weeks post injection, using a 15-MHz linear array transducer interfaced with a Acuson Sequoia C256 (Siemens, Munich, Germany). The animals were sedated with ketamine, the chest was shaved, and the sedated animal maintained in a supine position. For quantification of LV dimensions and wall thickness, we digitally record 2D clips and m-mode images in a short axis view from the mid-LV just below the papillary muscles. This anatomical location was chosen to consistently obtain measurements from the same anatomical location in different mice. Measurements were made offline using ProSolv (Indianapolis, IN). Each measurement in each animal was made 6 times, from 3

randomly chosen m-mode clips out of 5. As a measure of left ventricular functions, shortening fractions was calculated from M mode studies.

5.2.5 Immunohistochemistry

8 weeks after the injection of the plasmid, the animals were perfused with saline and histochoice and the hearts were harvested. Tissues were fixed in histochoice and embedded in paraffin blocks according to established protocols. Antigen retrieval was performed using 10 mM sodium citrate buffer (pH 6.0) and heat at 95℃ for 5 min. The buffer was replaced with fresh buffer and reheated for an additional 5 min, then cooled for 20 min. The slides were washed in deionized water three times for 2 min each. Specimens were then incubated with 1% normal blocking serum with goat and donkey serum in PBS for 60 min to suppress nonspecific binding of IgG. Slides were then incubated for 60 min with rabbit polyclonal von Willebrand factor (Abcam Cambridge, MA) at 1:100 dilutions in blocking buffer with serum. Myosin was stained with mouse monoclonal left ventricular myosin (Millipore, Billerica MA) at a dilution of 1:10 in blocking buffer with serum. Optimal antibody concentration was determined by titration. Slides were then washed with phosphate-buffered saline (PBS) and incubated for 45 min, with IgG donkey anti-rabbit Alexa fluor 594 (Molecular Probes, Invitrogen, Carlsbad, CA) at 1:800 dilution in blocking buffer with serum and IgG goat anti-mouse Alexa Fluor 488 (Molecular Probes, Invitrogen, Carlsbad CA) at 1:800 dilution in blocking buffer with serum respectively in a dark chamber. After washing extensively with PBS, coverslips were mounted with aqueous mounting medium. (Vectashield Mounting

Medium with DAPI, H-1200; Vector Laboratories, Burlingame, CA, USA). For arteriole imaging, a mouse monoclonal α-sarcomeric actin antibody was used at a 1:200 dilution (Sigma).

5.2.6 Masson's Trichrome Staining

8 weeks after the injection of the plasmid, the animals were perfused with saline and histochoice and the hearts were harvested. The hearts were fixed in histochoice for 7 days and then embedded in paraffin. Hearts were then sectioned and stained with Masson's Trichrome staining for identifying the infarct. Mason's trichrome was used to quantitate the collagen content. Fibrosis size or scar tissue was deduced by the percentage of area with collagen as compared to the total area.

5.3 Results:

5.3.1 Intra-myocardial injection of SDF-1 plasmid increased vessel density

Previous studies have shown that SDF-1 expression is increased after MI and recruits stem and/or progenitor cells to promote tissue preservation and promote vasculogenesis. We tested whether non-viral gene transfer of vector expressing SDF-1 would improve vasculogenesis following myocardial infarction. As described above, rodents were infarcted via LAD ligation and received direct injection of SDF-1 plasmid DNA one month post myocardial infarction. Myocardial sections obtained from animals that

received SDF-1 gene transfer, 8 weeks after injection, were stained with antibodies against von Willebrand Factor (vWF) to assess vasculogenesis (Figure 5-1). We observed a statistically significant increase in blood vessel density in the infarct zone in the animals that received pCMVe-hSDF-1 and pCMV-hSDF-1, as compared to saline controls ($p<0.0001$). The infarct border zone and infarct zone, on average, had a higher blood vessel density in the pCMVe-hSDF-1 group (21 vessels/mm^2) and pCMV-hSDF-1 group (17 vessels/mm^2) than those in the saline group (6 vessels/mm^2) (n=7 in all groups) (Figure 5-2). The vessels observed by vWF staining were also co-stained with α-smooth muscle actin. A co-localization of endothelial cells and actin filaments was observed (Fig 5-3), which further established the fact that the blood vessels observed were arterioles and arteries, and not capillaries.

Interestingly, the pCMVe vector that had the highest peak expression did not induce significantly greater vasculogenesis than the lesser expressing unenhanced pCMV vector. This result suggests that delivering a minimum threshold amount of SDF-1 was necessary to induce vasculogenesis but that more SDF-1 did not induce more.

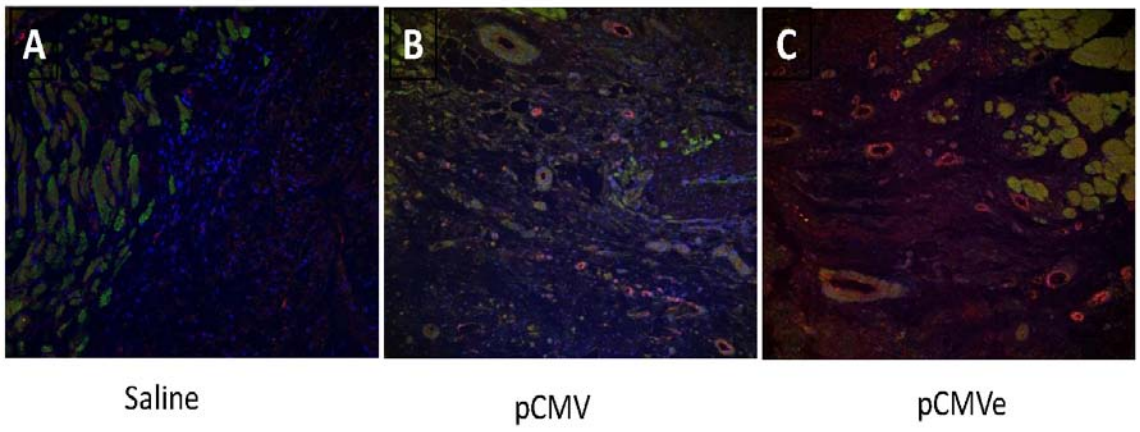

Figure 5-1: Vessel density count (vessels / mm^2) in rodents that received SDF-1 gene
Double staining with von Willebrand Factor and ventricular myosin showing blood vessels and myocytes respectively in the infarct zone after injection with saline as control, or plasmids; CMV pcDNA SDF-1 and CMV KCPIR SDF-1 (n=7 in all groups) are represented above. The number of arterioles observed in the SDF-1 treated groups is significantly greater than the controls. ($p<0.001$)
Red: vWF; Green: Myocytes; Blue: Dapi. Magnification = 20x

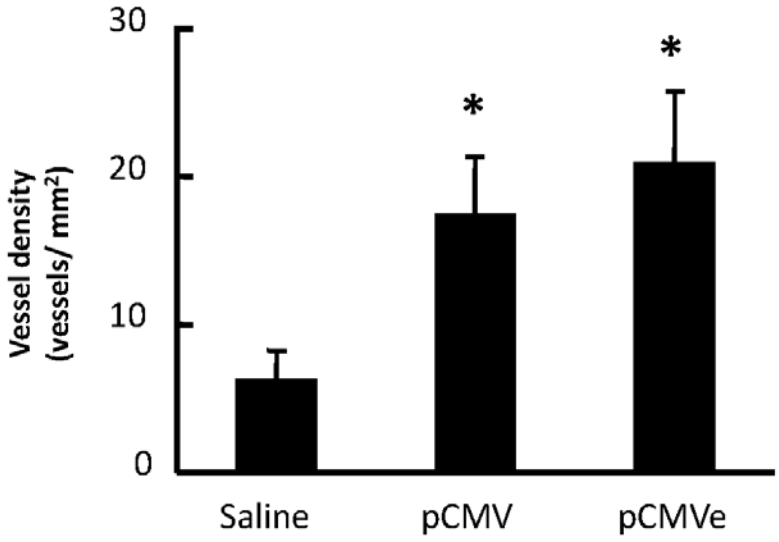

Figure 5-2 : Increase in blood vessels following SDF-1 gene therapy
Vessel density was significantly increased in the SDF-1 treated animals compared to saline controls.CMV KCPIR-SDF1, 21 ± 1.82 vessels/mm^2; CMV pcDNA-SDF1 17 ± 1.48 vessels/mm^2, and PBS 6 ± 0.73 vessels/mm^2. *, $p<0.001$.

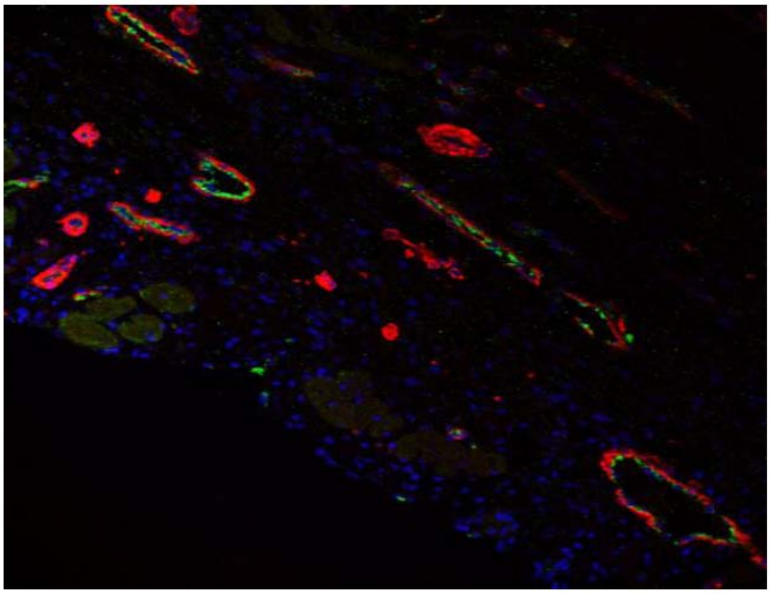

Figure 5-3 : Actin staining to determine the vessels to be arterioles
Immunohistochemistry with vWF and α- sarcomeric actin staining showing blood vessels and actin staining in the infarct zone, 8 weeks after injection with CMV KCPIR SDF-1 (n=7). The positive staining identifies the blood vessels as mature arterioles and not capillaries. Red: actin; Green: vWF for vessels, Blue: Dapi. Magnification = 20x

5.3.2 SDF-1 plasmid therapy improves ventricular function in ischemic rats

We hypothesized that the SDF-1 plasmids that induced vasculogenesis would also improve cardiac function post-MI. To test this hypothesis, ischemic hearts were injected with hSDF-1 pDNA vectors. Pre-injection (one month post infarct), all rats had fractional shortening (FS) < 30%. 4 weeks post-injection, control animals had a decrease in fractional shortening by 35.9%. In contrast, the pCMV-SDF1, and pCMVe-SDF1 groups showed statistically significant improvements of 4.62% and 24.97% respectively, by 4 weeks, ($p < 0.01$) compared to control. In contrast, a cardiac-specific promoter, αMHC-driven plasmid (pMHC-hSDF1) treated animals did not improve function compared to control animals exhibiting a decline in FS of 32.65% (Figure 5-4). Importantly, the

improvement in cardiac function correlated with an increase in blood vessel density strongly suggesting a link between vasculogenesis and cardiac functional improvement. However, the greater benefit seen with the pCMVe compared to pCMV suggests that there are other mechanisms in play as well since pCMVe did not induce significantly greater vascular density compared to pCMV. SDF-1 gene transfer induced cardiac benefit was sustained at 8 weeks, as the animals that received the CMV-driven plasmids continued to demonstrate improved cardiac function compared to saline control and αMHC vector groups (Fig 5-5).

Other parameters of cardiac function, such as the thickening of the anterior and posterior walls, trended toward significant improvement (i.e. an increase in wall thickness) in the pCMVe-hSDF1 treated animals. No significant change was observed in the pCMV-hSDF1 treated animals, the pMHC-SDF1 treated animals or the saline control animals. There was no change in left ventricular mass in any group. (Figure 5-6). Since the animals treated with the plasmid producing the highest peak expression had the largest cardiac benefit, these data suggest the importance of the magnitude of hSDF-1 vector expression rather than the length of plasmid expression in determining improvement in cardiac function.

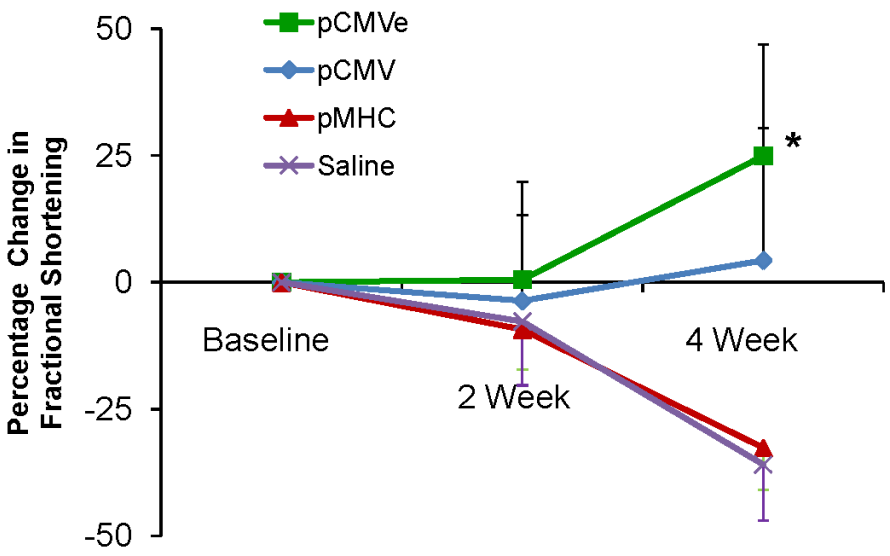

Figure 5-4 : Functional benefit observed *in vivo* with SDF-1 plasmid treatment
Pre-injection, (one month post infarct) all rats had a Fraction of Shortening % (FS%) < 30%. 4 week post injection, the control group (n=10) decreased in FS. In contrast, both CMV-driven plasmids showed a statistically significant improvement of 5% (CMV-SDF-1) (n=9) and 25% (CMVe-SDF-1) (n=10) respectively ($p<0.02$). The cardiac-specific promoter plasmid (αMHC- SDF1) (n=5) did not improve function compared to control.

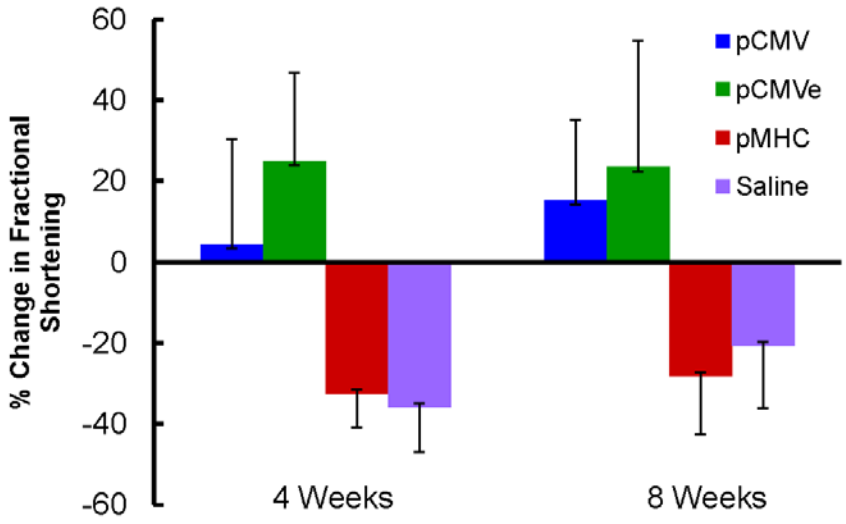

Figure 5-5 : Sustenance of benefit for 8 weeks post treatment
The improvement in cardiac function following plasmid injection is sustained 8 weeks after injection. CMV driven plasmids depict an increase in cardiac function as compared to saline controls and αMHC driven plasmids.

Other Echo Parameters

		pCMVe			pCMV			pMHC			Saline		
		BL	2 w	4 w	BL	2 w	4 w	BL	2 w	4 w	BL	2 w	4 w
FS %	Avg	0.13	0.12	0.15	0.16	0.15	0.15	0.16	0.14	0.10	0.15	0.14	0.10
	SEM	0.02	0.01	0.02	0.02	0.04	0.04	0.02	0.02	0.01	0.01	0.02	0.02
LV Mass Avg	Avg	1503.86	999.81	989.80	831.79	1035.44	953.02	981.72	952.74	925.30	891.53	943.39	941.74
	SEM	494.39	117.74	134.93	40.25	70.10	63.39	93.40	78.80	75.96	94.91	126.08	92.91
AW thickening	Avg	-0.01	-0.02	1.09	0.22	0.12	0.11	-0.13	0.04	-0.04	0.07	0.20	0.02
	SEM	0.13	0.10	0.73	0.16	0.08	0.10	0.05	0.20	0.12	0.05	0.07	0.06
PW thickening	Avg	0.27	0.34	0.37	0.43	0.50	0.29	0.60	0.36	0.32	0.43	0.28	0.16
	SEM	0.06	0.10	0.06	0.10	0.12	0.07	0.12	0.10	0.07	0.09	0.05	0.08

Figure 5-6 : Other physiological parameters associated with benefit
Other physiological parameters such as left ventricular mass, anterior wall and posterior wall thickening between rodents from the different treatment groups are assessed here. These parameters are symptomatic with ventricular remodeling.

5.3.3 SDF-1 gene transfer reduced fibrotic tissue in the infarct zone

We performed Masson's Trichrome staining to determine the infarct size, represented by fibrotic tissue, 4 weeks after treatment with plasmids. The infarct size was reduced in the animals that received SDF-1 plasmid when compared to the saline animals. The fibrotic area was smaller in the pCMVe-SDF1 group (16.92%) and pCMV-SDF1 group (17.81%), than in the saline group (23.82%) (n=7 in all groups). These results exhibit a strong trend towards reduction in cardiac fibrosis following SDF-1 treatment (p=0.08) (Figure 5-7).

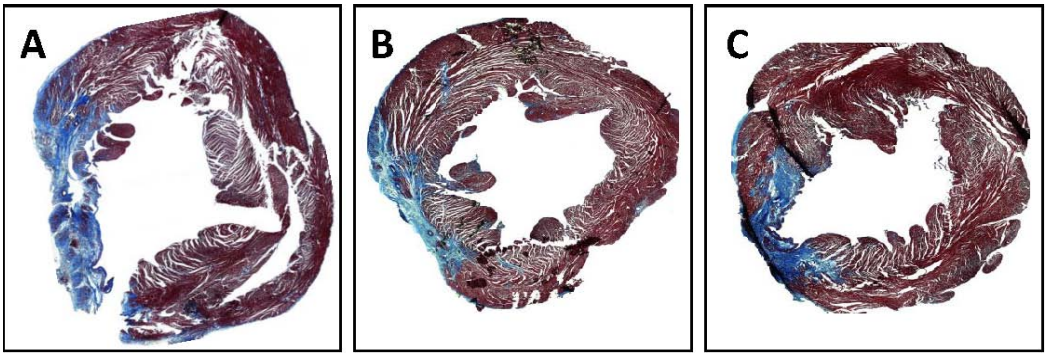

Figure 5-7 : Masson's Trichrome staining to determine infarct sizes *in vivo*
SDF-1 gene therapy reduces infarct size, 8 weeks after treatment in chronic heart failure. The left ventricular fibrotic area was significantly smaller in the SDF1 groups (compared to the saline group. (n=7 in all groups)

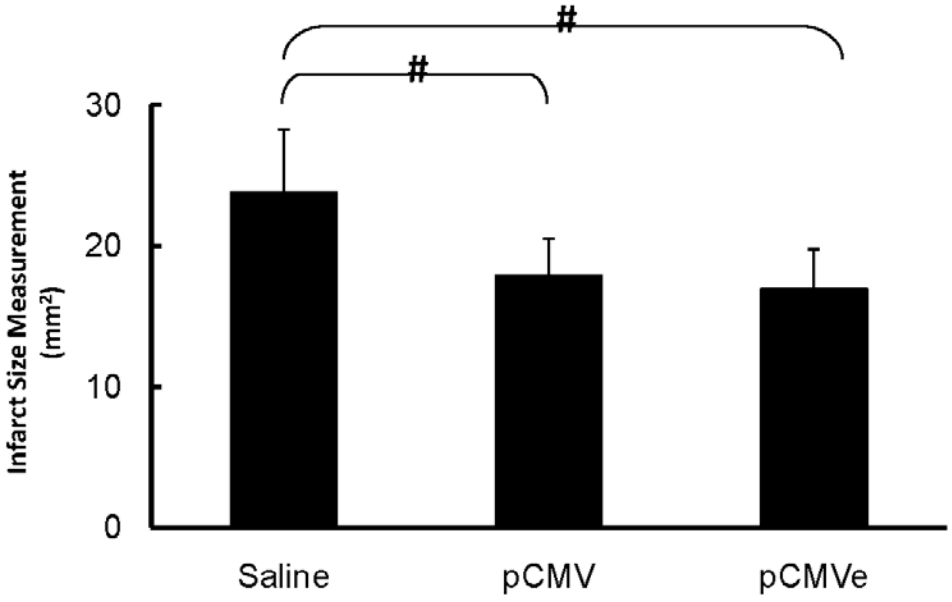

Figure 5-8 : Decrease in fibrotic scar following SDF-1 treatment
The left ventricular fibrotic area was significantly smaller in the CMV KCPIR-SDF1 (16.92 ±2.82 %) and CMV pcDNA-SDF1 groups (17.81 ±2.59 %), compared to the saline group (23.82 ±4.47 %). (n=7 in all groups)

5.4 Discussion

Regenerative medicine has significant potential for the treatment of ischemic cardiac disease because, unlike current treatments that focus on either alleviating symptoms or reducing cardiac work load, regenerative medicines provide an opportunity to repair and retain function in degenerating organs. Non-viral gene delivery, or the application of naked plasmid DNA to express a therapeutic protein at a specific site, is a simple delivery method that has been tested clinically in ischemic patients for over 15 years. A substantial body of literature, both preclinical and clinical, has demonstrated that non-viral vector delivery of therapeutic genes is safe and effective. The safety profile of non-viral gene delivery is also attractive when compared to viral vector therapy delivery because it does not produce a significant inflammatory response that viral vector delivery can cause; nor is there concern for antibody response to the vector due to prior viral exposure in the patient.

Cardiovascular gene therapy has been found to be a safe strategy to obtain transient protein expression in the heart. Skeletal and cardiac muscle have been shown to take up and express plasmid encoded genes as well as transgenes incorporated into viral vectors.[183, 184] While viral vectors yield increased transfection efficiencies compared to non-viral strategies, they induce inflammatory responses that may result in unwanted side effects and preclude repeat administrations.[185] *In vitro* and *in vivo* studies have shown that despite lower gene transfer efficiency with non-viral methods, site-specific administration of the gene still results in physiological effects within the tissue.[186, 187]

Some advantages of non-viral gene transfer are the ability for repeat administration of therapy and the potential for transient protein expression. Several clinical trials have demonstrated safety and efficacy for non-viral gene therapy in ischemic cardiovascular disease.[110]

We previously identified Stromal cell-Derived Factor-1, or SDF-1, as a naturally-occurring protein that is rapidly produced in response to ischemic tissue injury.[175] SDF-1 induction stimulates a number of protective anti-inflammatory pathways, is increased in the myocardium after a heart attack, but only lasts for a matter of days, and therefore the protective response quickly fades. This short duration of SDF-1 action reduces the potential for tissue repair. A non-viral plasmid producing SDF-1 for treatment of heart failure provides a potentially safe means through which to obtain longer, albeit transient (< 15 day) therapeutic protein production in the heart while allowing for the possibility of repeat injections.

In this study, we have demonstrated that the delivery of SDF-1 plasmid to the infarct border zone, 1 month after myocardial infarction, led to an increase in vascular density and improvement in cardiac function that was sustained 8 to 10 weeks after gene transfer. Our expression studies demonstrated that expression of our optimized plasmid peaked at day 2 post gene transfer and decreased over the following two weeks. These findings are consistent with previous literature showing a peak in CMV-driven gene expression, 2 days after injection in the rat heart.[169, 174] Peak expression in the presence of the RU5

element (pCMVe) was 10-fold greater than that seen in the non-enhanced CMV plasmid (pCMV).

The degree of functional changes with any given plasmid encoding hSDF-1 correlated with the level of luciferase expression achieved with that plasmid construct. We observed continued decline in cardiac function in the animals that received saline or the low expressing αMHC plasmid (pMHC). Four weeks after plasmid injection (8 weeks after MI) there was a decline in cardiac function in both these groups, which correlated with low expression profiles. Both CMV vectors resulted in an increase in cardiac vascular density. However, the animals that received the CMV plasmid with enhancer elements (pCMVe) increased cardiac function to a greater extent than those animals that received the CMV plasmid alone (pCMV).

Increased SDF-1 expression in the infarct border zone also led to a decrease in myocardial fibrosis at 8 to 10 weeks after plasmid injection. Similar to the change in vascular density, there was an inverse correlation between the degree of myocardial fibrosis and SDF-1 expression, suggesting that the mechanisms behind scar remodeling may be crucial to the understanding of the therapeutic response to SDF-1. These data suggest that SDF-1 treatment attenuates the progression of chronic ischemic heart failure and may partially reverse manifestations of the disease by increasing vasculogenesis, reducing scar formation and attenuating pathological cardiac remodeling after MI.

CHAPTER VI

IDENTIFICATION OF TARGETING PEPTIDES

6.1 Introduction

Gene therapy has evolved as a viable therapeutic option for treating patients with chronic conditions. We have optimized and established a vector system for delivering plasmid hSDF-1 to the myocardium in order to provide significant cardiac benefit, due to improved angiogenesis in the cardiac tissue. However, we injected this plasmid into the myocardial wall, thus requiring an invasive procedure in order to deliver the therapeutic gene. Injecting the plasmid directly into the myocardium, ensures maximum efficacy of the therapeutic gene, as it is delivered into the micro environment associated with the damaged tissue, therefore, improving the chances of the gene being taken up by these cells. However, delivery of naked plasmid into the tissues, increases the probability of

being subject to endosomal degradation. Therefore, only a smaller portion of the plasmid injected is taken up by the cells and then translated to the therapeutic protein. In order to protect the genes from degradation, scientists have studied various techniques to package the plasmid and safely deliver it to organs.[188,189] However, although this technique protects the DNA from being degraded, it does not eliminate the need for invasive surgery.

Systemic delivery of the plasmid, packaged into safe compartments is an optimal solution. Recent advances in identifying various polymeric carriers capable of encapsulating the DNA safely have spurred research into identifying efficient targeting ligands to direct the polymeric vectors to the organs of interest.

Phage libraries are able to provide a comprehensive list of peptide sequences that specifically bind to particular molecules. A large number of phage particles (approximately $10^{10\text{-}12}$) are exposed to a specific molecule, a certain organic compound, sugar molecule, or even cells in culture, to identify the few that bind to them.[160] An extension of this technique, is in vivo phage panning, where a similar number of phage particles are infused via a vein into an animal, to identify the few ones that specifically bind to the targeted organ.[158] These have shown to traverse intestinal mucosal layers, skin layers to target cells within them.[152] They have been used to identify targets for tumor cells, identify targets to the brain via an intra nasal pathway, and reach amyloid plaques with the help of antibodies.[150, 153, 155, 190] Infusion of phage display libraries within M13

bacteriophage may be useful in identifying specific ligands in the infarct region of the heart.

In this study, we hypothesized that delivering a large number of phage particles, with multiple copies of various peptides in the library, can lead us to one or a few targets to the infarcted zone in the heart. The main focus was to identify one or a few ligands that have a high affinity for infarct tissue and are specific to the heart. This can then be used to tag polymeric devices, or the naked plasmids to infuse therapeutic genes to the ischemic myocardium.

We infused the circular C7C peptide library in M13bacteriophages into rodents that exhibited chronic heart failure. 1.5 hours post infusion we removed the heart, separated the infarcted and border region, and eluted the phages in this region of the heart. This was amplified and panned for a second round. After 3 rounds of panning and sequencing of the peptides with affinity to the infarcted region of the heart, we identified the sequence to be a 7 peptide sequence of RQPRMKR (RR peptide) flanked on either sides by cysteines to provide a circular CRQPRMKRC ligand with selective affinity to the heart. On infusing this peptide tagged with a fluorescent label, we confirmed the targeting nature of this peptide with immunohistochemistry studies.

6.1.1 Mechanism of phage panning

The Ph.D. C7C library consists of random 7-mer peptides flanked by cysteines in order to conserve the 7-mer peptide by giving it a circular conformation. The cysteine residues are oxidized during phage assembly, and thus allow for a di-sulfide link that brings the 7-mer peptide to a circular construct, conserving its sequence. These 7-mer peptides are fused to the minor coat protein of the M13 bacteriophage via a linker sequence Gly-Gly-Gly-Ser. These variant libraries are expressed on the outside of the phage, while the genetic material encoding the 7 mer is inside the phage particle. The presence of the peptide on the surface, bound to the phage, creates a link that can bind the phage to selective targets, antibodies, receptors enzymes etc.

In vitro phage panning is carried out when multiple copies of each variant peptide is exposed to a surface antigen, the unbound phage is washed away and the resulting phage is eluted, amplified and exposed to a second surface with the antigen. Each such round is called panning. After 3 to 4 rounds of panning, an exclusive sequence is identified by DNA sequencing and ELISA, which binds to the antigen.[132, 150, 151]

In vivo phage panning refers to an extension of the *in vitro* phage panning, to identify potential ligands that bind to organs. Phage with its variant libraries is circulated through an animal, following infusion via a vein. The organs are harvested and the bound phage is eluted, amplified and identified.[155]

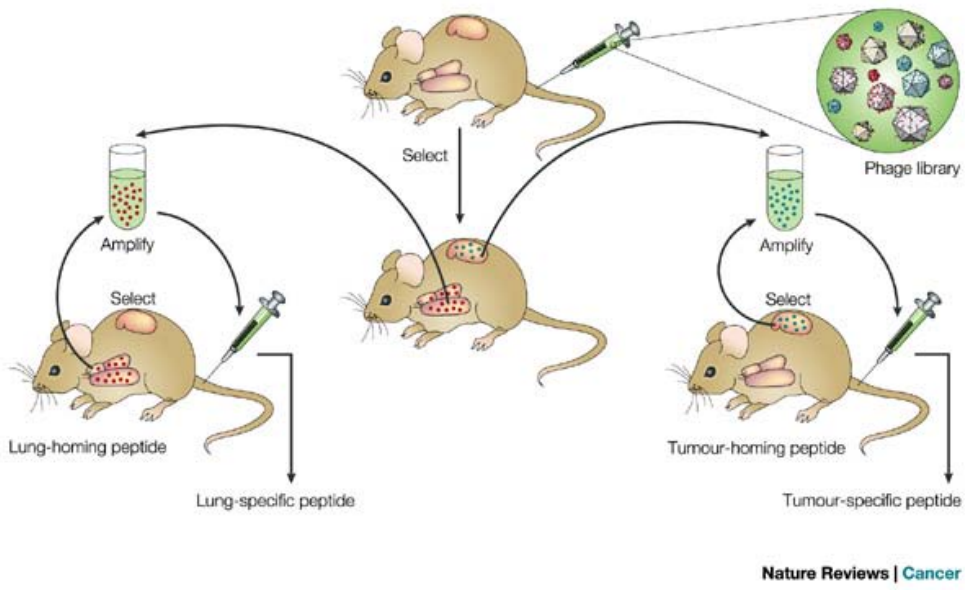

Figure 6-1 : Mechanism of *in vivo* phage panning technique in rodents.
Adapted from Nature Reviews Cancer 2, 83-90 (February 2002)

6.2 Methods:

6.2.1 Phage Panning

M13 phage library Ph.D.-7 (M13-based, complexity $\sim 2.8\times10^{9}$ transformants; New England BioLabs, Schwalbach, Germany) which displays random 7-mer peptides at the N-terminus of the pIII protein (high stringency: only 3–5 copies per phage particle) was used. 1.2×10^{11} pfu of phage library in 200 µl saline was delivered to three anesthetized Lewis rats (8–12 weeks old), one month post infarction via LAD ligation. LAD ligation is described above. These animals were sacrificed 1.5 hours post infusion. Following careful dissection to avoid any possible puncture of gastro-intestinal tract and exsanguinations by cutting jugular veins, the rats were perfused through the heart with

120 ml of saline to remove all blood. The hearts were removed and washed in ice cold saline. Tissues were weighed and, homogenized in 2 ml of tissue suspension buffer (DMEM, with 1% BSA and 10% protease inhibitors). Bound phage was eluted from this with glycine and stabilized with Tris. This was amplified with E Coli. 1.2×10^{11} pfu of amplified phage was re-infused via tail veins. This process was repeated three times. At the end of the 3rd round, eluted phage was sequenced and identified.

6.2.2 Peptide Synthesis and Analysis

The RQPRMKR peptide was synthesized by the Protein Core lab at the Cleveland Clinic and confirmed by mass spectrometry. This peptide was tagged with a His tag. A 6-His peptide was attached to the N terminal end, thus synthesizing a 6-His-RQPRMKR peptide (RR peptide).

Rats were infarcted via LAD ligation, as described before. One month post ligation, the RR peptide was infused via the tail vein. 1.5 hours later, the animal was sacrificed and the heart, lung, liver, spleen and kidney was excised, and washed in ice cold PBS.

6.2.3 Immunohistochemistry

Organs were embedded in OCT compound and were frozen immediately. The tissue samples were stored for long periods of time at -80°C. Frozen samples were cut in a cryotome at 5micron thickness and mounted on slides. Tissue specimens were fixed with

paraformaldehyde and incubated with 1% normal blocking serum with goat and donkey serum in PBS for 60 min to suppress nonspecific binding of IgG. Slides were then incubated for 60 min with mouse monoclonal anti His antibody (Abcam Cambridge, MA) at 1:200 dilutions in blocking buffer with serum. Slides were then washed with phosphate-buffered saline (PBS) and incubated for 45 min, with IgG goat anti-mouse Alexa fluor 488 (Molecular Probes, Invitrogen, Carlsbad, CA) at 1:800 dilution in blocking buffer with serum in a dark chamber. After washing extensively with PBS, coverslips were mounted with aqueous mounting medium. (Vectashield Mounting Medium with DAPI H-1200; Vector Laboratories, Burlingame, CA, USA).

6.3 Results

6.3.1 Identification of targeting peptide

In vivo phage panning was performed in rats with LAD ligation, one month post infraction. Infarction in the hearts was confirmed by echocardiography. $1.2x10^{12}$ particles was infused via the tail vein. 1.5 hours later, when the particles have had enough time to circulate through the body, hearts were excised. The blanched region was identified as the infarct zone. The region in between this zone and the healthy tissue is termed the border zone. Tissue sections were washed in ice cold saline, and the blanched region was sectioned out. Tissues were homogenized and the phage was eluted. Phage was sequenced using primers provided in the kit. Three colonies were picked after each round

of panning. After three rounds of panning, a common sequence of Arg-Glu-Pro-Arg-Met-Lys-Arg (RQPRMKR) was identified. (Figure 6-2)

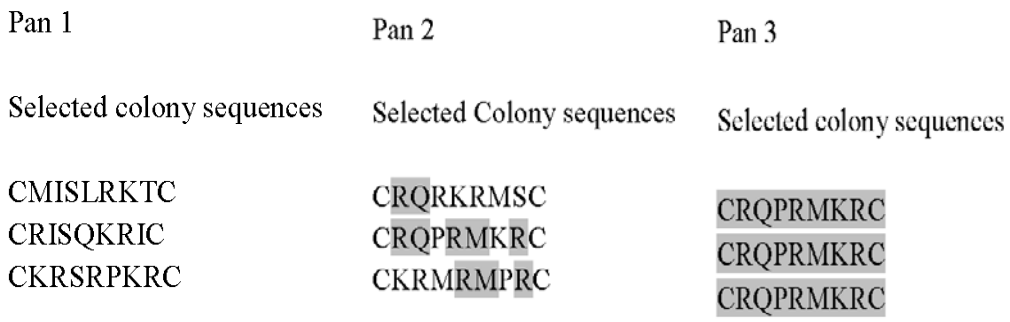

Figure 6-2 : Phage panning to determine a targeting sequence to the ischemic heart
Colonies obtained from rodents (n=3) after each panning cycle were sequenced to identify the phage that bound to the ischemic hearts in their respective cycles. The first pan identified multiple sequences but after the third round a common sequence was identified.

6.3.2 Synthetic Peptide Formulation and Analysis

This peptide was synthesized at the CC Proteomics Core lab. The peptides were synthesized with a fluorescent tag attached to one end. A $(His)_6$ – RQPRMKR peptide was synthesized and the purity was checked by reverse phase liquid chromatography. The mass was determined using a mass spectrometer and was recorded at 1794.60 units using a 4700 Reflector Spectrometer.

6.3.3 *In Vivo* Expression Profile of the RR peptide

The RR peptide tagged with His was infused at 200 µg of peptide in 200 µl of PBS into tail veins in rodents, one month after LAD ligation. Prior to infusion, rats hearts were imaged via echocardiography to ensure an akinetic wall motion and a loss in fractional shortening (<30%). The rats were then perfused with saline, and the organs were excised and embedded in OCT compound. Sections were made and the tissue samples were stained with fluorescent antibody markers against His and Dapi for nuclear detection. Heart sections were stained positive against the His antibody, thereby confirming the presence of the $(His)_6$ – RR peptide. All other organs, lungs, spleen, liver and kidney were stained negative for His, thus confirming the absence of this peptide in all other organs. (Figure 6-3)

The RR peptide specifically targets the heart tissues and has high affinity to the infarct region. This peptide may be used as a targeting molecule to direct therapeutic drugs and genes to the infarct region.

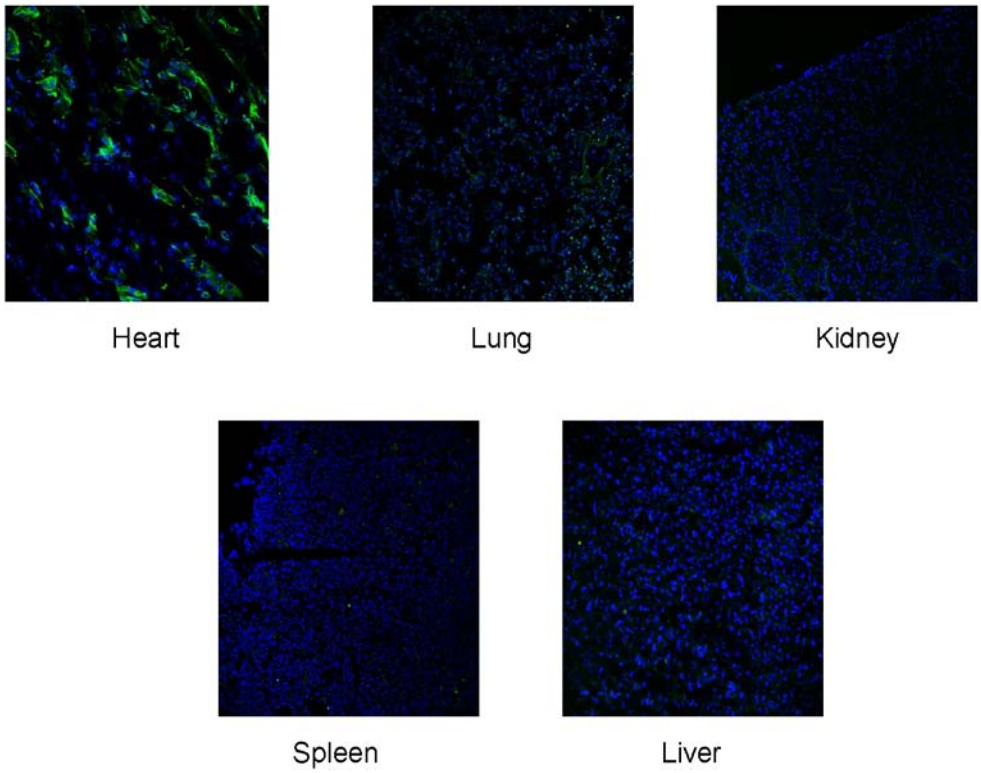

Figure 6-3 : Specificity of peptide interaction with heart tissues
Rodent hearts were frozen and then stained for His antibody. A "His" tag was attached to the peptide sequence thus a positive His stain correlated with a positive peptide identification. Peptides were infused via the tail vein and translocated to the heart tissue specifically.

6.3.4 BLAST Analysis of the targeting peptide

The RQPRMKR sequence with the genomic code of agg cag ccg cgc atg aag cgg was compared against all the known sequences n the rat genome using the BLAST software. There were some similarities in the sequence code with other known protein sequences such as FAS Associated Factor -1 (FAF-1) which has the sequence *qive**rqprm**ldfrveyrdrn* and another protein, Sodium-dependent phosphate transporter 1 or Solute carrier family 20 member 1 a.k.a. Phosphate transporter 1 (PiT-1) which has a sequence *wffvc**prmkr**kierevkssp*. But neither of these sequences possesses all the 7-mer

sequence, therefore a conclusive evidence of either of these two proteins is lacking. (Figure 6-4)

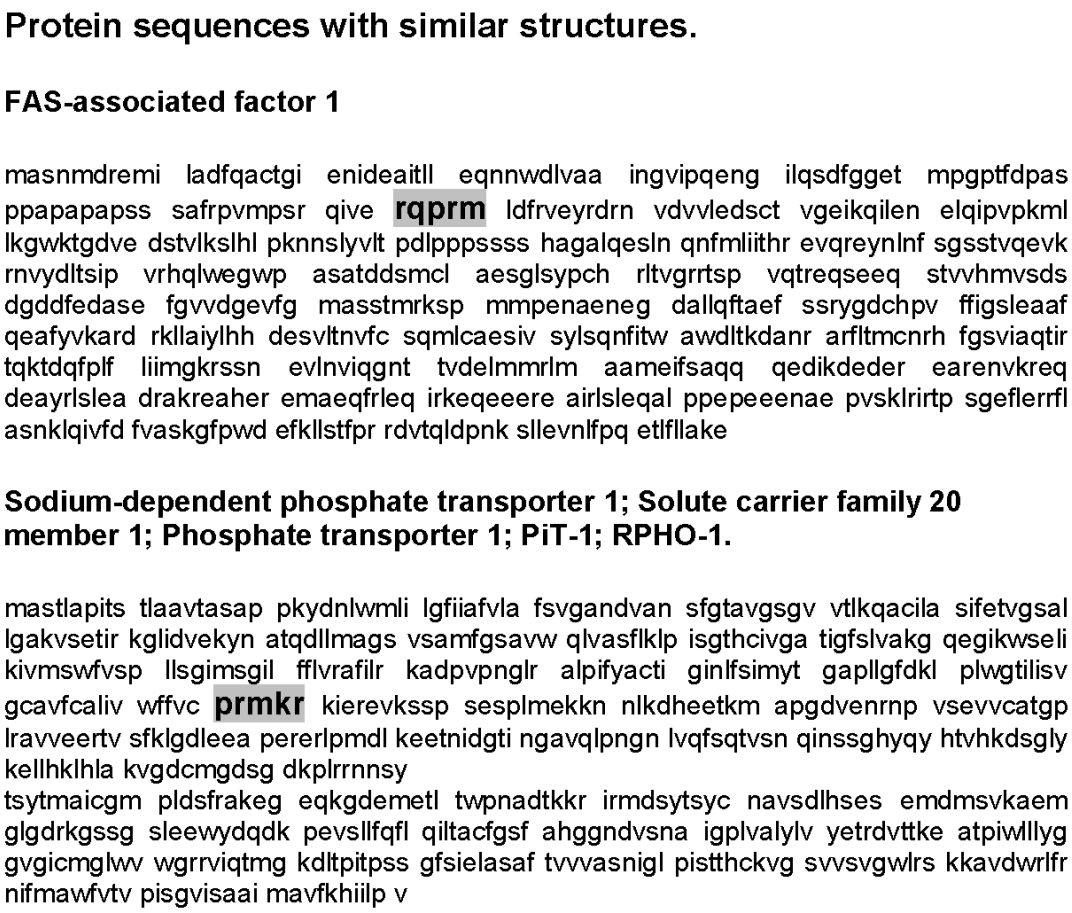

Figure 6-4 : BLAST Analysis of the peptide sequence with other known proteins
BLAST analysis provides a comparison between a known peptide sequence to the whole genome to identify potential peptide targets or proteins associated with the peptide. Analyzing the targeting peptide against the rat genome using the BLAST software provided two potential protein targets, FAF-1 and PiT-1.

6.4 Discussion

Targeting peptides are an essential component in delivering genes or encapsulated drugs to the organ of interest. There has been a growing body of researchers trying to develop micro particles, and other polymeric compounds to devise novel means to encapsulate genes and drugs to protect their safety from degradation.[191] However, on the other hand, research involving the identification of targeting ligands has been slow to progress. This is partly due to the lack of effective libraries required for screening of ligands. Previously, researchers studied various angiogenic and inflammatory pathways that were triggered during injury to build a library of possible ligands and then screened them to identify effective ones. This poses a problem with missing out on ligands that were not included as part of the list.[159]

The PhD library, using phages has revolutionized the screening for target compounds to complex diseases, such as cancer.[155] The PhD libraries provide every possible combination of the whole genome, and thus are useful in identifying ligands that may be involved in targeting.[150] However, the repeated panning cycles, are responsible for the high selectivity in this process. The prepared libraries have sufficient complexity to produce multiple DNA sequences encoding the same consensus peptide motifs. These libraries are used for various purposes, ranging from epitope mapping, material-specific peptide identification, in vitro testing and identification, small molecule discoveries, enzyme substrates and various in vivo applications.[148, 149, 151, 154, 160] The Ph.D. libraries have been used extensively for discovery of peptide antagonists of VEGF-mediated

angiogenesis, trans-dermal trafficking and trans-intestinal trafficking peptides, and cell targeting peptides.[151, 152, 155]

In our study we have identified and confirmed a peptide sequence of RQPRMKR, with some unknown binding sites that may relate to the FAF-1 peptide or the PiT-1 peptide. This sequence was identified after three different panning rounds. This peptide was synthetically made and tagged with a fluorescent label of 6-His. This peptide sequence was specific among $1.2x10^{11}$ pfu of phage and demonstrated specificity to the heart tissue as compared to the various other organs. When used as a tagging peptide to nanocarriers, this peptide will be capable of transporting the carriers to the heart alone, and thus reduce risks of secondary organ complications.

This study now opens the doors towards the application of this targeting peptide in multiple applications involving the failed heart, thus providing the solution to systemic delivery of drugs for patients, who are incapable of undergoing a surgical procedure.

CHAPTER VII

ENGINEERED NANOPARTICLES AS CARRIERS FOR SYSTEMIC DELIVERY

7.1 Introduction

Gene therapy has evolved as a promising option to deliver pro-angiogenic proteins to infarct zones, thus providing cardiac benefit. We have identified a gene design without viral promoters, using the ubiquitously-expressing CMV promoter and transcription enhancers, to improve the length and magnitude of gene expression as compared to traditional naked plasmid deliveries. Using this design we delivered therapeutic levels of Stromal Derived Cell Factor-1 (SDF-1) (which is pro-angiogenic) in rodents and pigs with chronic heart failure, by direct injection in the border zone, thereby improving cardiac function. To target cardiac myocytes in the infarct zone, we also generated a

vector with a cardiac-specific αMHC promoter. On assessing the gene expression, *in vivo*, we observed that non-enhanced αMHC driven plasmids have low magnitudes of expression which could be increased 10-fold, to therapeutic levels, with transcriptional enhancers. This therapy is safe, effective, and the benefits can last long after the expression of the gene is lost. We have also studied and identified targeting peptides that allow for systemic targeting to the heart.

However, the need for improving penetration of the genes into the cells has long been a challenge. Studies with cell penetrating peptides, such as TAT, VP22, etc have shown improvements in cell penetration of therapeutic drugs.[192-195] Encapsulations of drugs and plasmids within polymeric devices have been studied extensively. The need for biodegradable particles, to encapsulate drugs, and deliver them safely to injured tissue, in an active form, has been the reason for the development and growth of nanoparticulate systems. PLGA (poly lactide co glycolide) is a poly ester with growing interest due to its stability, ability to bind targeting ligands to the surface, regulated control of release of the encapsulated plasmid in the cytoplasm, ability to be degraded *in vivo*, following the release of the plasmid, and approval for use in human trials by the FDA.[114, 118] Our focus was to engineer a polymeric carrier that is capable of targeting the ischemic myocardium and delivering therapeutic drugs to it. PLGA polymeric devices may be able to encapsulate therapeutic genes and deliver them safely to tissues via the systemic circulation.

We hypothesized that encapsulating the gene of interest into PLGA polymeric particles, tagged with the RQPRMKR (RR) peptide will be able to provide a targeting encapsulated drug capable of homing to the ischemic myocardium via systemic delivery. The targeting peptide, RR, when tagged to the polymeric complex, will be viable and in its active form, and will be able to direct the polymeric complex to the injured myocardium. The PLGA polymer will then be able to release the encapsulated material into the area of injury.

To understand the behavior of encapsulated drugs *in vivo*, and to determine the efficacy of this system, various strategies have been studied in the past. Fluorescent nanoparticles with polystyrene have been used as models to understand tissue uptake and trafficking.[196] Other strategies have employed gold colloidal particles that can be viewed by transmission electron microscopy due to its dense matter.[197] 6 Coumarin (6C) is a lipophilic fluorescent dye that can be viewed by confocal microscopy, and its fluorescence activity can be accurately measured by High Performance Liquid Chromatography (HPLC) analysis.[127,198] Our focus was to design a nanoparticulate carrier capable of encapsulating 6C, a fluorescent dye, and delivering it to the myocardium, with the help of a tagging peptide. The uptake and in vivo trafficking would then be monitored to determine the dose, time, and other aspects associated with this delivery system.

In order to determine the release and uptake of nanoparticles *in vitro*, we added nanoparticles with or without the homing peptide to cardiac fibroblasts seeded on 6 well

plates. As expected, we did not see a difference in fluorescence between the two groups. The uptake took place in about 30 minutes and stayed for more than 24 hours. *In vivo*, we observed a greater uptake of nanoparticles, as determined by the amount of fluorescence in various organs, in the injured myocardium, as opposed to the healthy myocardium. RR peptide helps target the encapsulated material to the injured myocardium.

On replacing the 6C dye with a therapeutic gene, such as SDF-1 we may be able to show improved cardiac benefit via systemic delivery, capable of translating this complex, to patients with chronic heart failure.

7.2 Methods

7.2.1 Materials

BSA (Fraction V) and PVA (average molecular weight, 30,000–70,000) were purchased from Sigma (St. Louis, MO). 6-Coumarin was purchased from Polysciences (Warrington, PA). PLGA (50:50 lactide–glycolide ratio, 143,000 Da, viscosity 0.87dl/g) was purchased from Birmingham Polymers (Birmingham, AL). RR-peptide of the sequence $(His)_6$- Arg-Glu-Pro-Arg-Met-Lys-Arg (molecular weight 1784) was custom synthesized by Cleveland Clinic Proteomics Core(Cleveland, OH). Denacol_ EX-521 (Pentaepoxy, molecular weight 742) was a gift from Nagase Chemicals Ltd (Tokyo, Japan). Zinc tetrahydrofluroborate hydrate, poly(vinyl alcohol) (PVA, average molecular weight 30,000–70,000), dextran, boric acid, and ethanol were obtained from Sigma

Chemical Co. (St. Louis, MO). Chloroform was obtained from Fisher Scientific (Pittsburgh, PA).

7.2.2 Formulation of 6C loaded PLGA nanoparticles

Nanoparticles containing BSA and 6-coumarin were formulated using a double emulsion-solvent evaporation technique as described previously. An aqueous solution of BSA (60 mg/ml, 1 ml) was emulsified in a PLGA solution (180 mg in 6ml chloroform) containing 6-coumarin (100µg) using a probe sonicator (55W for 2 min) (Sonicator® XL, Misonix, NY). The water-in-oil emulsion formed was further emulsified into 50 ml of 2.5% w/v aqueous solution of PVA by sonication (55W for 5 min) to form a multiple water-in-oil-in-water emulsion. The multiple emulsion was stirred for ~18 h at room temperature followed by for 1 h in a desiccator under vacuum to remove the residual chloroform. Nanoparticles were recovered by ultracentrifugation (35,000 rpm for 20 min at 4 ℃, OptimaTM LE-80K, Beckman, Palo Alta, CA), washed two times with distilled water to remove PVA, unentrapped BSA and 6-coumarin, and then lyophilized (−80 ℃ and <10_m mercury pressure, SentryTM, Virtis, Gardiner, NY) for 48 h to obtain a dry powder. Dry lyophilized nanoparticle samples were stored in a desiccator at 4℃ and were reconstituted in a suitable medium (buffer or cell culture medium) prior to an experiment.

7.2.3 Conjugation of targeting peptide:

The peptide to be conjugated is the RQPRMKR peptide, identified via phage panning experiments. Prior to conjugation, the peptide is tagged with $(His)_6$ residues in its N terminal. The peptide was conjugated to the nanoparticles in two steps.

Step 1: Surface activation step: nanoparticles were suspended in borate buffer (50mM, pH 5.0) by sonication for 30 sec on an ice bath. This is followed by the addition of Denacol (40 mg), an epoxy that helps conjugation of the peptide on the surface and the catalyst zinc tetrahydrofluroborate hydrate (50 mg) also dissolved in an equal volume of buffer to the NP solution. This mixture was stirred gently for 30 minutes at 37C. NPs were separated by ultracentrifugation at 30000 rpm for 20 minutes at 4C. Any unreacted Denacol is removed by multiple wash steps.

Step 2 : Conjugation of peptide: Surface activated NPs were suspended in borate buffer (4 ml) and stirred into a solution containing three different initial amounts of peptides; 250ug, 500ug and 1 mg in borate buffer. This reaction is carried out for 2 hours at 37C. The unreacted peptide was removed by ultracentrifugation and the final nanoparticles suspension was lyophilized for 48 hours.

7.2.4 Nanoparticle characterization

Particle size and surface charge (zeta potential).

Particle size and size distribution were determined by photon correlation spectroscopy (PCS) using quasi-elastic light scattering equipment (ZetaPlusTM equipped with particle sizing mode, Brookhaven Instrument Crop., Holtsville, NY). A dilute suspension (100µg/ml) of nanoparticles was prepared in double distilled water and sonicated on an ice bath for 30 s. The sample was subjected to particle size analysis. Zeta potential of nanoparticles in 0.001M double distilled water, was determined using ZetaPlusTM in the zeta potential analysis mode.

7.2.5 *In vitro* expression and uptake of 6-coumarin

Rat cardiac fibroblasts (abbreviated as rCFs,) cultured in DMEM Medium with 10% fetal bovine serum (Gibco, NY) and 1% penicillin G and streptomycin (Gibco BRL, Grand Island, NY), were used for all the cell culture studies. The cells were seeded at 200,000 cells per well/1 ml (50% confluency) in a 6-well plate and allowed to attach overnight. Nanoparticles were added at different doses in 1 ml of the medium and incubated for 2 days. Untreated cells (plain medium) were used as a control. At the end of the incubation period, cells were washed twice with phosphate buffered saline (PBS, pH 7.4) to remove nanoparticles and 1 ml of fresh medium was added to each well. The

uptake of the nanoparticles in the cells was determined using optical microscopy studies, and high performance liquid chromatography (HPLC) analysis

7.2.6 Extraction and quantitation of 6C fluorescence in cells

Cells were washed with PBS three times and were solubilized in 1% Triton X 100 solution. This suspension was stored at -80°C overnight and lyophilized for 48 hours. Lyophilized cell lysates were reconstituted in methanol (500ul) and incubated at 37°C for 18 hours to extract the dye. Samples were centrifuged at 14000 rpm for 10 minutes at 4°C to remove cell debris. Supernatants were collected for HPLC analysis. A standard curve is obtained by adding 8 µg to 40 µg of nanoparticles in Triton X 100 solution and lyophilized as the cell samples.

7.2.7 Confocal Microscopy Analysis

rCFs were plated on coverslips in 6 well plates at 50,000 cells per well (50% confluency) in 1 ml of culture medium and allowed to attach for 24 h. Cells were then incubated with 6-coumarin loaded nanoparticle suspension (200µg/ml) in growth medium for 60 min. Cells were then washed twice with PBS and visualized with a Zeiss Confocal LSM410 microscope equipped with 488 nm excitation laser (Carl Zeiss Microimaging, Inc., Thornwood, NY).

7.2.8 *In vivo* Expression Analysis

Rats were infarcted via LAD ligation, as described above. 4 weeks post infarction, nanoparticles with or without the tagging peptide was infused via the tail vein at 200 µg of particles per animal in 200µl of PBS. The nanoparticles were allowed to circulate overnight, after which the animals were sacrificed by de-sanguination by perfusion with saline, and the organs (heart and liver) were excised. Heart tissues were divided based on the region of infarct or the healthy region. The wet weight of the tissues was recorded. Samples were homogenized in 2 ml of distilled water using a tissue homogenizer. The homogenized samples were then lyophilized for 48 hours. The 6C dye from the homogenized tissue was extracted by shaking with 5 ml of methanol at 37°C for 24 hours at 100 rpm using an Environ orbital shaker. Standard curve was obtained by samples varying from 8 µg to 40µg of the nanoparticles in methanol. Tissue extracts were centrifuged at 14000 rpm for 10 minutes to remove cell debris. The supernatant was collected and this was used for HPLC analysis.

7.2.9 HPLC Analysis

A Shimadzu HPLC system (Shimadzu Scientific Instruments, Columbia, MO) fitted with an SCL-10A system controller, an SIL-10A auto-injector, LC-10AT pump, a RF-10A XL fluorescence detector, and Class VP chromatography data system software version 4.2 was used. A Nova pak C-8 column with spherical particles (4 mm) and pore size of 60A ° (Waters, Milford, MA) and the mobile phase consisting of acetonitrile

/water (65:35) containing 5mM sodium salt of 1-heptane sulfonic acid (Aldrich, Milwaukee, WI) set at a flow rate of 0.8 ml/min were used to resolve the dye peak. Excitation and emission wavelengths were 450 and 490 nm respectively. A 20 ml aliquot of each sample was injected into HPLC. The retention time of 6-coumarin was 2.6 min. The amount of nanoparticles in different tissue samples was determined from a calibration curve plotted between the fluorescent intensity and the amount of fluorescently labeled nanoparticles that were treated similar to the tissue samples. There was no background peak for the control tissue (without nanoparticles). The assay is sensitive enough to detect as low as 5 ng nanoparticles in the tissue samples.

7.3 Results

7.3.1 Formulation of Nanoparticles

Nanoparticles with 6 Coumarin as a fluorescent marker and BSA as a model protein were formulated. Nanoparticles had a typical protein loading of 20% (w/w). As in, 20 mg of BSA was present in 100 mg of nanoparticles.

7.3.2 Particle Size Analysis and Zeta Potential

Particle size distribution was analyzed by dynamic light scattering technique. The size of the unconjugated PLGA polymer encapsulating the 6C dye in BSA was found to be 0.095 microns or 95 ±12.3 nm. The conjugated PLGA polymer with the tagging

peptide on the surface had an average size of 103 ± 11 nm indicating uniform particle size distribution. When these particle sizes were analyzed before sonicating them, the mean particle size was 600 ± 350 nm indicating the importance of sonicating on these particles.

The zeta potential, corresponding to the surface charge was recorded at -14.72 ± 0.95 mV for the unconjugated particles and -11.04 ± 6.22 mV for the conjugated particles.

Nanoparticles were resuspended easily after lyophilization to form a stable colloidal dispersion without any change in size or content. In previous studies, it has been shown that 99.4% of the entrapped dye remains associated with the nanoparticles even after 48 h of in vitro release study under constant conditions. [199]Therefore, these nanoparticles serve as a good model formulation to study the tissue uptake in vivo in acute experiments. Furthermore, one can use these nanoparticles to quantitate the uptake as well as to study their localization in the cells/tissue by fluorescence microscopy

7.3.3 *In vitro* Expression Analysis

Dose Analysis

Rat cardiac fibroblasts were cultured in DMEM Medium with 10% fetal bovine serum and 1% penicillin and streptomycin. The cells were seeded at 50,000 cells per well in 1 ml of culture medium (50% confluency) in a 6-well plate and allowed to attach

overnight. Nanoparticles with the conjugated peptides were added at different doses ranging between 10 µg of nanoparticles to 1 mg of nanoparticles per well in 1 ml of the medium and incubated overnight. At the end of the incubation period, cells were washed twice with phosphate buffered saline (PBS, pH 7.4) to remove nanoparticles and 1 ml of fresh medium was added to each well. The cells were then viewed using optical microscopy (Figure 7-1).

When less than 100 µg of particles were added to the wells, the signal obtained was almost inconceivable. On the other hand a strong signal was observed at 500 µg of particles and 1 mg of particles per well. A minimum of 200 µg per well of particles are required for an observable signal. For future studies 200 µg of particles per well was used.

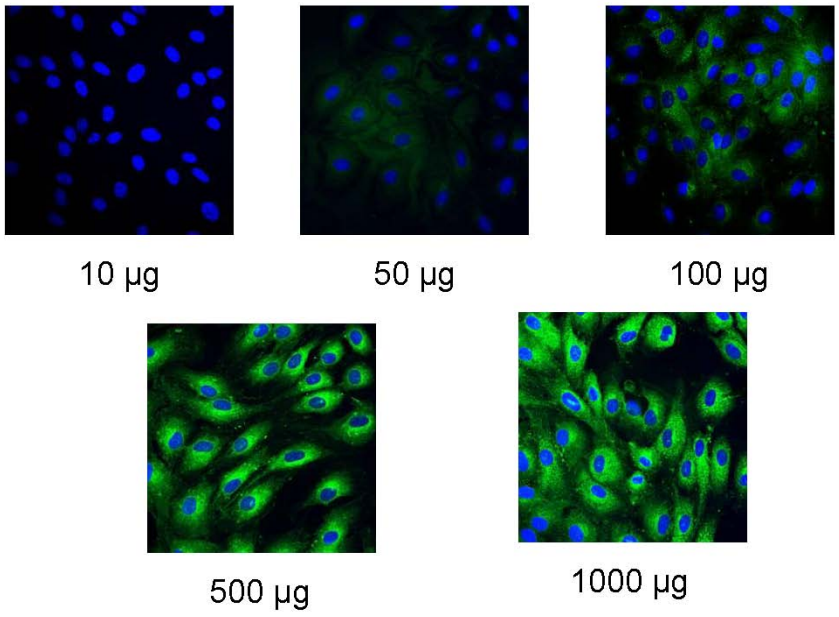

Figure 7-1 : Dose response with un-conjugated nanoparticles encapsulating 6C
Cardiac fibroblasts were cultured and nanoparticles encapsulating a fluorescent dye, 6C, were added to this in varying doses. The signal obtained correlates to the amount of 6C that released inside the cells. A 200µg dose was used for future studies.

7.3.4 Time for Uptake

Rat cardiac fibroblasts were cultured in DME Medium with 10% fetal bovine serum and 1% penicillin and streptomycin. The cells were seeded at 50,000 cells per well / 1 ml of culture medium (50% confluency) in a 6-well plate and allowed to attach overnight. Nanoparticles with and without the conjugated peptides were added at 200 µg of nanoparticles per well in 1 ml of the medium and incubated for varying lengths of time varying between 30 minutes and 24 hours to determine the optimum time for uptake. Unconjugated nanoparticles were used as controls. At the end of the incubation period, cells were washed twice with phosphate buffered saline (PBS, pH 7.4) to remove nanoparticles and 1 ml of fresh medium was added to each well. The cells were then viewed using optical microscopy

When the cells were analyzed at 30 minutes or less, no significant signal was observed. However, after 1 hour there was an observable signal that increased for upto 3 hours, following which the signal remained constant for up to 24 hours. For future in vitro studies, nanoparticles will be added for a period of 2 hours before it is washed away. (Figure 7-2)

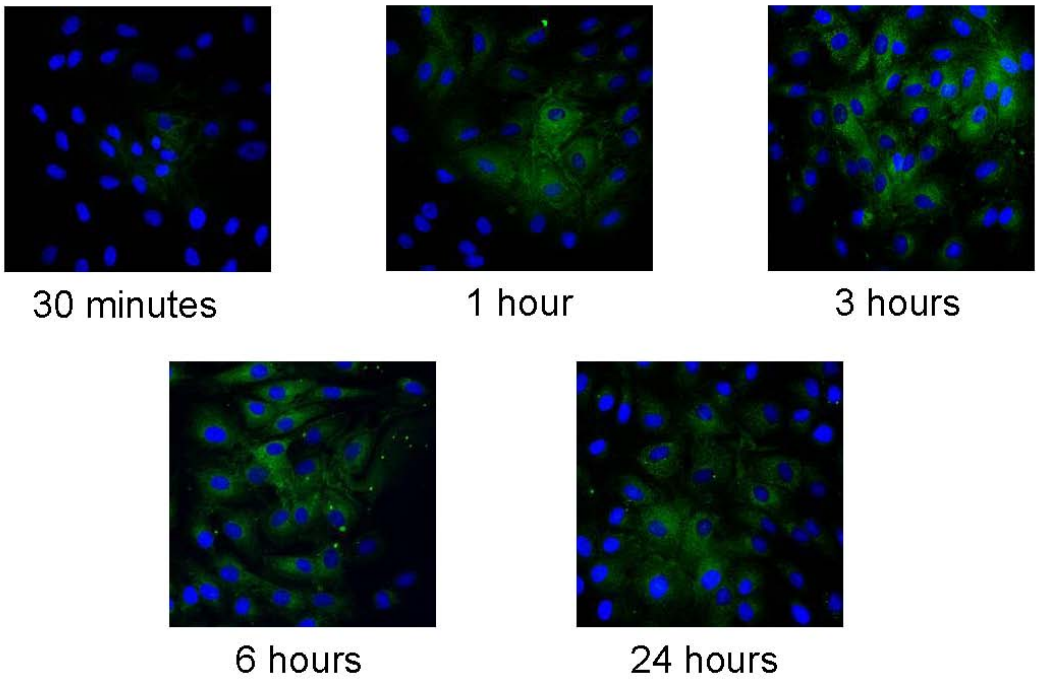

Figure 7-2 : Time response with un-conjugated nanoparticles encapsulating 6C
Rat cardiac fibroblasts were cultured onto 6 well plated and 200µg of nanoparticles without any targeting peptide were added to this. The time taken for release of the nanoparticles into the cells and the endocytosis was determined by imaging cells ant various time points following the addition of nanoparticles. 6C signal was obtained 1 hour following the addition and lasted for more than 24 hours.

As expected, there was no significant difference in signal between the two nanoparticles types, whether conjugated or un-conjugated. Particles were added to the wells and did not have to target any specific cell type. In fact, there seemed to be a slight increase in particle uptake with un-conjugated particles. (Figure 7-3) Therefore in order to address this, a quantitative study was performed with conjugated and un-conjugated particles, at 200 µg of particles per well following 2 hours of uptake.

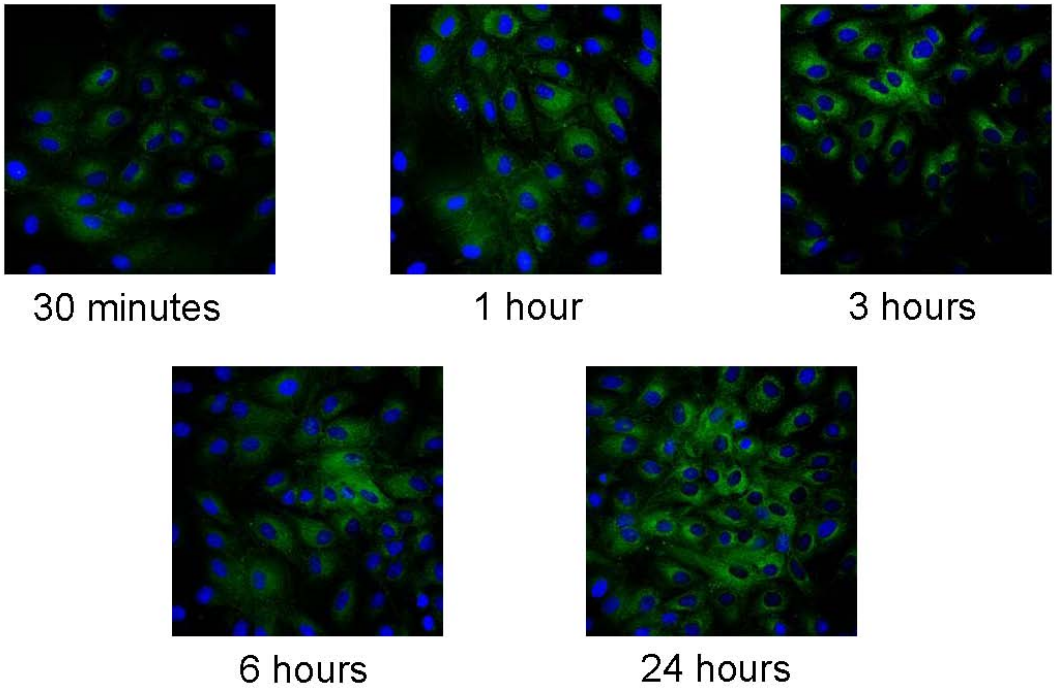

Figure 7-3 : Time response of nanoparticles with 6C conjugated with RR peptide
Rat cardiac fibroblasts were cultured onto 6 well plated and 200µg of nanoparticles with targeting peptide were added to this. On imaging these cells at various time points, 6C signal was obtained 1 hour following the addition and lasted for more than 24 hours similar to the results obtained from un-conjugated nanoparticles

7.3.5 HPLC Analysis with *in vitro* particle study

Rat cardiac fibroblasts were cultured in the appropriate medium at 50,000 cells per well/1 ml of culture medium (50% confluency) in a 6-well plate and allowed to attach overnight. Nanoparticles with and without the conjugated peptides were added at 200 µg of nanoparticles per well in 1 ml of the medium and incubated 2 hours. Unconjugated nanoparticles were used as controls. At the end of the incubation period, cells were washed twice with phosphate buffered saline (PBS, pH 7.4) to remove nanoparticles and 1 ml of fresh medium was added to each well and were solubilized in 1% Triton X 100

solution. This solution was lyophilized for 48 hours, and cell lysates were reconstituted in methanol (500ul) and incubated at 37℃ for 18 hours to extract the dye. Samples were centrifuged at 14000 rpm for 10 minutes at 4℃ to remove cell debris. Supernatants were collected for HPLC analysis. A Standard curve was obtained by adding 8 µg to 40 µg of nanoparticles in Triton X 100 solution and lyophilized as with the cell samples.

Following the HPLC analysis, the amount of fluorescent dye extracted from the un-conjugated particles was 14.89 ±2.1 µg per well and the amount of 6C dye extracted from conjugated nanoparticles was 11.97 ± 3.24 µg per well. There is a slight decrease in the loading of conjugated particles that may be attributed to the slightly smaller sizes as compared to the un-conjugated particles. However, this difference is not significant. However, when unsonicated 6C unconjugated nanoparticles were used, this uptake dropped to almost half, indicating the importance of particle size on uptake. (Figure 7-4)

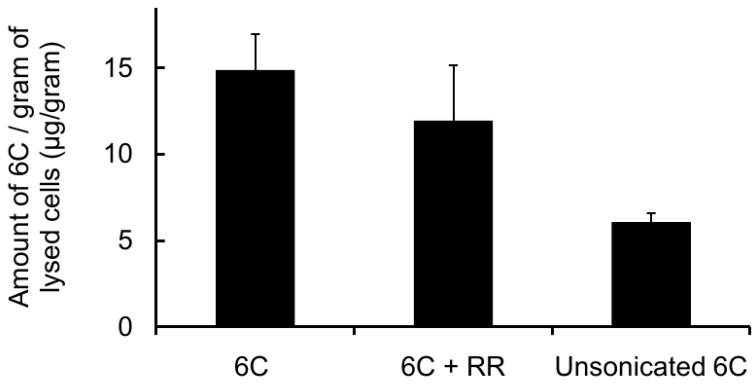

Figure 7-4 : *In vitro* HPLC analysis to determine amount of 6C in cardiac fibroblasts

Both conjugated and unconjugated nanoparticles had similar sizes. A quantitative analysis between the unconjugated and conjugated nanoparticles revealed similar amounts of nanoparticles being taken up by cardiac fibroblasts in culture. However, unsonicated nanoparticles that had a larger size exhibited lower uptake.

7.3.6 *In vivo* nanoparticle uptake in rodents

4 weeks post infarction via LAD ligation in rodents, nanoparticles with or without the tagging peptide was infused via the tail vein at 200 µg of particles per animal in 200µl of PBS. The nanoparticles were allowed to circulate overnight, and the organs (heart and liver) were excised. Heart tissues were divided between infarcted and healthy regions. The wet weight of the tissues was recorded. Samples were homogenized, lyophilized and the 6C dye from the homogenized tissue was extracted by shaking with 5 ml of methanol at 37°C for 24 hours at 100 rpm. Tissue extracts were centrifuged at 14000 rpm for 10 minutes to remove cell debris. The supernatant was collected and this was used for HPLC analysis. Standard curve was obtained by samples varying from 8 µg to 40µg of the nanoparticles in methanol.

On analyzing the HPLC results, it was observed that infarcted tissue regions had more 6 C extracted from them, as compared to healthy tissues (n=3) (Figure 7-5). Also, the amount of fluorescence intensity observed in the infarcted region of the heart increased when nanoparticles with the homing peptide were infused as compared to when nanoparticles alone were used. This increase in fluorescence intensity was significant, with a p value of < 0.01 (Figure 7-6). When particles were conjugated with the ischemic heart targeting peptide, they travelled to the infarcted region of the heart.

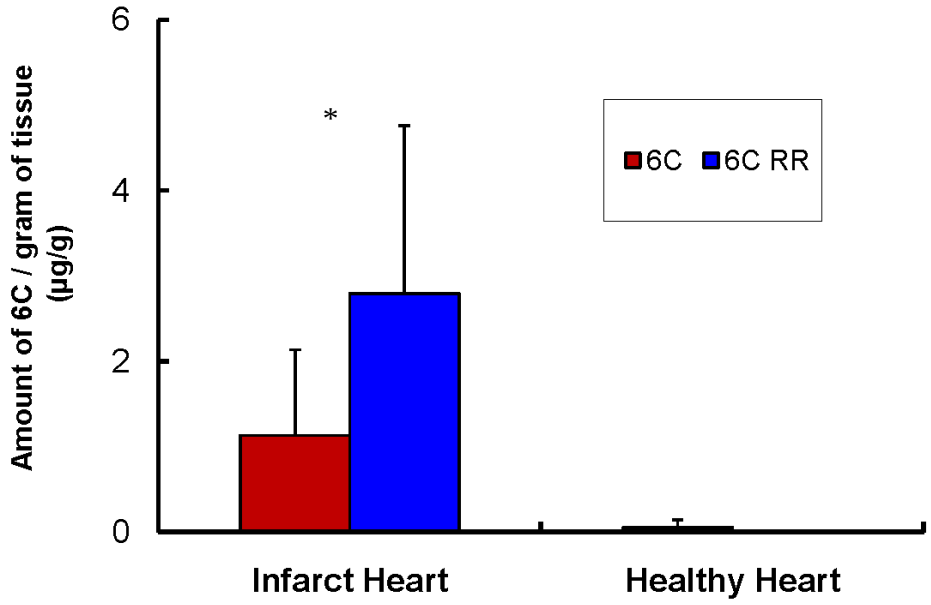

Figure 7-5 : *In vivo* HPLC analysis between infarct and healthy regions of the heart
On comparing infarcted tissue and healthy tissue for the amount of nanoparticles that released the fluorescent dye, 6C in them, we observed a greater amount of nanoparticles that targeted the infarct heart as compared to the healthy heart when a targeting peptide was used to conjugate the nanoparticles.

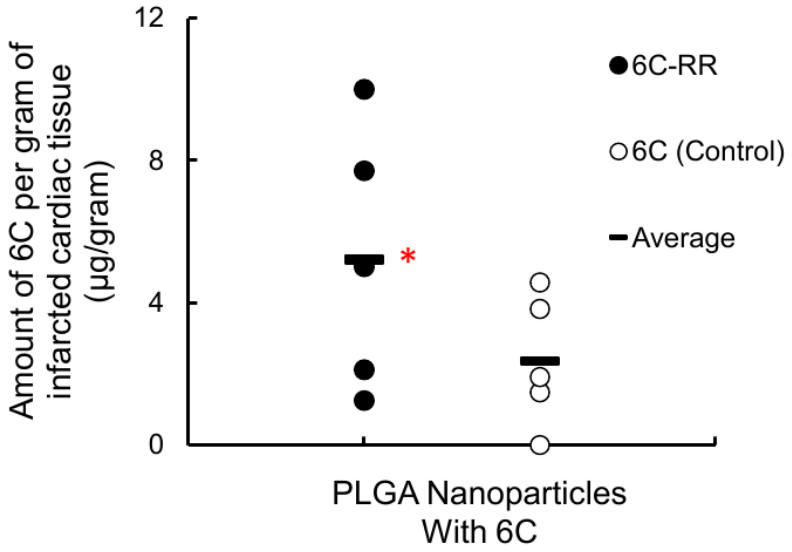

Figure 7-6 : Difference in uptake in infarcted tissue with conjugation of nanoparticles
A greater number of nanoparticles targeted the infarct heart when a targeting peptide was conjugated to the surface of the PLGA polymer. (n=5), $p<0.05$

7.4 Discussion

Regenerative medicine aims to repair and retain the function of cardiac tissues following ischemia. The most viable of these therapeutic options is the use of genes that can trigger various other pathways responsible for alleviating the symptoms of cardiac failure. The use of non viral gene therapy is a safe and non toxic method of providing these genes to injured tissues, allowing them to repair and regenerate the tissue to mediate benefit in function. However, although non viral naked gene therapy may be a viable option in vitro, it is subject to degradation in vivo, by lysosomes in the cytoplasm.[109] DNA plasmids have a polynucleotide structure and thus are negatively charged and hydrophobic in nature. This poses a challenge for traversing the tissue layers, and they are easily degraded in the system.[191] In order to overcome this, genes need to be properly condensed to a size that can be taken up by cells. The encapsulation of these genes within polymeric carriers may provide an efficient, non toxic, yet safe delivery mechanism for sustained intra cellular delivery of these therapeutic agents. However this delivery platform has some limitations as the plasmid needs to be condensed to allow encapsulation within the nanoparticle. Following that, the whole assembly needs to be stable during formulation and in vivo. This complex should be capable of being targeted to the tissue or cells of choice by either a surface ligand or by possessing a specific promoter element in the plasmid, or both. And lastly, following intra cellular delivery, these encapsulated particles need to be released in their viable form else they will be sequestered and exited from the cells by lysosomal endosmosis.[114]

PLGA offers a viable, effective and safe delivery of therapeutic agents; drugs and genes, due to its capability release the encapsulated material intra cellular. Also, it is capable of attaching surface ligands and can thus be modified for specific tissue targeting.[114,118] We wanted to test the efficacy and safety of PLGA polymers in being able to deliver a fluorescent dye within ischemic heart tissue and thus develop a model capable of delivering therapeutic genes responsible for cardiac regeneration.

In this study we formulated PLGA nanoparticles via the double emulsion process and encapsulated a fluorescent dye, 6C that can be viewed via optical microscopy analysis. This dye is capable of being excited and emitted at certain wavelengths therefore the amount can be quantitated by using HPLC analysis. The surface of these particles was activated with PVA thus making it hydrophilic and being capable of attaching to surface ligands. We previously identified a peptide sequence RQPRMKR which is a specific ligand to ischemic cardiac tissues via phage panning studies. We tagged the surface of the PLGA nanoparticles with this ligand in order to mediate its delivery specifically to the ischemic heart.

Intracellular levels of nanoparticles increased with dose and time, and an optimum 200 µg of particles per well for a mean incubation time of 2 hours was selected for our study. In vitro studies with and without the surface ligands demonstrated that the size of the particles and not the ligands associated on its surface mediates the uptake into cells. The uptake of nanoparticles was proportional to the size of the particles, however, there was no significant difference between the particle uptake as the size between the

conjugated and un-conjugated particles was not very different from each other with average sizes around 100 nms.[119] When un-sonicated particles, of an average size of 500 nm were used the uptake changed dramatically, with the amount of extracted 6C from these cells reducing to more than half of the sonicated particles.

In vivo studies with PLGA nanoparticles demonstrated the selective targeting of conjugated nanoparticles to the ischemic heart specifically, as compared to the healthy heart or the liver as a response to the targeting ligand on the surface. Un-conjugated particles did not get taken up by the heart tissues and instead were found to be flushed into the liver.

This study provides a viable option for the encapsulation of a fluorescent agent and has demonstrated the intracellular characteristics, *in vitro* and *in vivo* associated with this. This can be used as a model for future studies, as a mechanism for the delivery and uptake of other genetic or drug therapies responsible for mediating benefit to the cardiac tissue.

CHAPTER VIII

IDENTIFICATION OF NOVEL CARDIAC PATHWAYS IN REVERSE VENTRICULAR REMODELING FOLLOWING STEM CELL THERAPY

8.1 Introduction

Cell therapy, especially stem cell therapy has emerged as a promising method for the repair and/or regeneration of ischemic myocardium following myocardial infarct. This includes the use of Hematopoietic Stem Cells (HSCs), Mesenchymal Stem Cells (MSCs), and Multipotent Adult Progenitor Cells (MAPCs).[31,36,37,200] MSCs have been extensively tested for the repair of diseases involved in the heart, brain, liver and the skin.[13,48,201-204] Various mechanisms have been demonstrated for cardiac repair mediated by MSCs,

some of which include differentiation of recruited or cardiac stem cells, fusion between host and recruited stem cells, promotion of angiogenesis and thus improved tissue perfusion.[31,46,200,205] In the past, MSCs have been shown to differentiate to cells of the endothelial lineage providing for angiogenesis and thus improvement in micro circulation.[205] Also, functional recovery of cardiac tissue following MSC engraftment has shown to be coupled with increase in various other paracrine factors, including Vascular Endothelial Growth Factor (VEGF), basic Fibroblast Growth Factor (bFGF), and Angiopoietin-I which induces the growth of blood vessels.[34,49,53] However, due to the complexity involved in the mechanism of repair followed by mesenchymal stem cell therapy, the exact pathways that determine this change in functional improvement is not yet determined.

Similar results obtained from the varied stem cell sources combined with limited evidence that these different cell types actually differentiate into cardiac myocytes has led to the conclusion that the majority of the improvement observed is not due to the regeneration of cardiac myocytes, but rather due to the paracrine factors released by the engrafted stem cells.[52, 206]

Consistent with this hypothesis are our recent studies demonstrating that the benefit of MSC therapy is increased by the over-expression of specific factors, namely Stromal Cell Derived Factor -1 (SDF-1)[35] and Monocyte Chemoattractant Protein-3 (MCP-3).[52] Studies in our laboratory have demonstrated that MSC home to myocardial tissue in response to MCP-3, and that re-establishment of MCP-3 weeks after Acute Myocardial

Infarction (AMI) re-establishes MSC homing to the heart leading to improved cardiac function. The expression of MCP-3 in the absence of MSC infusion had no effect. Interestingly, unlike virtually all preclinical cell transplantation studies published to date, the improvement in LV dimensions and function was achieved in the absence of neovascularization or an increase in vascular density.[52] These observations suggest that the MCP-3 based recruitment of MSC late after AMI leads to the expression of as yet undefined paracrine factors that are able to reverse LV remodeling without inducing vessel development or growth.

We thus hypothesize that this MSC-MCP3 mediated improvement in ventricular function is attributed to reverse ventricular remodeling. Also, this reverse ventricular remodeling is ascribed to paracrine factors secreted in the microenvironment.

The main focus of this aim was to identify key pathways and candidate proteins that are modified as a result of the improvement in cardiac function when MCP-3 is expressed followed by MSC infusions, in chronic heart failure hearts. Whole genome analysis provides a comprehensive list of information on all genes in the genome that are affected as a result of the application of therapy. Therefore this would be a viable option to identify these proteins and the pathways associated in the changes that lead to functional improvement.

The primary focus is to identify candidates associated with reversing ventricular remodeling, following therapy with mesenchymal stem cells. To understand and identify

these proteins we employed whole genome analysis studied pathways upregulated following treatments with MSC therapy. Important aspects of genome wide experiments are the large number of genes and their associated pathways assessed and the high sensitivity of this approach. We investigated secreted proteins, and thus were able to eliminate specific genes associated with the respective tissue types either host or engrafted. Moreover, we looked specifically for pathways associated with the cardiac lineage and the changes mediated in the cardiac tissue.

8.2 Methods

8.2.1 Experimental Plan

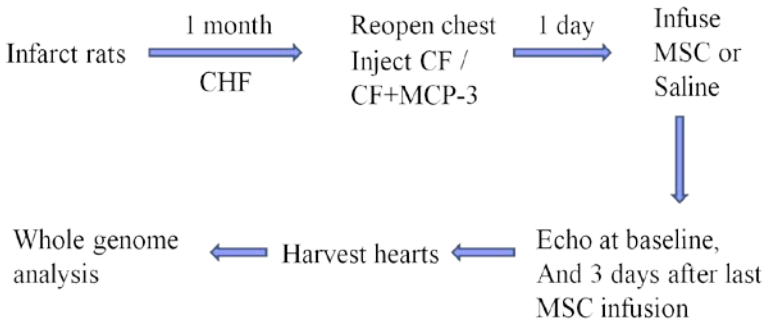

Group 1	MCP-3 transfected cardiac fibroblasts	MSC x 6 doses
Group 2 (control)	MCP-3 transfected cardiac fibroblasts	Saline
Group 3 (control)	Cardiac fibroblasts	MSC x 6 doses
Group 4 (control)	Cardiac Fibroblasts	Saline
Group 5 (control)	Saline	MSC x 6 dose
Group 6 (control)	Saline	Saline

Table 8-1 : Animal groups involved in stem cell therapy

8.2.2 Isolation of MSCs

Rat bone marrow was isolated by flushing rat femurs and tibias with 0.6 ml DMEM repeatedly till all of it is extracted. Clumps of bone marrow were gently minced using a 20 gauge needle and a 10 ml syringe. Cells were then be removed by Percoll density gradient. This bone marrow was washed with PBS three times to remove all debris and then plated in a dish with MSC media, comprising 10% FBS and 1% antibiotic in low glucose DMEM, and incubated at 37ºC for three days. The mesenchymal stem cells adhere to the plate leaving the endothelial cells in suspension. The media was changed in order to obtain a pure population of MSC cells. This culture is then sorted negatively after 4 passages for CD45 and CD34, by magnetic cell sorting techniques in order to obtain a double purified and pure population of MSCs.

8.2.3 Isolation of Cardiac Fibroblasts

The left ventricles of 3 to 5 rats were pooled together, minced and placed in 100 U/ml of collagenase XI and trypsin at 37 ºC for 10 minutes in a shaking incubator. The cell suspension was filtered out using gauze filtration and minced tissue was collected. The cell suspension was centrifuged at 2000 rpm for 10 minutes to sediment the cells. The cells were seeded in Ham's modified DME medium supplemented with 10 % FBS and 1% antibiotic containing Penicillin and Streptomycin. Non adherent cells were removed after 2 hours of incubation and the adherent cells were washed twice with phosphate buffered solution (PBS). The resulting adherent fibroblasts were cultured in

Ham's modified DMEM medium supplemented with 10% FBS and 1% antibiotic containing Penicillin and Streptomycin on T75 flasks and incubated in 37ºC and 5% CO2.

8.2.4 Transfection of Cardiac Fibroblasts with MCP-3

MCP-3 from total RNA was cloned into expression vector pcDNA3.1 and a MYC TAG was attached in order to detect the gene. The cardiac fibroblast culture dish was treated with the MCP-3 encoding expression vector, or the control pcDNA vector overnight in the presence of FUGENE. MCP-3 expression was selected by neomycin by the addition of Geneticin to the media for two weeks. The surviving cells were expanded and used for the experiment.

8.2.5 Experimental animals

We used male Lewis rats (Jackson Laboratories) for the chronic heart failure study. All animals were 8 week old weighing 200-225 grams. There were 5 animals in each group involved in the study (Table 8-1).

8.2.6 Intramyocardial Cardiac Fibroblast delivery

To inject the cardiac fibroblasts, the chest will be reopened two weeks post MI, applying the same procedure as above, and using a 30 gauge needle, 100µl of DNA solution will be injected per injection site. There will be 4 injection sites in all, around the

border zone. The border zone will be identified by the blanched region around the LAD. The DNA will be injected into the wall and blanching will be observed when the DNA is injected. The chest will be closed as mentioned above for the LAD ligation.

8.2.7 Infusion of Mesenchymal Stem Cells

Mesenchymal stem cells will be infused via the tail vein using a 30 gauge needle. The needle will be inserted and blood will be drawn from the vein to ensure the site of injection. 2 million MSCs in 100 µl volume will be injected over a period of 1 minute to avoid any emboli formation.

8.2.8 Isolation of total RNA

RNA from tissue samples will be isolated using the Trizol reagents. Briefly, the tissues are homogenized in Trizol in dry ice and chloroform is added to this. The aqueous phase obtained is collected and mixed with isopropanol and centrifuged to collect the samples. RNAgents denaturing solution (from Qiagen) is then added to this to dissolve the pellet. Samples are again collected with isopropanol and are centrifuged to collect the samples at the bottom. This sample is not treated with 75% ethanol and again centrifuged to collect samples. The supernatant is again discarded without disturbing the pellet and the pellet is dissolved in DEPC water for future use. Further clean up of the RNA will be done with the use of the Qiagen kit as per the manufacturer's instructions.

8.2.9 Preparation of cRNA

First-strand cDNA was synthesized using Oligo dT and Superscript II RT (Invitrogen, Grand Island, NY). Alternatively, cDNA will be prepared using OVATION RNA Amplification System (NuGen Technologies, Inc., San Carlos, CA). cDNA amplification products will then be fragmented and chemically-labeled with biotin to generate biotinylated cDNA targets. Each Affymetrix gene chip for rat genome will be hybridized with fragmented and biotin-labeled target (2.5 μg) in 200 μl of hybridization cocktail. Target denaturation is performed at 99°C for 2 minutes, followed by hybridization for 18 hours. Arrays then will be washed and stained using Genechip Fluidic Station 450, and hybridization signals will be amplified using antibody amplification with goat IgG (Sigma-Aldrich) and anti-streptavidin biotinylated antibody (Vector Laboratories, Burlingame, CA).

8.2.10 Affymetrix Analysis

Eight micrograms of total RNA from rats treated with MSC and MCP-3 and control rats with MCP-3 without MSCs was tested. Affymetrix GeneChip Rat Exon Arrays 1.0, which allow analysis of >23,000 transcripts, was performed in triplicates and analyzed with Affymetrix Microarray Suite (MAS 5.0). All possible comparisons Comparison between MSC-MCP-3 treated animals vs. Saline MCP-3 treated control animals was tested. Chips were scanned on a Affymetrix Gene Chip Scanner 3000, using GeneChip Operating Software (GCOS) version 3.0. Background correction and normalization was

done using Robust Multichip Average (RMA) with GeneSpring V 7.3.1 software (Silicon Genetics, Redwood City, CA). Volcano plots were used to identify differentially expressed genes using the parametric testing assuming variances are equal (filters based on the results of a Student's two-sample t-test for two groups or a one-way analysis of variance (ANOVA) for multiple groups) and no multiple testing correction. Comparisons were done between MSC MCP-3 treated group and the Saline MCP-3 treated control group. The differentially expressed gene list was loaded into IPA 5.0 software (www.ingenuity.com) to perform biological network and functional analyses.

8.3 Results

8.3.1 Stem cell therapy improves cardiac function in chronic heart failure

8 week old rats were infarcted via LAD ligation. 4 weeks post ligation, all rats had a diminished fractional shortening of < 30%. The chests were re opened and cardiac fibroblasts were transplanted into the heart wall at 2 million cells per animal. Cardiac fibroblasts were modified to secrete increased levels of MCP-3 or were used as is, as controls. One day post transplantation, 2 million mesenchymal stem cells were infused via the tail vein, 6 times in a period of 12 days. 3 days after the last infusion, rats were analyzed for cardiac function, via echocardiographic analysis.

Pre injection all rats had a fractional shortening less than 30%. Rats that received mesenchymal stem cells showed increase in cardiac function, immediately post stem cell

therapy, as compared to the rats that did not receive stem cell therapy. Among the ones that received stem cell therapy, rodents with boosted MCP-3 activity showed the maximum benefit as compared to the all other groups. (Figure 8-1)

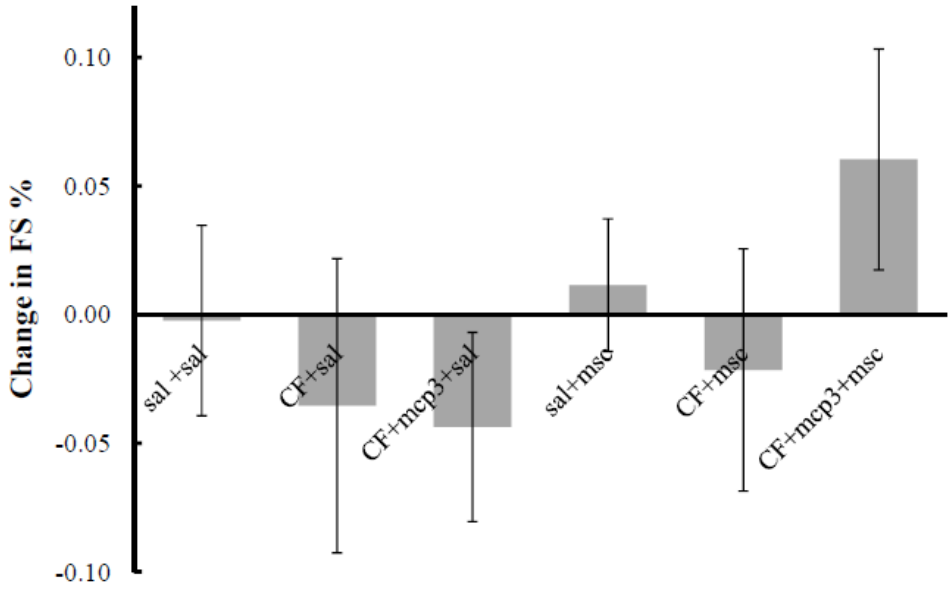

Figure 8-1 : Change in cardiac function with MSC therapy *in vivo*
Ischemic rat hearts were injected with cardiac fibroblasts overexpressing the homing factor for mesenchymal stem cells, MCP-3 and infused with mesenchymal stem cells. Animals that received both treatments showed an improvement in cardiac function, 3 days post treatment, as compared to the ones that did not receive mesenchymal stem cells. (n=5)

8.3.2 Identification of pathways and genes involved in cardiac repair

Among all the groups, the RNA from the group with MSC and MCP-3 treatment and the animals from the MCP-3 with saline group were sent for whole genome analysis. The results from the whole genome analysis were sorted in order to identify a sub set of genes that were maximally affected by the therapy, thus leading to improved cardiac

functioning, via reverse ventricular remodeling. The gene expression results were supplied by whole genome analysis. Gene profiling were conducted with RNA isolated from the left ventricles of treated and control rats.

Microarray analysis was performed on RNA isolated from each group to identify differentially expressed genes, using the Affymetrix Rat exon 2.0 array. Signals were loaded into Gene Chip Operating Software (GCOS) and normalized using the Robust Multichip Average (RMA) algorithm. The normalized set was further sorted to provide a more ideal normalization with the GC-RMA software. Instead of eliminating the mismatch genes, as provided by RMA analysis, the GC RMA, supplies a graded average for each gene, with a simulated number for the mismatch, as provided by the number of G and C rich regions in the probe. This subset of genes was then sorted based on Significance of Microarray studies, to remove false positives for p values with a False Detection Rate of 20%. The expressed genes were finally sorted based on p values (<0.05) and fold changes.

To provide a more specific subset of differentially expressed genes, with a p value of 0.05 and a Fold change of 2, these genes were subject to ANOVA to determine the number of genes that are expressed differentially. Following these sorting measures a small subset of secreted genes were identified, based on their locations in the cell either in the cytoplasm, the cell wall, or extra cellular matrix. (Table 8-2). Among these genes, some were upregulated and some were down regulated. PSG-19 and LIF were upregulated and our focus was on these genes.

Gene ID	Gene Name	Function
Upregulated Genes		
PSG-18	Pregnancy Specific Glycoprotein 18	Induces IL10
LIF	Leukemia Inhibitory factor	Proliferation of cells
Downregulated Genes		
CTF1	Cardiotrophin 1	cardioprotective
SERPINH1	Serpin Peptidase Inhibitor	Cell survival
MIP/CCL3	Macrophage Inflammatory Protein	Pro-inflammation
VCAN	Versican	Macrophage adhesion
REG3A	Regenerating Islet-Derived 3 alpha	Pancreatitis associated protein

Table 8-2 : Genes of secreted proteins involved in cardiac repair with MSC therapy

8.3.3 RT PCR Analysis for individual paracrine factors

RT-PCR analysis was carried out with primers specific for the PSG-19 gens with the RNA isolated from the tissues of all animal groups. Primers were designed with the software provided in the NCBI website. For RT-PCR analysis, forward primer of GAGCCTTGTTGGAGCTGAAG and reverse primer of AGGGCTACACCCTGA ACAGA were used. However, there was no difference between the amount of this protein expressed by the various groups.

8.3.4 Pathway Analysis with Ingenuity Pathway Analysis Software

Pathway analysis provides highly sophisticated information on the interactions between genes and the relationship between one another, with respect to various functions. The various analyses were performed as described above. Briefly, the results from the Affymetrix data analysis was subject to normalization software with GC-RMA, and sorted based on p values. This data set is referred to as the reference set. Instead of using all the genes in the rat genome as the reference set, this subset of affected and normalized genes was used as the reference. This data set was further subject to a 20% false detection rate in the SAM analysis, to identify and eliminate false p-values. The following subset that ensued was the data set for the pathway analysis. This data set was analyzed to determine the interactions between these differentially significant genes.

Pathway analysis was able to provide us with information regarding specific genes (either up or down regulated) that was associated with cardiovascular functions, including development and disorder. These genes were then sorted into a subset that can provide leads into factors that may affect ventricular remodeling. (Table 8-3)

Symbol	Gene Name	Fold Change	Location	Type(s)
Upregulated genes				
MIF	macrophage migration inhibitory factor (glycosylation-inhibiting factor)	2.84	Extracellular Space	cytokine
LIF	leukemia inhibitory factor (cholinergic differentiation factor)	2.27	Extracellular Space	cytokine
SFRP4	secreted frizzled-related protein 4	2.27	Plasma Membrane	Trans-membrane receptor
TNNI3	troponin I type 3 (cardiac)	2.24	Cytoplasm	transporter
MEF2B	myocyte enhancer factor 2B	2.24	Nucleus	transcription regulator
APOH	apolipoprotein H (beta-2-glycoprotein I)	2.21	Extracellular Space	transporter
FSHB	follicle stimulating hormone, beta polypeptide	2.19	Extracellular Space	other
UTS2	urotensin 2	2.18	Extracellular Space	other
CYSLTR2	cysteinyl leukotriene receptor 2	2.14	Plasma Membrane	GPCR
DRD1	dopamine receptor D1	2.13	Plasma Membrane	GPCR
HCN2	hyperpolarization activated cyclic nucleotide-gated potassium channel 2	2.12	Plasma Membrane	ion channel
CLEC11A	C-type lectin domain family 11, member A	2.12	Extracellular Space	growth factor
GLRX3	glutaredoxin 3	2.12	Cytoplasm	enzyme
VEGFA	vascular endothelial growth factor A	2.10	Extracellular Space	growth factor
GRIN2A	glutamate receptor, ionotropic, N-methyl D-aspartate 2A	2.10	Plasma Membrane	ion channel
MAX	MYC associated factor X	2.09	Nucleus	transcription regulator
ES22	esterase 22	2.08	Cytoplasm	enzyme
EGF	epidermal growth factor	2.07	Extracellular Space	growth factor
GHR	growth hormone	2.07	Plasma Membrane	

	receptor			transmembrane receptor
MAPT	microtubule-associated protein tau	2.05	Cytoplasm	other
GRM5	glutamate receptor, metabotropic 5	2.05	Plasma Membrane	GPCR
AGTR1B	angiotensin II receptor, type 1b	2.05	Plasma Membrane	GPCR
PIK3C2G	phosphoinositide-3-kinase, class 2, gamma polypeptide	2.04	Cytoplasm	kinase
IFNG	interferon, gamma	2.03	Extracellular Space	cytokine
KRT1	keratin 1	2.03	Cytoplasm	other
CSF3	colony stimulating factor 3 (granulocyte)	2.02	Extracellular Space	cytokine
CAV3	caveolin 3	2.02	Plasma Membrane	enzyme
NOS2	nitric oxide synthase 2, inducible	2.02	Cytoplasm	enzyme
GRIA2	glutamate receptor, ionotropic, AMPA 2	2.02	Plasma Membrane	ion channel
AMPD1	adenosine monophosphate deaminase 1	2.01	unknown	enzyme
PDGFA	platelet-derived growth factor alpha polypeptide	2.01	Extracellular Space	growth factor
ATP2B3	ATPase, Ca++ transporting, plasma membrane 3	2.01	Plasma Membrane	transporter
AACS	acetoacetyl-CoA synthetase	2.00	Cytoplasm	enzyme
CEBPA	CCAAT/enhancer binding protein (C/EBP), alpha	2.00	Nucleus	transcription regulator
Downregulated genes				
TIMP1	TIMP metallopeptidase inhibitor 1	-3.99	Extracellular Space	other
FN1	fibronectin 1	-3.74	Plasma Membrane	enzyme
VCAN	versican	-3.54	Extracellular Space	other
C3AR1	complement component 3a receptor 1	-3.45	Plasma Membrane	GPCR

CXCL13	chemokine (C-X-C motif) ligand 13	-3.43	Extracellular Space	cytokine
SERPINA3	serpin peptidase inhibitor, clade A member 3	-3.23	Extracellular Space	other
KCNJ2	potassium inwardly-rectifying channel, subfamily J, member 2	-3.19	Plasma Membrane	ion channel
SERPINE1	serpin peptidase inhibitor, clade E	-3.18	Extracellular Space	other
CCR5	chemokine (C-C motif) receptor 5	-3.17	Plasma Membrane	GPCR
VCAM1	vascular cell adhesion molecule 1	-3.16	Plasma Membrane	other
HSPB1	heat shock 27kDa protein 1	-3.11	Cytoplasm	other
LOX	lysyl oxidase	-3.03	Extracellular Space	enzyme
CCR2	chemokine (C-C motif) receptor 2	-2.99	Plasma Membrane	GPCR
CCL13	chemokine (C-C motif) ligand 13	-2.98	Extracellular Space	cytokine
NOV	nephroblastoma overexpressed gene	-2.97	Extracellular Space	growth factor
HTR1B	5-hydroxytryptamine (serotonin) receptor 1B	-2.91	Plasma Membrane	GPCR
ANXA2	annexin A2	-2.86	Plasma Membrane	other
THY1	Thy-1 cell surface antigen	-2.85	Plasma Membrane	other
ANPEP	alanyl (membrane) aminopeptidase	-2.85	Plasma Membrane	peptidase
MET	met proto-oncogene (hepatocyte growth factor receptor)	-2.84	Plasma Membrane	kinase
ENPP3	ectonucleotide pyrophosphatase/phosphodiesterase 3	-2.82	Plasma Membrane	enzyme
MSLN	mesothelin	-2.80	Extracellular Space	other
CP	ceruloplasmin (ferroxidase)	-2.79	Extracellular Space	enzyme
SIRPA	signal-regulatory protein alpha	-2.77	Plasma Membrane	phosphatase
ITGAM	integrin, alpha M (complement component 3 receptor 3 subunit)	-2.76	Plasma Membrane	other
NCAM1	neural cell adhesion	-2.75	Plasma	other

	molecule 1		Membrane	
CYBB	cytochrome b-245, beta polypeptide	-2.75	Cytoplasm	enzyme
SELE	selectin E	-2.74	Plasma Membrane	other
MMP2	matrix metallopeptidase 2	-2.73	Extracellular Space	peptidase
FZD2	frizzled homolog 2 (Drosophila)	-2.71	Plasma Membrane	GPCR
FIGF	c-fos induced growth factor (vascular endothelial growth factor D)	-2.69	Extracellular Space	growth factor
PTPRC	protein tyrosine phosphatase, receptor type, C	-2.69	Plasma Membrane	phosphatase
CD14	CD14 molecule	-2.69	Plasma Membrane	transmembrane receptor
RRAD	Ras-related associated with diabetes	-2.68	Cytoplasm	enzyme
LGALS3	lectin, galactoside-binding, soluble, 3	-2.66	Extracellular Space	other
DMBT1	deleted in malignant brain tumors 1	-2.65	Plasma Membrane	transmembrane receptor
RPS6	ribosomal protein S6	-2.65	Cytoplasm	other
UTS2R	urotensin 2 receptor	-2.65	Plasma Membrane	GPCR
S100A4	S100 calcium binding protein A4	-2.63	Cytoplasm	other
UGCG	UDP-glucose ceramide glucosyltransferase	-2.63	Cytoplasm	enzyme
APLNR	apelin receptor	-2.62	Plasma Membrane	GPCR
CD53	CD53 molecule	-2.62	Plasma Membrane	other
TGFB2	transforming growth factor, beta 2	-2.62	Extracellular Space	growth factor
ACTN1	actinin, alpha 1	-2.61	Cytoplasm	other
TGM2	transglutaminase 2	-2.60	Cytoplasm	enzyme
PRRX1	paired related homeobox 1	-2.59	Nucleus	transcription regulator
TRH	thyrotropin-releasing hormone	-2.59	Extracellular Space	other
PMP22	peripheral myelin protein 22	-2.58	Plasma Membrane	other

IGF1	insulin-like growth factor 1	-2.57	Extracellular Space	growth factor
TGFBR2	transforming growth factor, beta receptor II	-2.57	Plasma Membrane	kinase
JAK2	Janus kinase 2	-2.56	Cytoplasm	kinase
CD44	CD44 molecule (Indian blood group)	-2.55	Plasma Membrane	other
CITED2	Cbp/p300-interacting transactivator	-2.55	Nucleus	transcription regulator
EMP1	epithelial membrane protein 1	-2.55	Plasma Membrane	other
DAB2	disabled homolog 2, mitogen-responsive phosphoprotein	-2.55	Plasma Membrane	other
CPT1A	carnitine palmitoyltransferase 1A (liver)	-2.55	Cytoplasm	enzyme
HSPA5	heat shock 70kDa protein 5 (glucose-regulated protein, 78kDa)	-2.55	Cytoplasm	other
PTPN6	protein tyrosine phosphatase, non-receptor type 6	-2.54	Cytoplasm	phosphatase
FGG	fibrinogen gamma chain	-2.54	Extracellular Space	other
ADD3	adducin 3 (gamma)	-2.54	Cytoplasm	other
CTSB	cathepsin B	-2.54	Cytoplasm	peptidase
HIF1A	hypoxia inducible factor 1, alpha subunit	-2.53	Nucleus	transcription regulator
SNCG	synuclein, gamma (breast cancer-specific protein 1)	-2.53	Cytoplasm	other
HTR2A	5-hydroxytryptamine (serotonin) receptor 2A	-2.52	Plasma Membrane	GPCR
AP2A2	adaptor-related protein complex 2, alpha 2 subunit	-2.51	Cytoplasm	transporter
EGR1	early growth response 1	-2.51	Nucleus	transcription regulator
MAGED1	melanoma antigen family D, 1	-2.51	Plasma Membrane	transcription regulator
APP	amyloid beta (A4) precursor protein	-2.50	Plasma Membrane	other
GRN	granulin	-2.50	Extracellular Space	growth factor
BMP2	bone morphogenetic protein 2	-2.49	Extracellular Space	growth factor
EDNRA	endothelin receptor type A	-2.49	Plasma	

			Membrane	transmembrane receptor
TP53	tumor protein p53	-2.49	Nucleus	transcription regulator
AXL	AXL receptor tyrosine kinase	-2.49	Plasma Membrane	kinase
CASP3	caspase 3, apoptosis-related cysteine peptidase	-2.49	Cytoplasm	peptidase
TGFB1	transforming growth factor, beta 1	-2.49	Extracellular Space	growth factor
ARHGDIB	Rho GDP dissociation inhibitor (GDI) beta	-2.48	Cytoplasm	other
SELP	selectin P (granule membrane protein 140kDa, antigen CD62)	-2.48	Plasma Membrane	other
ITGB1	integrin, beta 1	-2.48	Plasma Membrane	transmembrane receptor
HBEGF	heparin-binding EGF-like growth factor	-2.48	Extracellular Space	growth factor
OLR1	oxidized low density lipoprotein (lectin-like) receptor 1	-2.48	Plasma Membrane	transmembrane receptor
JUP	junction plakoglobin	-2.47	Plasma Membrane	other
GJA1	gap junction protein, alpha 1, 43kDa	-2.47	Plasma Membrane	transporter
SERPINF1	serpin peptidase inhibitor, clade F	-2.47	Extracellular Space	other
TNFRSF1A	tumor necrosis factor receptor superfamily, member 1A	-2.47	Plasma Membrane	transmembrane receptor
PDGFC	platelet derived growth factor C	-2.46	Extracellular Space	growth factor
TLR2	toll-like receptor 2	-2.46	Plasma Membrane	transmembrane receptor
GSK3B	glycogen synthase kinase 3 beta	-2.45	Nucleus	kinase
PTGS1	prostaglandin-endoperoxide synthase 1	-2.45	Cytoplasm	enzyme
CYB5R3	cytochrome b5 reductase 3	-2.45	Cytoplasm	enzyme
SCAMP2	secretory carrier membrane protein 2	-2.44	Cytoplasm	transporter
JAG1	jagged 1 (Alagille syndrome)	-2.44	Extracellular Space	growth factor

GPAM	glycerol-3-phosphate acyltransferase, mitochondrial	-2.44	Cytoplasm	enzyme
IL6ST	interleukin 6 signal transducer	-2.44	Plasma Membrane	transmembrane receptor
LYN	v-yes-1 Yamaguchi sarcoma viral related oncogene homolog	-2.43	Cytoplasm	kinase
STAT3	signal transducer and activator of transcription 3	-2.43	Nucleus	transcription regulator
EXTL3	exostoses (multiple)-like 3	-2.43	Cytoplasm	enzyme
NPPA	natriuretic peptide precursor A	-2.43	Extracellular Space	other
LPAR1	lysophosphatidic acid receptor 1	-2.42	Plasma Membrane	GPCR
NOTCH2	Notch homolog 2 (Drosophila)	-2.42	Plasma Membrane	transcription regulator
P4HB	prolyl 4-hydroxylase, beta polypeptide	-2.42	Cytoplasm	enzyme
ATP6AP1	ATPase, H+ transporting, lysosomal accessory protein 1	-2.42	Cytoplasm	transporter
TPM2	tropomyosin 2 (beta)	-2.41	Cytoplasm	other
ATP2B4	ATPase, Ca++ transporting, plasma membrane 4	-2.41	Plasma Membrane	transporter
MYO5A	myosin VA (heavy chain 12, myoxin)	-2.41	Cytoplasm	enzyme
DMD	dystrophin	-2.40	Plasma Membrane	other
CLU	clusterin	-2.40	Extracellular Space	other
FSTL1	follistatin-like 1	-2.40	Extracellular Space	other
OGG1	8-oxoguanine DNA glycosylase	-2.40	Nucleus	enzyme
CTNNB1	catenin (cadherin-associated protein), beta 1, 88kDa	-2.40	Nucleus	transcription regulator
GNB1	guanine nucleotide binding protein (G protein), beta polypeptide 1	-2.40	Plasma Membrane	enzyme
PSEN1	presenilin 1	-2.40	Plasma Membrane	peptidase
NCSTN	nicastrin	-2.39	Plasma	peptidase

			Membrane	
VIM	vimentin	-2.39	Cytoplasm	other
TAGLN	transgelin	-2.38	Cytoplasm	other
CD81	CD81 molecule	-2.38	Plasma Membrane	other
CSPG4	chondroitin sulfate proteoglycan 4	-2.38	Plasma Membrane	other
NRAS	neuroblastoma RAS viral (v-ras) oncogene homolog	-2.38	Plasma Membrane	enzyme
ACTN4	actinin, alpha 4	-2.37	Cytoplasm	other
SHMT2	serine hydroxymethyltransferase 2 (mitochondrial)	-2.37	Cytoplasm	enzyme
ACVR1B	activin A receptor, type IB	-2.37	Plasma Membrane	kinase
ADORA1	adenosine A1 receptor	-2.37	Plasma Membrane	GPCR
IL1R1	interleukin 1 receptor, I	-2.37	Plasma Membrane	transmembrane receptor
EPHA7	EPH receptor A7	-2.37	Plasma Membrane	kinase
HCN4	hyperpolarization activated cyclic nucleotide-gated potassium channel 4	-2.37	Plasma Membrane	ion channel
ODC1	ornithine decarboxylase 1	-2.37	Cytoplasm	enzyme
LCN2	lipocalin 2	-2.36	Extracellular Space	transporter
LIPE	lipase, hormone-sensitive	-2.36	Cytoplasm	enzyme
PTPRF	protein tyrosine phosphatase, receptor, F	-2.36	Plasma Membrane	phosphatase
RXRA	retinoid X receptor, alpha	-2.36	Nucleus	receptor
CACNA1G	calcium channel, voltage-dependent, T type, alpha 1G subunit	-2.36	Plasma Membrane	ion channel
CASP2	caspase 2, apoptosis-related cysteine peptidase	-2.36	Cytoplasm	peptidase
ECE1	endothelin converting enzyme 1	-2.36	Plasma Membrane	peptidase
CREBBP	CREB binding protein	-2.36	Nucleus	transcription regulator
LIPA	lipase A, lysosomal acid, cholesterol esterase	-2.36	Cytoplasm	enzyme
CD47	CD47 molecule	-2.35	Plasma Membrane	other
GJB6	gap junction protein, beta 6, 30kDa	-2.35	Plasma Membrane	transporter

MCM7	minichromosome maintenance complex component 7	-2.35	Nucleus	enzyme
TIMP2	TIMP metallopeptidase inhibitor 2	-2.35	Extracellular Space	other
DYNC1H1	dynein, cytoplasmic 1, heavy chain 1	-2.34	Cytoplasm	peptidase
GAB2	GRB2-associated binding protein 2	-2.34	Cytoplasm	other
PDPK1	3-phosphoinositide dependent protein kinase-1	-2.34	Cytoplasm	kinase
TGIF1	TGFB-induced factor homeobox 1	-2.34	Nucleus	transcription regulator
TRPC6	transient receptor potential cation channel, subfamily C, member 6	-2.34	Plasma Membrane	ion channel
IGF1R	insulin-like growth factor 1 receptor	-2.34	Plasma Membrane	Trans-membrane receptor
GRIA3	glutamate receptor, ionotrophic, AMPA 3	-2.33	Plasma Membrane	ion channel
VEGFC	vascular endothelial growth factor C	-2.33	Extracellular Space	growth factor
REST	RE1-silencing transcription factor	-2.33	Nucleus	transcription regulator
GALR2	galanin receptor 2	-2.33	Plasma Membrane	GPCR
ICAM1	intercellular adhesion molecule 1	-2.33	Plasma Membrane	transmembrane receptor
IRS1	insulin receptor substrate 1	-2.33	Cytoplasm	other
LXN	latexin	-2.33	Cytoplasm	other
GPI	glucose-6-phosphate isomerase	-2.32	Extracellular Space	enzyme
AMPD3	adenosine monophosphate deaminase 3	-2.32	unknown	enzyme
FST	follistatin	-2.32	Extracellular Space	other
NOTCH3	Notch homolog 3 (Drosophila)	-2.32	Plasma Membrane	transcription regulator
JAK1	Janus kinase 1	-2.31	Cytoplasm	kinase
ADM	adrenomedullin	-2.31	Extracellular Space	other
CDS2	CDP-diacylglycerol synthase	-2.31	Cytoplasm	enzyme
DUSP5	dual specificity phosphatase 5	-2.31	Nucleus	phosphatase

SCARB2	scavenger receptor class B, member 2	-2.31	Plasma Membrane	other
APAF1	apoptotic peptidase activating factor 1	-2.31	Cytoplasm	other
CLTC	clathrin, heavy chain (Hc)	-2.31	Plasma Membrane	other
MAP3K1	mitogen-activated protein kinase kinase kinase 1	-2.31	Cytoplasm	kinase
OGT	O-linked N-acetylglucosamine (GlcNAc) transferase	-2.31	Cytoplasm	enzyme
DYNLT1	dynein, light chain, Tctex-type 1	-2.30	Cytoplasm	other
ITGA1	integrin, alpha 1	-2.30	Plasma Membrane	other
STXBP1	syntaxin binding protein 1	-2.30	Cytoplasm	transporter
CCND2	cyclin D2	-2.30	Nucleus	other
DIO2	deiodinase, iodothyronine, type II	-2.30	Cytoplasm	enzyme
HNRNPD	heterogeneous nuclear ribonucleoprotein D	-2.30	Nucleus	transcription regulator
HYOU1	hypoxia up-regulated 1	-2.30	Cytoplasm	other
IGF2	insulin-like growth factor 2 (somatomedin A)	-2.30	Extracellular Space	growth factor
PLD2	phospholipase D2	-2.30	Cytoplasm	enzyme
DIO3	deiodinase, iodothyronine, type III	-2.30	Plasma Membrane	enzyme
AGRN	agrin	-2.29	Plasma Membrane	other
ATP6V0C	ATPase, H+ transporting, lysosomal 16kDa, V0 subunit c	-2.29	Cytoplasm	transporter
CXCR3	chemokine (C-X-C motif) receptor 3	-2.29	Plasma Membrane	GPCR
MYD88	myeloid differentiation primary response gene (88)	-2.29	Plasma Membrane	other
NRP1	neuropilin 1	-2.29	Plasma Membrane	transmembrane receptor
ADAM17	ADAM metallopeptidase domain 17	-2.29	Plasma Membrane	peptidase
CAPN1	calpain 1, (mu/I) large subunit	-2.29	Cytoplasm	peptidase
CXCR4	chemokine (C-X-C motif) receptor 4	-2.28	Plasma Membrane	GPCR
FYN	FYN oncogene related to	-2.28	Plasma	kinase

	SRC, FGR, YES		Membrane	
PDE3A	phosphodiesterase 3A, cGMP-inhibited	-2.28	Cytoplasm	enzyme
SMPD1	sphingomyelin phosphodiesterase 1, acid lysosomal	-2.28	Cytoplasm	enzyme
STEAP3	STEAP family member 3	-2.28	Cytoplasm	transporter
ITPR1	inositol 1,4,5-triphosphate receptor, type 1	-2.28	Cytoplasm	ion channel
SMAD1	SMAD family member 1	-2.28	Nucleus	transcription regulator
CDH2	cadherin 2, type 1, N-cadherin (neuronal)	-2.28	Plasma Membrane	other
CDK9	cyclin-dependent kinase 9	-2.28	Nucleus	kinase
EGFR	epidermal growth factor receptor	-2.28	Plasma Membrane	kinase
APC	adenomatous polyposis coli	-2.27	Nucleus	enzyme
CXCL2	chemokine (C-X-C motif) ligand 2	-2.27	Extracellular Space	cytokine
MAP3K11	mitogen-activated protein kinase kinase kinase 11	-2.27	Cytoplasm	kinase
PDE5A	phosphodiesterase 5A, cGMP-specific	-2.27	Cytoplasm	enzyme
PPP1R12A	protein phosphatase 1, regulatory (inhibitor) subunit 12A	-2.27	Cytoplasm	phosphatase
CCND1	cyclin D1	-2.27	Nucleus	other
CDH13	cadherin 13, H-cadherin (heart)	-2.27	Plasma Membrane	other
ITSN1	intersectin 1 (SH3 domain protein)	-2.27	Cytoplasm	other
MYO9B	myosin IXB	-2.27	Cytoplasm	enzyme
HTT	huntingtin	-2.26	Cytoplasm	transcription regulator
TSC2	tuberous sclerosis 2	-2.26	Cytoplasm	other
ERBB2	v-erb-b2 erythroblastic leukemia viral oncogene homolog 2,	-2.26	Plasma Membrane	kinase
NSF	N-ethylmaleimide-sensitive factor	-2.26	Cytoplasm	transporter
VLDLR	very low density lipoprotein receptor	-2.26	Plasma Membrane	transporter
PSEN2	presenilin 2 (Alzheimer disease 4)	-2.26	Cytoplasm	peptidase
CXCL12	chemokine (C-X-C motif) ligand 12	-2.25	Extracellular Space	cytokine

BID	BH3 interacting domain death agonist	-2.25	Cytoplasm	other
PRKCD	protein kinase C, delta	-2.25	Cytoplasm	kinase
IKBKB	inhibitor of kappa light polypeptide gene enhancer in B-cells, kinase beta	-2.25	Cytoplasm	kinase
ITPKB	inositol 1,4,5-trisphosphate 3-kinase B	-2.25	Cytoplasm	kinase
ARHGAP20	Rho GTPase activating protein 20	-2.25	unknown	other
CACNA1C	calcium channel, voltage-dependent, L type, alpha 1C subunit	-2.24	Plasma Membrane	ion channel
ERBB3	v-erb-b2 erythroblastic leukemia viral oncogene homolog 3 (avian)	-2.24	Plasma Membrane	kinase
PLAU	plasminogen activator, urokinase	-2.24	Extracellular Space	peptidase
MMP9	matrix metallopeptidase 9	-2.24	Extracellular Space	peptidase
BIN1	bridging integrator 1	-2.23	Nucleus	other
GATA4	GATA binding protein 4	-2.23	Nucleus	transcription regulator
ETS1	v-ets erythroblastosis virus E26 oncogene homolog 1 (avian)	-2.23	Nucleus	transcription regulator
EP300	E1A binding protein p300	-2.23	Nucleus	transcription regulator
MADD	MAP-kinase activating death domain	-2.22	Cytoplasm	other
ADRA1A	adrenergic, alpha-1A-, receptor	-2.22	Plasma Membrane	GPCR
MTOR	mechanistic target of rapamycin (serine/threonine kinase)	-2.22	Nucleus	kinase
APOE	apolipoprotein E	-2.22	Extracellular Space	transporter
GNB2L1	guanine nucleotide binding protein (G protein), beta polypeptide 2-like 1	-2.22	Cytoplasm	enzyme
SRC	v-src sarcoma (Schmidt-Ruppin A-2) viral oncogene homolog (avian)	-2.22	Cytoplasm	kinase
SF1	splicing factor 1	-2.21	Nucleus	transcription regulator
AXIN1	axin 1	-2.20	Cytoplasm	other

DNM1	dynamin 1	-2.20	Cytoplasm	enzyme
CXCL1	chemokine (C-X-C motif) ligand 1	-2.20	Extracellular Space	cytokine
ARHGEF7	Rho guanine nucleotide exchange factor (GEF) 7	-2.20	Cytoplasm	other
ATG7	ATG7 autophagy related 7 homolog (S. cerevisiae)	-2.19	Cytoplasm	enzyme
CTF1	cardiotrophin 1	-2.19	Extracellular Space	cytokine
DCTN1	dynactin 1 (p150, glued homolog, Drosophila)	-2.19	Cytoplasm	other
KHSRP	KH-type splicing regulatory protein	-2.19	Nucleus	enzyme
GRB2	growth factor receptor-bound protein 2	-2.18	Cytoplasm	other
APH1A	anterior pharynx defective 1a homolog (C. elegans)	-2.18	Cytoplasm	peptidase
CASP9	caspase 9, apoptosis-related cysteine peptidase	-2.18	Cytoplasm	peptidase
CABIN1	calcineurin binding protein 1	-2.18	Nucleus	other
MAPK1	mitogen-activated protein kinase 1	-2.18	Cytoplasm	kinase
SMAD3	SMAD family member 3	-2.18	Nucleus	transcription regulator
GIT1	G protein-coupled receptor kinase interacting ArfGAP 1	-2.17	Nucleus	other
CDK5	cyclin-dependent kinase 5	-2.16	Nucleus	kinase
SNAP29	synaptosomal-associated protein, 29kDa	-2.16	Cytoplasm	transporter
DLG4	discs, large homolog 4 (Drosophila)	-2.15	Plasma Membrane	kinase
PDE3B	phosphodiesterase 3B, cGMP-inhibited	-2.15	Cytoplasm	enzyme
PPP1CC	protein phosphatase 1, catalytic subunit, gamma isozyme	-2.15	Cytoplasm	phosphatase
NOS3	nitric oxide synthase 3 (endothelial cell)	-2.14	Cytoplasm	enzyme
PTEN	phosphatase and tensin homolog	-2.14	Cytoplasm	phosphatase
IL4	interleukin 4	-2.14	Extracellular Space	cytokine
PTK2	PTK2 protein tyrosine kinase 2	-2.14	Cytoplasm	kinase

CLIP2	CAP-GLY domain containing linker protein 2	-2.13	Cytoplasm	transcription regulator
MAPK3	mitogen-activated protein kinase 3	-2.13	Cytoplasm	kinase
CASP4	caspase 4, apoptosis-related cysteine peptidase	-2.13	Cytoplasm	peptidase
PRL	prolactin	-2.11	Extracellular Space	cytokine
ZNF423	zinc finger protein 423	-2.10	Nucleus	transcription regulator
NFKB2	nuclear factor of kappa light polypeptide gene enhancer in B-cells 2	-2.10	Nucleus	transcription regulator
CREB1	cAMP responsive element binding protein 1	-2.10	Nucleus	transcription regulator
CD2AP	CD2-associated protein	-2.09	Cytoplasm	other
NPPB	natriuretic peptide precursor B	-2.09	Extracellular Space	other
PXN	paxillin	-2.09	Cytoplasm	other
CRYAB	crystallin, alpha B	-2.08	Nucleus	other
VEGFB (includes EG:89811)	vascular endothelial growth factor B	-2.08	Extracellular Space	other
TNF	tumor necrosis factor	-2.08	Extracellular Space	cytokine
AGT	angiotensinogen (serpin peptidase inhibitor, clade A, member 8)	-2.07	Extracellular Space	other
DCTN2	dynactin 2 (p50)	-2.07	Cytoplasm	other
WNT4	wingless-type MMTV integration site family, member 4	-2.06	Extracellular Space	other
SHH	sonic hedgehog homolog (Drosophila)	-2.05	Extracellular Space	peptidase
ADRB2	adrenergic, beta-2-, receptor, surface	-2.04	Plasma Membrane	GPCR
BCL2	B-cell CLL/lymphoma 2	-2.03	Cytoplasm	other
GRIN2B	glutamate receptor, ionotropic, N-methyl D-aspartate 2B	-2.03	Plasma Membrane	ion channel
PPARG	peroxisome proliferator-activated receptor gamma	-2.03	Nucleus	ligand-dependent nuclear receptor
NOTCH4	Notch homolog 4 (Drosophila)	-2.02	Plasma Membrane	transcription regulator

GRIN1	glutamate receptor, ionotropic, N-methyl D-aspartate 1	-2.01	Plasma Membrane	ion channel
GRM1	glutamate receptor, metabotropic 1	-2.01	Plasma Membrane	GPCR
FSHR	follicle stimulating hormone receptor	-2.01	Plasma Membrane	GPCR
PKIG	protein kinase (cAMP-dependent, catalytic) inhibitor gamma	-2.01	unknown	other
CDK5R1	cyclin-dependent kinase 5, regulatory subunit 1 (p35)	-2.01	Nucleus	kinase
REN	renin	-2.01	Extracellular Space	peptidase

Table 8-3 : Genes associated with cardiac function

8.4 Discussion

The repair of ventricular tissues, following ischemia can lead to an improvement in the quality of life in patients suffering from chronic heart failure. Various studies have focused on the need for angiogenesis in ischemic tissue, in order to stimulate hibernating myocardium and provide for cardiac functional benefit.[12,34,48] However, the application of mesenchymal stem cells delivered peri infarct, as a response to the MSC homing factor, monocyte chemoattractant protein-3 (MCP-3) led to a significant improvement in cardiac benefit, without any improvement in angiogenesis, or the differentiation of MSCs to cardiac myocytes in the infarct tissue.[52] Therefore, in order to understand the molecular mechanisms involved, and to identify lead paracrine factors responsible for reverse ventricular remodeling, we analyzed these tissues for all up and down regulated genes, following MSC therapy, using microarray studies. We approached the microarray

analysis data with two different aspects, one primarily to look for secreted proteins in the tissue based on fold changes and p-values, and another to look for specific proteins associated with cardiovascular functions, based on p values and interactions between the differentially expressed genes.

Secreted proteins in the treated group were based on the location of these proteins, in the extra cellular space. We identified 6 secreted proteins that were differentially expressed with a fold change of greater than 2. Among these proteins, two were upregulated, and we looked at these 2 genes, Leukemia inhibitory factor, is a gene that promotes proliferation of cells, but there hasn't been any studies to see its effect on cardiac benefit. However, PSG-18 (pregnancy specific glycoprotein 18) has been shown to induce a cardioprotective protein IL10.[207] IL10 has been implicated in heart failure to promote cardiac functional benefit, by preventing the infiltration of macrophages.[208,209] However, on studying the expression of PSG-19 based on RT PCR analysis between all the groups, we did not obtain any conclusive evidence of this being a differentially expressed gene between all the groups.

Differentially expressed genes, associated with cardiovascular functions, were then analyzed based on pathway analysis networks. Network studies allow us to understand the interactions between the various genes and the role they play within the various pathways that they are involved in.[165, 166] This data is provided by literature from previous studies performed and uploaded onto the software. However, the lack of a complete library does not provide accurate and updated information, but can still provide various

leads that can be pursued in order to understand the molecular pathways associated with reverse ventricular remodeling.[147] A list of the complete genes, as obtained from the pathway analysis software has been provided. Some of the upregulated genes have been shown to provide cardiac benefit and some have been shown to increase the risk involved with the disease, and circulating levels of these proteins are used as diagnostic markers for the disease. Some proteins, such as macrophage migration inhibition factor (MIF), and interferon gamma (IFNg) have been shown to increase the risk for heart failure.[210, 211] Other proteins such as SFRP-4 (secreted frizzled receptor protein 4) promotes cardiac protection by reducing fibrosis size in ischemic models,[54, 212] MEF2b (myocyte enhancer protein 2b) is essential for heart development,[213] CLEC11A, also known as SCGF (Stem cell growth factor) is secreted and is required by an autocrine process responsible for the proliferation of hematopoietic stem cells,[214] VEGf (Vascular endothelial growth factor) is responsible for angiogenesis in infarct tissues,[215] GLRX3 (glutaredoxin 3) reduces the risks involved with cardiac failure in diabetic mice, [216] and CAV3 (caveolin 3) overexpression has been studied as a means to provide cardiac protection.[217] Taking cue from the various studies performed earlier, and correlating them to this cardiovascular gene list provided by this study, we are able to identify novel molecular mechanisms involved in reverse ventricular remodeling.

This study paves the way for future studies, where these specific genes can be focused on for ventricular repair, and can be validated by protein and RT PCR analysis.

CHAPTER IX

SUMMARY AND CONCLUSIONS

Overall, we have developed and designed a gene drug that can provide significant improvements in cardiac function, capable of translating to a clinical setting. We have engineered a delivery package, using nanoparticlulate carriers with homing ligands, capable of targeting the polymeric carrier to ischemic tissues. We have analyzed pathways responsible for reverse ventricular leads and have paved the way for future research responsible for improving the quality of life in patients, by inducing the reversal of ventricular remodeling. The conclusions and outcomes, based on *in vivo* and *in vitro* studies, as elucidated by previous chapters above, are outlined here.

We investigated the use of optical imaging as a tool for detecting gene expression studies. We used a Luciferase gene, one that emits chemiluminescence in the presence of

an i.p. injection of luciferin, as our gene of interest for the bioluminescence studies in chronic heart failure rodent models. The chemiluminescence emitted was quantified and analyzed in order to understand the genetic profile of this plasmid.

We noticed the changes in expression profiles, with the use of enhancer elements in the gene design, thus correlating to the boosts in gene expression. Utilizing a cooled camera to detect bioluminescence can help understand the genetic profile in gene therapy and eliminate the need for complicated bioassays.

We designed a gene vector with enhancer elements, supported from the expression data collected by the bioluminescence studies and used this vector to now express the hSDF-1 gene, responsible for providing cardiac benefit in ischemic myocardium

We observed the improvements in cardiac function, *in vivo* and its correlation to the expression profiles, and were able to design a gene vector, capable of delivering the SDF-1 gene to ischemic myocardiums and provide sustained benefit, lasting up to 2 months following therapy.

We investigated the mechanism by which SDF-1 gene transfer provides cardiac benefit and attributed that to improved angiogenesis in the infarcted region of the cardiac tissue. We also observed a reduction in fibrosis area, but this did not correspond to the amount of benefit.

Employing phage panning techniques, we identified a targeting ligand out of millions of peptides that is specific to the infarcted region of the heart. This ligand was determined to be a 7 mer sequence of RQPRMKR.

We synthesized this peptide and tagged it with a fluorescent tag, to be able to view it with optical microscopy. This peptide is specific to the heart and not other organs.

We engineered nanoparticles made with polymeric PLGA and investigated the distribution patterns, uptake and release, *in vitro*, in cardiac fibroblasts and *in vivo* in chronic heart failure rodents. We identified the uptake to happen in the first one hour after the addition of particles, and continued release for up to 24 hours post addition, in culture dishes.

The role of the size of particles was determined, when we observed that size and uptake was inversely co related. The addition of larger particles (un sonicated ones) mediated lower uptake than sonicated, smaller sized particles.

The presence of targeting peptides did not affect the amount of uptake in cells growing on culture plates specifying its role in targeting of the particles, and not in cell penetration.

In vivo studies with nanoparticles, in rodents with chronic heart failure, determined the role of targeting peptides. More particles, with targeting peptides, released the dye in

the infarcted region as compared to particles without the targeting peptide. The non targeting particles were found flushed away from circulation, into the liver.

To determine novel pathways responsible for ventricular remodeling, we investigated the role of mesenchymal stem cells with whole genome analysis. Whole genome analysis was able to provide accurate and detailed information, regarding all the pathways and nodal genes, up regulated due to stem cell therapy.

The recruitment of mesenchymal stem cells by monocyte chemoattractant protein-3, late after acute myocardial infarction, was able to provide cardiac benefit in function, due to paracrine effects.

We identified a list of differentially expressed genes responsible for ventricular remodeling. Some of these genes have been studied to provide cardiac benefit.

Overall, we have developed a non viral gene therapy based delivery of h-Stromal derived cell factor -1 plasmid to benefit regeneration of cardiac myocardium due to improved angiogenesis. We have developed a carrier system, capable of transporting this gene, via the circulation, to the area of injury, in the heart, and deliver the drug gene. We have paved the way for new research in cardiac regeneration by identifying novel pathways responsible for reverse ventricular regeneration.

Significance and Clinical Impact

This study has identified a key gene drug responsible for providing benefit to the myocardium. On the other hand, we have designed and optimized this drug to sustain long enough and translate clinically viable quantities of protein in order to provide significant benefit long after the loss of gene expression. We have been able to able to verify our findings, and develop a method for improvement in cardiac function without the use of any cell types, or viral particles involved. This principle and gene and vector design can now be extended to larger animals and clinical populations towards AMI leading to CHF patients.

As mentioned above, over 10% of the US population over the age of 65 years has the diagnosis of congestive heart failure (CHF). The majority of the patients have CHF due to a history MI. These findings could be particularly useful in treating these patients.

Apart from the drug design we have identified a nanoparticulate carrier system, capable of encapsulating this drug. If we are able to verify these findings and extend this system towards targeted and effective drug delivery to ischemic cardiac tissue, this will eliminate the need for painful surgeries and will provide an easier yet effective strategy to treat the older populations, for whom, surgery may be a cause for risk.

Future Directions

This study has provided an extensive insight into the design and delivery of gene drugs to the myocardium. However, we anticipate that the future studies will be in many aspects. One will bring about extensive research in utilizing gene therapy without the use of viral or cellular delivery methods not only for cardiovascular but in all areas of gene therapy.

Another aspect will be to utilize this novel engineered nanoparticle delivery mechanism for any delivery of drug or gene to an ischemic myocardium. This will pave the way for future studies of taking these findings of this experiment into studies involving larger animals and into the clinical populations.

A third aspect will be to study defined cardiac pathways and genes identified by the microarray study and launch into a series of experiments involving animal studies and protein analysis to identify nodal proteins responsible for reverse ventricular remodeling. These proteins can then be packaged into the nanocarriers identified above, in a vector design as constructed above, in order to come up with more effective strategies for the repair of cardiac tissue following ischemic damage.

BIBLIOGRAPHY

1. Rosamond, W., et al., Heart disease and stroke statistics--2008 update: a report from the American Heart Association Statistics Committee and Stroke Statistics Subcommittee. Circulation, 2008. 117(4): p. e25-146.
2. Morrow, D.A., Cardiovascular risk prediction in patients with stable and unstable coronary heart disease. Circulation, 2010. 121(24): p. 2681-91.
3. Starling, R., *The Cleveland Clinic guide to heart failure* 2009.
4. Akiyama, T., *Ventricular arrhythmias and sudden cardiac death: an insight from recent multicenter randomized clinical trials.* Keio J Med, 1996. 45(4): p. 313-7.
5. Liu, L., *A New Epidemic of Heart Failure in the United States.* Scientific Sessions of the American Heart Association, 2008.
6. Nagano, M., N. Takeda, and N.S. Dhalla., *The Cardiomyopathic Heart.* 1994.
7. Balmforth, A.J., *Angiotensin II type 2 receptor gene polymorphisms in cardiovascular disease.* J Renin Angiotensin Aldosterone Syst, 2010. 11(1): p. 79-85.
8. Lemarie, C.A. and E.L. Schiffrin, *The angiotensin II type 2 receptor in cardiovascular disease.* J Renin Angiotensin Aldosterone Syst, 2010. 11(1): p. 19-31.
9. Plunkett, L.M. and R.L. Tackett, *Increases in CSF norepinephrine associated with the onset of digoxin-induced arrhythmias.* Eur J Pharmacol, 1987. 136(1): p. 119-22.

10. Bryant, D., et al., *Cardiac failure in transgenic mice with myocardial expression of tumor necrosis factor-alpha*. Circulation, 1998. 97(14): p. 1375-81.

11. Maeder, M.T., J.A. Mariani, and D.M. Kaye, *Hemodynamic Determinants of Myocardial B-Type Natriuretic Peptide Release. Relative Contributions of Systolic and Diastolic Wall Stress*. Hypertension, 2010.

12. Depre, C. and S.F. Vatner, *Cardioprotection in stunned and hibernating myocardium.* Heart Fail Rev, 2007. 12(3-4): p. 307-17.

13. Min, J.Y., et al., *Significant improvement of heart function by cotransplantation of human mesenchymal stem cells and fetal cardiomyocytes in postinfarcted pigs.* Ann Thorac Surg, 2002. 74(5): p. 1568-75.

14. Hodgson, D.M., et al., *Stable benefit of embryonic stem cell therapy in myocardial infarction.* Am J Physiol Heart Circ Physiol, 2004. 287(2): p. H471-9.

15. Assmus, B., et al., *Transplantation of Progenitor Cells and Regeneration Enhancement in Acute Myocardial Infarction (TOPCARE-AMI).* Circulation, 2002. 106(24): p. 3009-17.

16. Leor, J., et al., *Transplantation of fetal myocardial tissue into the infarcted myocardium of rat. A potential method for repair of infarcted myocardium?* Circulation, 1996. 94(9 Suppl): p. II332-6.

17. Leor, J., et al., *Bioengineered cardiac grafts: A new approach to repair the infarcted myocardium?* Circulation, 2000. 102(19 Suppl 3): p. III56-61.

18. Sakai, T., et al., *The fate of a tissue-engineered cardiac graft in the right ventricular outflow tract of the rat.* J Thorac Cardiovasc Surg, 2001. 121(5): p. 932-42.

19. Reinecke, H., et al., *Survival, integration, and differentiation of cardiomyocyte grafts: a study in normal and injured rat hearts.* Circulation, 1999. 100(2): p. 193-202.

20. Ruhparwar, A., et al., *Transplanted fetal cardiomyocytes as cardiac pacemaker.* Eur J Cardiothorac Surg, 2002. 21(5): p. 853-7.

21. Xiao, Y.F., J.Y. Min, and J.P. Morgan, *Immunosuppression and xenotransplantation of cells for cardiac repair.* Ann Thorac Surg, 2004. 77(2): p. 737-44.

22. Taylor, D.A., et al., *Regenerating functional myocardium: improved performance after skeletal myoblast transplantation.* Nat Med, 1998. 4(8): p. 929-33.

23. He, K.L., et al., *Autologous skeletal myoblast transplantation improved hemodynamics and left ventricular function in chronic heart failure dogs.* J Heart Lung Transplant, 2005. 24(11): p. 1940-9.

24. Menasche, P., et al., *Myoblast transplantation for heart failure.* Lancet, 2001. 357(9252): p. 279-80.

25. Veltman, C.E., et al., *Four-year follow-up of treatment with intramyocardial skeletal myoblasts injection in patients with ischaemic cardiomyopathy*. Eur Heart J, 2008. 29(11): p. 1386-96.

26. Ince, H., et al., *Transcatheter transplantation of autologous skeletal myoblasts in postinfarction patients with severe left ventricular dysfunction.* J Endovasc Ther, 2004. 11(6): p. 695-704.

27. Ghostine, S., et al., *Long-term efficacy of myoblast transplantation on regional structure and function after myocardial infarction.* Circulation, 2002. 106(12 Suppl 1): p. I131-6.

28. Aharinejad, S., et al., *Colony-stimulating factor-1 transfection of myoblasts improves the repair of failing myocardium following autologous myoblast transplantation.* Cardiovasc Res, 2008. 79(3): p. 395-404.

29. Formigli, L., et al., *Skeletal myoblasts overexpressing relaxin improve differentiation and communication of primary murine cardiomyocyte cell cultures.* J Mol Cell Cardiol, 2009. 47(2): p. 335-45.

30. Britten, M.B., et al., *Infarct remodeling after intracoronary progenitor cell treatment in patients with acute myocardial infarction (TOPCARE-AMI): mechanistic insights from serial contrast-enhanced magnetic resonance imaging.* Circulation, 2003. 108(18): p. 2212-8.

31. Orlic, D., et al., *Bone marrow stem cells regenerate infarcted myocardium.* Pediatr Transplant, 2003. 7 Suppl 3: p. 86-8.

32. Losordo, D.W., et al., *Intramyocardial transplantation of autologous CD34+ stem cells for intractable angina: a phase I/IIa double-blind, randomized controlled trial.* Circulation, 2007. 115(25): p. 3165-72.

33. Tang, Y.L., et al., *Mobilizing of haematopoietic stem cells to ischemic myocardium by plasmid mediated stromal-cell-derived factor-1alpha (SDF-1alpha) treatment.* Regul Pept, 2005. 125(1-3): p. 1-8.

34. Tang, Y.L., et al., *Autologous mesenchymal stem cell transplantation induce VEGF and neovascularization in ischemic myocardium.* Regul Pept, 2004. 117(1): p. 3-10.

35. Zhang, M., et al., *SDF-1 expression by mesenchymal stem cells results in trophic support of cardiac myocytes after myocardial infarction.* FASEB J, 2007. 21(12): p. 3197-207.

36. Agbulut, O., et al., *Can bone marrow-derived multipotent adult progenitor cells regenerate infarcted myocardium?* Cardiovasc Res, 2006. 72(1): p. 175-83.

37. Padin-Iruegas, M.E., et al., *Cardiac progenitor cells and biotinylated insulin-like growth factor-1 nanofibers improve endogenous and exogenous myocardial regeneration after infarction.* Circulation, 2009. 120(10): p. 876-87.

38. Kehat, I., et al., *Electromechanical integration of cardiomyocytes derived from human embryonic stem cells.* Nat Biotechnol, 2004. 22(10): p. 1282-9.

39. E, L.L., et al., *Enrichment of cardiomyocytes derived from mouse embryonic stem cells.* J Heart Lung Transplant, 2006. 25(6): p. 664-74.

40. Penn, M.S., *Cell-based gene therapy for the prevention and treatment of cardiac dysfunction.* Nat Clin Pract Cardiovasc Med, 2007. 4 Suppl 1: p. S83-8.

41. Wright, C.E., *Effects of vascular endothelial growth factor (VEGF)A and VEGFB gene transfer on vascular reserve in a conscious rabbit hindlimb ischaemia model.* Clin Exp Pharmacol Physiol, 2002. 29(11): p. 1035-9.

42. Comerota, A.J., et al., *Naked plasmid DNA encoding fibroblast growth factor type 1 for the treatment of end-stage unreconstructible lower extremity ischemia: preliminary results of a phase I trial.* J Vasc Surg, 2002. 35(5): p. 930-6.

43. Penn, M.S., et al., *Role of stem cell homing in myocardial regeneration.* Int J Cardiol, 2004. 95 Suppl 1: p. S23-5.

44. Orlic, D., et al., *Bone marrow cells regenerate infarcted myocardium.* Nature, 2001. 410(6829): p. 701-5.

45. Pozzobon, M., et al., *Human Bone Marrow-Derived Cd133+ Cells Delivered to a Collagen Patch on Cryoinjured Rat Heart Promote Angiogenesis and Arteriogenesis.* Cell Transplant, 2010.

46. Reinecke, H., et al., *Cardiogenic differentiation and transdifferentiation of progenitor cells.* Circ Res, 2008. 103(10): p. 1058-71.

47. Penn, M.S., *Stem-cell therapy after acute myocardial infarction: the focus should be on those at risk.* Lancet, 2006. 367(9505): p. 87-8.

48. Huang, N.F., et al., *Bone marrow-derived mesenchymal stem cells in fibrin augment angiogenesis in the chronically infarcted myocardium.* Regen Med, 2009. 4(4): p. 527-38.

49. Shabbir, A., et al., *Heart failure therapy mediated by the trophic activities of bone marrow mesenchymal stem cells: a noninvasive therapeutic regimen.* Am J Physiol Heart Circ Physiol, 2009. 296(6): p. H1888-97.

50. Nguyen, B.K., et al., *Improved Function and Myocardial Repair of Infarcted Heart by Intracoronary Injection of Mesenchymal Stem Cell-Derived Growth Factors.* J Cardiovasc Transl Res, 2010.

51. Askari, A.T., et al., *Myeloperoxidase and plasminogen activator inhibitor 1 play a central role in ventricular remodeling after myocardial infarction.* J Exp Med, 2003. 197(5): p. 615-24.

52. Schenk, S., et al., *Monocyte chemotactic protein-3 is a myocardial mesenchymal stem cell homing factor*. Stem Cells, 2007. 25(1): p. 245-51.

53. Gnecchi, M., et al., *Evidence supporting paracrine hypothesis for Akt-modified mesenchymal stem cell-mediated cardiac protection and functional improvement.* Faseb J, 2006. 20(6): p. 661-9.

54. Mirotsou, M., et al., *Secreted frizzled related protein 2 (Sfrp2) is the key Akt-mesenchymal stem cell-released paracrine factor mediating myocardial survival and repair*. Proc Natl Acad Sci U S A, 2007. 104(5): p. 1643-8.

55. Abbott, J.D., et al., *Stromal cell-derived factor-1alpha plays a critical role in stem cell recruitment to the heart after myocardial infarction but is not sufficient to induce homing in the absence of injury*. Circulation, 2004. 110(21): p. 3300-5.

56. Lataillade, J.J., et al., *Chemokine SDF-1 enhances circulating CD34(+) cell proliferation in synergy with cytokines: possible role in progenitor survival.* Blood, 2000. 95(3): p. 756-68.

57. Nagasawa, T., et al., *Defects of B-cell lymphopoiesis and bone-marrow myelopoiesis in mice lacking the CXC chemokine PBSF/SDF-1*. Nature, 1996. 382(6592): p. 635-8.

58. Tachibana, K., et al., *The chemokine receptor CXCR4 is essential for vascularization of the gastrointestinal tract.* Nature, 1998. 393(6685): p. 591-4.

59. Kocher, A.A., et al., *Myocardial homing and neovascularization by human bone marrow angioblasts is regulated by IL-8/Gro CXC chemokines.* J Mol Cell Cardiol, 2006. 40(4): p. 455-64.

60. Liesveld, J.L., et al., *Response of human CD34+ cells to CXC, CC, and CX3C chemokines: implications for cell migration and activation.* J Hematother Stem Cell Res, 2001. 10(5): p. 643-55.

61. Unzek, S., et al., *SDF-1 recruits cardiac stem cell-like cells that depolarize in vivo*. Cell Transplant, 2007. 16(9): p. 879-86.

62. Leone, A.M., et al., *Endogenous G-CSF and CD34+ cell mobilization after acute myocardial infarction.* Int J Cardiol, 2006. 111(2): p. 202-8.

63. Penn, M.S., *Importance of the SDF-1:CXCR4 axis in myocardial repair.* Circ Res, 2009. 104(10): p. 1133-5.

64. Kucia, M., J. Ratajczak, and M.Z. Ratajczak, *Bone marrow as a source of circulating CXCR4+ tissue-committed stem cells.* Biol Cell, 2005. 97(2): p. 133-46.

65. Sasaki, T., et al., *Stromal cell-derived factor-1alpha improves infarcted heart function through angiogenesis in mice.* Pediatr Int, 2007. 49(6): p. 966-71.

66. Elmadbouh, I., et al., *Ex vivo delivered stromal cell-derived factor-1alpha promotes stem cell homing and induces angiomyogenesis in the infarcted myocardium.* J Mol Cell Cardiol, 2007. 42(4): p. 792-803.

67. Segers, V.F. and R.T. Lee, *Local delivery of proteins and the use of self-assembling peptides.* Drug Discov Today, 2007. 12(13-14): p. 561-8.

68. Zhang, G., et al., *Controlled release of stromal cell-derived factor-1 alpha in situ increases c-kit+ cell homing to the infarcted heart.* Tissue Eng, 2007. 13(8): p. 2063-71.

69. Askari, A.T., et al., *Effect of stromal-cell-derived factor 1 on stem-cell homing and tissue regeneration in ischaemic cardiomyopathy*. Lancet, 2003. 362(9385): p. 697-703.

70. Mohle, R., et al., *The chemokine receptor CXCR-4 is expressed on CD34+ hematopoietic progenitors and leukemic cells and mediates transendothelial migration induced by stromal cell-derived factor-1*. Blood, 1998. 91(12): p. 4523-30.

71. Wynn, R.F., et al., *A small proportion of mesenchymal stem cells strongly expresses functionally active CXCR4 receptor capable of promoting migration to bone marrow.* Blood, 2004. 104(9): p. 2643-5.

72. Kucia, M., et al., *The migration of bone marrow-derived non-hematopoietic tissue-committed stem cells is regulated in an SDF-1-, HGF-, and LIF-dependent manner*. Arch Immunol Ther Exp (Warsz), 2006. 54(2): p. 121-35.

73. Naiyer, A.J., et al., *Stromal derived factor-1-induced chemokinesis of cord blood CD34(+) cells (long-term culture-initiating cells) through endothelial cells is mediated by E-selectin*. Blood, 1999. 94(12): p. 4011-9.

74. Peled, A., et al., *The chemokine SDF-1 activates the integrins LFA-1, VLA-4, and VLA-5 on immature human CD34(+) cells: role in transendothelial/stromal migration and engraftment of NOD/SCID mice.* Blood, 2000. 95(11): p. 3289-96.

75. Lee, B.C., et al., *Involvement of the chemokine receptor CXCR4 and its ligand stromal cell-derived factor 1alpha in breast cancer cell migration through human brain microvascular endothelial cells*. Mol Cancer Res, 2004. 2(6): p. 327-38.

76. Peled, A., et al., *The chemokine SDF-1 stimulates integrin-mediated arrest of CD34(+) cells on vascular endothelium under shear flow.* J Clin Invest, 1999. 104(9): p. 1199-211.

77. Vlahakis, S.R., et al., *G protein-coupled chemokine receptors induce both survival and apoptotic signaling pathways.* J Immunol, 2002. 169(10): p. 5546-54.

78. Gnecchi, M., et al., *Paracrine action accounts for marked protection of ischemic heart by Akt-modified mesenchymal stem cells.* Nat Med, 2005. 11(4): p. 367-8.

79. Zheng, H., et al., *SDF-1alpha/CXCR4 decreases endothelial progenitor cells apoptosis under serum deprivation by PI3K/Akt/eNOS pathway.* Atherosclerosis, 2008. 201(1): p. 36-42.

80. Petit, I., et al., *Atypical PKC-zeta regulates SDF-1-mediated migration and development of human CD34+ progenitor cells.* J Clin Invest, 2005. 115(1): p. 168-76.

81. Damas, J.K., et al., *Stromal cell-derived factor-1alpha in unstable angina: potential antiinflammatory and matrix-stabilizing effects.* Circulation, 2002. 106(1): p. 36-42.

82. Damas, J.K., et al., *Enhanced expression of the homeostatic chemokines CCL19 and CCL21 in clinical and experimental atherosclerosis: possible pathogenic role in plaque destabilization.* Arterioscler Thromb Vasc Biol, 2007. 27(3): p. 614-20.

83. Edelstein, M.L., M.R. Abedi, and J. Wixon, *Gene therapy clinical trials worldwide to 2007--an update.* J Gene Med, 2007. 9(10): p. 833-42.

84. Edelstein, M.L., et al., *Gene therapy clinical trials worldwide 1989-2004-an overview.* J Gene Med, 2004. 6(6): p. 597-602.

85. Wencker, D., et al., *A mechanistic role for cardiac myocyte apoptosis in heart failure.* J Clin Invest, 2003. 111(10): p. 1497-504.

86. Hirota, H., et al., *Loss of a gp130 cardiac muscle cell survival pathway is a critical event in the onset of heart failure during biomechanical stress.* Cell, 1999. 97(2): p. 189-98.

87. Shiojima, I., et al., *Akt signaling mediates postnatal heart growth in response to insulin and nutritional status.* J Biol Chem, 2002. 277(40): p. 37670-7.

88. Matsui, T., et al., *Akt activation preserves cardiac function and prevents injury after transient cardiac ischemia in vivo.* Circulation, 2001. 104(3): p. 330-5.

89. Matsui, T., et al., *Adenoviral gene transfer of activated phosphatidylinositol 3'-kinase and Akt inhibits apoptosis of hypoxic cardiomyocytes in vitro.* Circulation, 1999. 100(23): p. 2373-9.

90. van Weel, V., et al., *Expression of vascular endothelial growth factor, stromal cell-derived factor-1, and CXCR4 in human limb muscle with acute and chronic ischemia.* Arterioscler Thromb Vasc Biol, 2007. 27(6): p. 1426-32.

91. Witzenbichler, B., et al., *Intramuscular gene transfer of fibroblast growth factor-1 using improved pCOR plasmid design stimulates collateral formation in a rabbit ischemic hindlimb model.* J Mol Med, 2006. 84(6): p. 491-502.

92. Henry, T.D., et al., *The VIVA trial: Vascular endothelial growth factor in Ischemia for Vascular Angiogenesis.* Circulation, 2003. 107(10): p. 1359-65.

93. Lederman, R.J., et al., *Therapeutic angiogenesis with recombinant fibroblast growth factor-2 for intermittent claudication (the TRAFFIC study): a randomised trial.* Lancet, 2002. 359(9323): p. 2053-8.

94. Lazarous, D.F., et al., *Adenoviral-mediated gene transfer induces sustained pericardial VEGF expression in dogs: effect on myocardial angiogenesis.* Cardiovasc Res, 1999. 44(2): p. 294-302.

95. Ueno, H., et al., *Adenovirus-mediated expression of the secreted form of basic fibroblast growth factor (FGF-2) induces cellular proliferation and angiogenesis in vivo.* Arterioscler Thromb Vasc Biol, 1997. 17(11): p. 2453-60.

96. Baumgartner, I., et al., *Constitutive expression of phVEGF165 after intramuscular gene transfer promotes collateral vessel development in patients with critical limb ischemia.* Circulation, 1998. 97(12): p. 1114-23.

97. Muhlhauser, J., et al., *In vivo angiogenesis induced by recombinant adenovirus vectors coding either for secreted or nonsecreted forms of acidic fibroblast growth factor.* Hum Gene Ther, 1995. 6(11): p. 1457-65.

98. Vale, P.R., et al., *Randomized, single-blind, placebo-controlled pilot study of catheter-based myocardial gene transfer for therapeutic angiogenesis using left ventricular electromechanical mapping in patients with chronic myocardial ischemia.* Circulation, 2001. 103(17): p. 2138-43.

99. Symes, J.F., *Gene therapy for ischemic heart disease: therapeutic potential.* Am J Cardiovasc Drugs, 2001. 1(3): p. 159-66.

100. Walther, W., et al., *Uptake, biodistribution, and time course of naked plasmid DNA trafficking after intratumoral in vivo jet injection.* Hum Gene Ther, 2006. 17(6): p. 611-24.

101. Wolff, J.A. and V. Budker, *The mechanism of naked DNA uptake and expression.* Adv Genet, 2005. 54: p. 3-20.

102. Wright, M.J., et al., *In vivo myocardial gene transfer: optimization, evaluation and direct comparison of gene transfer vectors.* Basic Res Cardiol, 2001. 96(3): p. 227-36.

103. Tio, R.A., et al., *Intramyocardial gene therapy with naked DNA encoding vascular endothelial growth factor improves collateral flow to ischemic myocardium.* Hum Gene Ther, 1999. 10(18): p. 2953-60.

104. Munier, S., et al., *Cationic PLA nanoparticles for DNA delivery: comparison of three surface polycations for DNA binding, protection and transfection properties.* Colloids Surf B Biointerfaces, 2005. 43(3-4): p. 163-73.

105. Li, K., et al., *Direct gene transfer into the mouse heart.* Journal of Molecular and Cellular Cardiology, 1997. 29(5): p. 1499-1504.

106. Hong, J.W., et al., *PEGylated polyethylenimine for in vivo local gene delivery based on lipiodolized emulsion system.* J Control Release, 2004. 99(1): p. 167-76.

107. Aoki, M., et al., *Efficient in vivo gene transfer into the heart in the rat myocardial infarction model using the HVJ (Hemagglutinating Virus of Japan)--liposome method.* J Mol Cell Cardiol, 1997. 29(3): p. 949-59.

108. Ding, W., et al., *Intracellular trafficking of adeno-associated viral vectors.* Gene Ther, 2005. 12(11): p. 873-80.

109. Muller, O.J., H.A. Katus, and R. Bekeredjian, *Targeting the heart with gene therapy-optimized gene delivery methods.* Cardiovasc Res, 2007. 73(3): p. 453-62.

110. Shah, P.B. and D.W. Losordo, *Non-viral vectors for gene therapy: clinical trials in cardiovascular disease.* Adv Genet, 2005. 54: p. 339-61.

111. Kozak, M., *An analysis of 5'-noncoding sequences from 699 vertebrate messenger RNAs.* Nucleic Acids Res, 1987. 15(20): p. 8125-48.

112. Jobling, S.A. and L. Gehrke, *Enhanced translation of chimaeric messenger RNAs containing a plant viral untranslated leader sequence.* Nature, 1987. 325(6105): p. 622-5.

113. Attal, J., et al., *The stimulation of gene expression by the R region from HTLV-1 and BLV.* J Biotechnol, 2000. 77(2-3): p. 179-89.

114. Panyam, J. and V. Labhasetwar, *Biodegradable nanoparticles for drug and gene delivery to cells and tissue.* Adv Drug Deliv Rev, 2003. 55(3): p. 329-47.

115. Lemoine, D., et al., *Stability study of nanoparticles of poly(epsilon-caprolactone), poly(D,L-lactide) and poly(D,L-lactide-co-glycolide).* Biomaterials, 1996. 17(22): p. 2191-7.

116. Lobenberg, R., et al., *Body distribution of azidothymidine bound to hexyl-cyanoacrylate nanoparticles after i.v. injection to rats.* J Control Release, 1998. 50(1-3): p. 21-30.

117. Guterres, S.S., et al., *Poly(D,L-lactide) nanocapsules containing non-steroidal anti-inflammatory drugs: gastrointestinal tolerance following intravenous and oral administration.* Pharm Res, 1995. 12(10): p. 1545-7.

118. Panyam, J., et al., *Rapid endo-lysosomal escape of poly(DL-lactide-co-glycolide) nanoparticles: implications for drug and gene delivery.* Faseb J, 2002. 16(10): p. 1217-26.

119. Prabha, S., et al., *Size-dependency of nanoparticle-mediated gene transfection: studies with fractionated nanoparticles.* Int J Pharm, 2002. 244(1-2): p. 105-15.

120. Sahoo, S.K., et al., *Residual polyvinyl alcohol associated with poly (D,L-lactide-co-glycolide) nanoparticles affects their physical properties and cellular uptake.* J Control Release, 2002. 82(1): p. 105-14.

121. Prabha, S. and V. Labhasetwar, *Critical determinants in PLGA/PLA nanoparticle-mediated gene expression.* Pharm Res, 2004. 21(2): p. 354-64.

122. Allemann, E., et al., *In vitro extended-release properties of drug-loaded poly(DL-lactic acid) nanoparticles produced by a salting-out procedure.* Pharm Res, 1993. 10(12): p. 1732-7.

123. Mosqueira, V.C., et al., *Poly(D,L-lactide) nanocapsules prepared by a solvent displacement process: influence of the composition on physicochemical and structural properties.* J Pharm Sci, 2000. 89(5): p. 614-26.

124. Acharya, S., F. Dilnawaz, and S.K. Sahoo, *Targeted epidermal growth factor receptor nanoparticle bioconjugates for breast cancer therapy.* Biomaterials, 2009. 30(29): p. 5737-50.

125. Quintanar-Guerrero, D., et al., *Preparation and characterization of nanocapsules from preformed polymers by a new process based on emulsification-diffusion technique.* Pharm Res, 1998. 15(7): p. 1056-62.

126. Quellec, P., et al., *Protein encapsulation within polyethylene glycol-coated nanospheres. I. Physicochemical characterization.* J Biomed Mater Res, 1998. 42(1): p. 45-54.

127. Panyam, J. and V. Labhasetwar, *Dynamics of endocytosis and exocytosis of poly(D,L-lactide-co-glycolide) nanoparticles in vascular smooth muscle cells.* Pharm Res, 2003. 20(2): p. 212-20.

128. Prabha, S. and V. Labhasetwar, *Nanoparticle-mediated wild-type p53 gene delivery results in sustained antiproliferative activity in breast cancer cells.* Mol Pharm, 2004. 1(3): p. 211-9.

129. Mok, H. and T.G. Park, *Functional polymers for targeted delivery of nucleic acid drugs.* Macromol Biosci, 2009. 9(8): p. 731-43.

130. Schiffelers, R.M., et al., *Cancer siRNA therapy by tumor selective delivery with ligand-targeted sterically stabilized nanoparticle.* Nucleic Acids Res, 2004. 32(19): p. e149.

131. Suh, W., et al., *An angiogenic, endothelial-cell-targeted polymeric gene carrier.* Mol Ther, 2002. 6(5): p. 664-72.

132. Koivunen, E., B. Wang, and E. Ruoslahti, *Phage libraries displaying cyclic peptides with different ring sizes: ligand specificities of the RGD-directed integrins.* Biotechnology (N Y), 1995. 13(3): p. 265-70.

133. Kunath, K., et al., *Integrin targeting using RGD-PEI conjugates for in vitro gene transfer.* J Gene Med, 2003. 5(7): p. 588-99.

134. Beljaars, L., et al., *Successful targeting to rat hepatic stellate cells using albumin modified with cyclic peptides that recognize the collagen type VI receptor.* J Biol Chem, 2000. 275(17): p. 12743-51.

135. Stupack, D.G. and D.A. Cheresh, *Integrins and angiogenesis.* Curr Top Dev Biol, 2004. 64: p. 207-38.

136. Cai, W. and X. Chen, *Anti-angiogenic cancer therapy based on integrin alphavbeta3 antagonism.* Anticancer Agents Med Chem, 2006. 6(5): p. 407-28.

137. Jin, H., et al., *Tumor-specific nano-entities for optical detection and hyperthermic treatment of breast cancer.* Adv Exp Med Biol, 2008. 614: p. 275-84.

138. Huang, R., et al., *The use of lactoferrin as a ligand for targeting the polyamidoamine-based gene delivery system to the brain.* Biomaterials, 2008. 29(2): p. 238-46.

139. Widera, A., F. Norouziyan, and W.C. Shen, *Mechanisms of TfR-mediated transcytosis and sorting in epithelial cells and applications toward drug delivery.* Adv Drug Deliv Rev, 2003. 55(11): p. 1439-66.

140. Gao, H.L., et al., *Effect of lactoferrin- and transferrin-conjugated polymersomes in brain targeting: in vitro and in vivo evaluations.* Acta Pharmacol Sin, 2010. 31(2): p. 237-43.

141. Riese, D.J., 2nd, R.M. Gallo, and J. Settleman, *Mutational activation of ErbB family receptor tyrosine kinases: insights into mechanisms of signal transduction and tumorigenesis.* Bioessays, 2007. 29(6): p. 558-65.

142. Agarwal, A., et al., *Ligand based dendritic systems for tumor targeting.* Int J Pharm, 2008. 350(1-2): p. 3-13.

143. Kim, T.G., et al., *Gene transfer into human hepatoma cells by receptor-associated protein/polylysine conjugates.* Bioconjug Chem, 2004. 15(2): p. 326-32.

144. Cook, S.E., et al., *Galactosylated polyethylenimine-graft-poly(vinyl pyrrolidone) as a hepatocyte-targeting gene carrier.* J Control Release, 2005. 105(1-2): p. 151-63.

145. Jiang, H.L., et al., *The potential of mannosylated chitosan microspheres to target macrophage mannose receptors in an adjuvant-delivery system for intranasal immunization.* Biomaterials, 2008. 29(12): p. 1931-9.

146. Narayanan, S., et al., *Folate targeted polymeric 'green' nanotherapy for cancer.* Nanotechnology, 2010. 21(28): p. 285107.

147. Jostock, T. and S. Dubel, *Screening of molecular repertoires by microbial surface display.* Comb Chem High Throughput Screen, 2005. 8(2): p. 127-33.

148. Kolonin, M.G., et al., *Synchronous selection of homing peptides for multiple tissues by in vivo phage display.* Faseb J, 2006. 20(7): p. 979-81.

149. Smith, J., et al., *Antibody phage display technologies with special reference to angiogenesis.* Faseb J, 2005. 19(3): p. 331-41.

150. Pasqualini, R. and E. Ruoslahti, *Organ targeting in vivo using phage display peptide libraries.* Nature, 1996. 380(6572): p. 364-6.

151. Kang, S.K., et al., *Identification of a peptide sequence that improves transport of macromolecules across the intestinal mucosal barrier targeting goblet cells.* J Biotechnol, 2008. 135(2): p. 210-6.

152. Chen, Y., et al., *Transdermal protein delivery by a coadministered peptide identified via phage display*. Nat Biotechnol, 2006. 24(4): p. 455-60.

153. Yao, V.J., et al., *Targeting pancreatic islets with phage display assisted by laser pressure catapult microdissection.* Am J Pathol, 2005. 166(2): p. 625-36.

154. Bockmann, M., M. Drosten, and B.M. Putzer, *Discovery of targeting peptides for selective therapy of medullary thyroid carcinoma*. J Gene Med, 2005. 7(2): p. 179-88.

155. Laakkonen, P., et al., *A tumor-homing peptide with a targeting specificity related to lymphatic vessels.* Nat Med, 2002. 8(7): p. 751-5.

156. Arap, W., et al., *Targeting the prostate for destruction through a vascular address*. Proc Natl Acad Sci U S A, 2002. 99(3): p. 1527-31.

157. Landon, L.A. and S.L. Deutscher, *Combinatorial discovery of tumor targeting peptides using phage display*. J Cell Biochem, 2003. 90(3): p. 509-17.

158. Krag, D.N., et al., *Phage-displayed random peptide libraries in mice: toxicity after serial panning.* Cancer Chemother Pharmacol, 2002. 50(4): p. 325-32.

159. Arap, W., et al., *Steps toward mapping the human vasculature by phage display.* Nat Med, 2002. 8(2): p. 121-7.

160. Maruta, F., et al., *Use of a phage display library to identify oligopeptides binding to the lumenal surface of polarized endothelium by ex vivo perfusion of human umbilical veins.* J Drug Target, 2003. 11(1): p. 53-9.

161. Pasqualini, R., W. Arap, and D.M. McDonald, *Probing the structural and molecular diversity of tumor vasculature.* Trends Mol Med, 2002. 8(12): p. 563-71.

162. Rosenwald, A., et al., *The proliferation gene expression signature is a quantitative integrator of oncogenic events that predicts survival in mantle cell lymphoma*. Cancer Cell, 2003. 3(2): p. 185-97.

163. Thirunavukkarasu, M., et al., *Heterozygous disruption of Flk-1 receptor leads to myocardial ischaemia reperfusion injury in mice: application of affymetrix gene chip analysis.* J Cell Mol Med, 2008. 12(4): p. 1284-302.

164. Schiekofer, S., et al., *Microarray analysis of Akt1 activation in transgenic mouse hearts reveals transcript expression profiles associated with compensatory hypertrophy and failure*. Physiol Genomics, 2006. 27(2): p. 156-70.

165. Clark, T.A., et al., *Discovery of tissue-specific exons using comprehensive human exon microarrays.* Genome Biol, 2007. 8(4): p. R64.

166. Seo, J., H. Gordish-Dressman, and E.P. Hoffman, *An interactive power analysis tool for microarray hypothesis testing and generation*. Bioinformatics, 2006. 22(7): p. 808-14.

167. Wu, Z. and R.A. Irizarry, *Preprocessing of oligonucleotide array data*. Nat Biotechnol, 2004. 22(6): p. 656-8; author reply 658.

168. Beller, G.A., *The case for cardiac magnetic resonance and positron emission tomography multimodality imaging of myocardial viability*. J Nucl Cardiol, 2010. 17(4): p. 527-8.

169. Inubushi, M., et al., *Positron-emission tomography reporter gene expression imaging in rat myocardium.* Circulation, 2003. 107(2): p. 326-32.

170. Contag, C.H., et al., *Visualizing gene expression in living mammals using a bioluminescent reporter*. Photochem Photobiol, 1997. 66(4): p. 523-31.

171. Contag, C.H., et al., *Use of reporter genes for optical measurements of neoplastic disease in vivo.* Neoplasia, 2000. 2(1-2): p. 41-52.

172. Yamaguchi, S., et al., *Bioluminescence imaging of c-fos gene expression accompanying filial imprinting in the newly hatched chick brain.* Neurosci Res, 2010

67(2): p. 192-5.

173. Pietrella, D., et al., *A beta-glucan-conjugate vaccine and anti-beta-glucan antibodies are effective against murine vaginal candidiasis as assessed by a novel in vivo imaging technique.* Vaccine, 2010

28(7): p. 1717-25.

174. Herweijer, H., et al., *Time course of gene expression after plasmid DNA gene transfer to the liver.* J Gene Med, 2001. 3(3): p. 280-91.

175. Lapidot, T. and I. Petit, *Current understanding of stem cell mobilization: the roles of chemokines, proteolytic enzymes, adhesion molecules, cytokines, and stromal cells.* Exp Hematol, 2002. 30(9): p. 973-81.

176. Hu, X., et al., *Stromal cell derived factor-1 alpha confers protection against myocardial ischemia/reperfusion injury: role of the cardiac stromal cell derived factor-1 alpha CXCR4 axis.* Circulation, 2007. 116(6): p. 654-63.

177. Zheng, H., et al., *SDF-1alpha/CXCR4 decreases endothelial progenitor cells apoptosis under serum deprivation by PI3K/Akt/eNOS pathway.* Atherosclerosis, 2008.

178. Deglurkar, I., et al., *Mechanical and electrical effects of cell-based gene therapy for ischemic cardiomyopathy are independent.* Hum Gene Ther, 2006. 17(11): p. 1144-51.

179. Segers, V.F., et al., *Local delivery of protease-resistant stromal cell derived factor-1 for stem cell recruitment after myocardial infarction.* Circulation, 2007. 116(15): p. 1683-92.

180. Wang, T., et al., *Bone marrow stem cells implantation with alpha-cyclodextrin/MPEG-PCL-MPEG hydrogel improves cardiac function after myocardial infarction.* Acta Biomater, 2009. 5(8): p. 2939-44.

181. Thai, H.M., et al., *Implantation of a three-dimensional fibroblast matrix improves left ventricular function and blood flow after acute myocardial infarction.* Cell Transplant, 2009. 18(3): p. 283-95.

182. French, B.A., et al., *Direct in vivo gene transfer into porcine myocardium using replication-deficient adenoviral vectors.* Circulation, 1994. 90(5): p. 2414-24.

183. Giordano, F.J., et al., *Intracoronary gene transfer of fibroblast growth factor-5 increases blood flow and contractile function in an ischemic region of the heart.* Nat Med, 1996. 2(5): p. 534-9.

184. Wolff, J.A., et al., *Direct gene transfer into mouse muscle in vivo.* Science, 1990. 247(4949 Pt 1): p. 1465-8.

185. Yang, Y., et al., *Cellular immunity to viral antigens limits E1-deleted adenoviruses for gene therapy.* Proc Natl Acad Sci U S A, 1994. 91(10): p. 4407-11.

186. Pickering, J.G., et al., *Liposome-mediated gene transfer into human vascular smooth muscle cells.* Circulation, 1994. 89(1): p. 13-21.

187. Takeshita, S., et al., *Gene transfer of naked DNA encoding for three isoforms of vascular endothelial growth factor stimulates collateral development in vivo.* Lab Invest, 1996. 75(4): p. 487-501.

188. Boussif, O., et al., *A versatile vector for gene and oligonucleotide transfer into cells in culture and in vivo: polyethylenimine.* Proc Natl Acad Sci U S A, 1995. 92(16): p. 7297-301.

189. Kumari, A., S.K. Yadav, and S.C. Yadav, *Biodegradable polymeric nanoparticles based drug delivery systems.* Colloids Surf B Biointerfaces, 2010. 75(1): p. 1-18.

190. Mori, T., *Cancer-specific ligands identified from screening of peptide-display libraries.* Curr Pharm Des, 2004. 10(19): p. 2335-43.

191. Dincer, S., M. Turk, and E. Piskin, *Intelligent polymers as nonviral vectors.* Gene Ther, 2005. 12 Suppl 1: p. S139-45.

192. Juliano, R.L., et al., *Cell-targeting and cell-penetrating peptides for delivery of therapeutic and imaging agents.* Wiley Interdiscip Rev Nanomed Nanobiotechnol, 2009. 1(3): p. 324-35.

193. Torchilin, V.P., *Tat peptide-mediated intracellular delivery of pharmaceutical nanocarriers.* Adv Drug Deliv Rev, 2008. 60(4-5): p. 548-58.

194. Bian, J., et al., *Engineered cell therapy for sustained local myocardial delivery of nonsecreted proteins.* Cell Transplant, 2006. 15(1): p. 67-74.

195. Bian, J., et al., *Effect of cell-based intercellular delivery of transcription factor GATA4 on ischemic cardiomyopathy.* Circ Res, 2007. 100(11): p. 1626-33.

196. Zauner, W., N.A. Farrow, and A.M. Haines, *In vitro uptake of polystyrene microspheres: effect of particle size, cell line and cell density*. J Control Release, 2001. 71(1): p. 39-51.

197. McIntosh, D.P., et al., *Targeting endothelium and its dynamic caveolae for tissue-specific transcytosis in vivo: a pathway to overcome cell barriers to drug and gene delivery*. Proc Natl Acad Sci U S A, 2002. 99(4): p. 1996-2001.

198. Panyam, J., et al., *Fluorescence and electron microscopy probes for cellular and tissue uptake of poly(D,L-lactide-co-glycolide) nanoparticles.* Int J Pharm, 2003. 262(1-2): p. 1-11.

199. Desai, M.P., et al., *The mechanism of uptake of biodegradable microparticles in Caco-2 cells is size dependent.* Pharm Res, 1997. 14(11): p. 1568-73.

200. Penn, M.S., et al., *Autologous cell transplantation for the treatment of damaged myocardium*. Prog Cardiovasc Dis, 2002. 45(1): p. 21-32.

201. Chen, S., et al., *Intracoronary transplantation of autologous bone marrow mesenchymal stem cells for ischemic cardiomyopathy due to isolated chronic occluded left anterior descending artery*. J Invasive Cardiol, 2006. 18(11): p. 552-6.

202. Wilkins, A., et al., *Human bone marrow-derived mesenchymal stem cells secrete brain-derived neurotrophic factor which promotes neuronal survival in vitro.* Stem Cell Res, 2009.

203. Chen, Y., et al., *Recruitment of endogenous bone marrow mesenchymal stem cells towards injured liver*. J Cell Mol Med, 2010

14(6B): p. 1494-508.

204. Deng, W., et al., *Engrafted bone marrow-derived flk-(1+) mesenchymal stem cells regenerate skin tissue.* Tissue Eng, 2005. 11(1-2): p. 110-9.

205. Pelacho, B., et al., *Multipotent adult progenitor cell transplantation increases vascularity and improves left ventricular function after myocardial infarction.* J Tissue Eng Regen Med, 2007. 1(1): p. 51-9.

206. Tang, Y.L., et al., *Paracrine action enhances the effects of autologous mesenchymal stem cell transplantation on vascular regeneration in rat model of myocardial infarction.* Ann Thorac Surg, 2005. 80(1): p. 229-36; discussion 236-7.

207. Wessells, J., et al., *Pregnancy specific glycoprotein 18 induces IL-10 expression in murine macrophages.* Eur J Immunol, 2000. 30(7): p. 1830-40.

208. Stumpf, C., et al., *Interleukin-10 improves left ventricular function in rats with heart failure subsequent to myocardial infarction.* Eur J Heart Fail, 2008. 10(8): p. 733-9.

209. Burchfield, J.S., et al., *Interleukin-10 from transplanted bone marrow mononuclear cells contributes to cardiac protection after myocardial infarction.* Circ Res, 2008. 103(2): p. 203-11.

210. Aritaka Makino, et al., *High plasma levels of macrophage migrationinhibitory factor predict future cardiovascular events inpatients with impaired glucose tolerance or Type 2 Diabetes Mellitus.* Circulation, 2008. 118: p. S_1113.

211. Schroecksnadel, K., et al., *Crucial role of interferon-gamma and stimulated macrophages in cardiovascular disease.* Curr Vasc Pharmacol, 2006. 4(3): p. 205-13.

212. Matsushima, K., et al., *Secreted Frizzled Related Protein 4 Reduces Fibrosis Scar Size and Ameliorates Cardiac Function After Ischemic Injury*. Tissue Eng Part A, 2010.

213. Molkentin, J.D., et al., *MEF2B is a potent transactivator expressed in early myogenic lineages*. Mol Cell Biol, 1996. 16(7): p. 3814-24.

214. Hiraoka, A., *Leukemia cell lines require self-secreted stem cell growth factor (SCGF) for their proliferation.* Leuk Res, 2008. 32(10): p. 1623-5.

215. Schratzberger, P., et al., *Therapeutic angiogenesis by gene transfer in critical limb and myocardial ischemia*. Curr Pharm Des, 2003. 9(13): p. 1041-7.

216. Lekli, I., et al., *Functional recovery of diabetic mouse hearts by glutaredoxin-1 gene therapy: role of Akt-FoxO-signaling network*. Gene Ther, 2010. 17(4): p. 478-85.

217. Tsutsumi, Y.M., et al., *Cardiac-specific overexpression of caveolin-3 induces endogenous cardiac protection by mimicking ischemic preconditioning*. Circulation, 2008. 118(19): p. 1979-88.